Master's Thesis

Master's degree in Biomedicine
May 2021

Establishment of a new quantitative method for *in situ* detection of DNA breaks in human spermatozoa

Pia Skovholt Halvorsen

MABIO5900

60 ECTS

Faculty of Health Sciences

OSLO METROPOLITAN UNIVERSITY
STORBYUNIVERSITETET

Establishment of a new quantitative method for *in situ* detection of DNA breaks in human spermatozoa

by

Pia Skovholt Halvorsen

Main supervisor: Erwan Delbarre

Co-supervisors: Oliwia Witczak and Mette Haug Stensen

Master of Biomedicine

60 ECTS

Faculty of Health Science,

Department of Science and Health

OsloMet – Oslo Metropolitan University

OSLO METROPOLITAN UNIVERSITY
STORBYUNIVERSITETET

FERTILITETSSENTERET

Acknowledgements

The work presented in this thesis has been performed at the Faculty of Health Sciences, Oslo Metropolitan University (OsloMet) from August 2020 to May 2021 for the master's degree in Biomedicine at OsloMet.

First, I would like to thank my main supervisor, Erwan Delbarre that proofread every word and offered suggestions that really improved my thesis. Thank you for your continuously patience over the last year and for pushing me to be more reflective. I would also like to thank my other supervisors, Oliwia Witczak for her high scientific and literary standards that lifted my thesis and to Mette Haug Stensen for valuable suggestions and for her clinical point of view. I am so grateful to have such brilliant and encouraging supervisors.

I would like to give special thanks to Eldri Undlien Due for her presence and motivation, and to Mario Iliceto for helping me with practical protocols and for giving me several advices through this year.

Furthermore, I want to show gratitude to Trine Haugen and the rest of the research group "Male Reproductive Health" for welcoming me into the group and helping me out with solution storming when I was struggling.

Throughout this year, I have received enormously support from my family and belongings. Thank you for always being there, I could not have done this without you.

Abstract

Background: There is increasing evidence that infertile men have higher levels of DNA fragmentation compared to fertile men. It was also shown that spermatozoa with highly fragmented DNA are less motile. Several tests are available to measure DNA fragmentation in spermatozoa, but they all focus on different aspects of it and most of them lack standardization. Sperm Chromatin Structure Assay (SCSA) is a standardized method that relies on fluorescence detection by flow cytometry and involve use of a licensed software. In 2020, a new method for measuring DNA fragmentation was published: STRIDE (SensiTive Recognition of Individual DNA Ends). The method is based on fluorescence microscopy and can detect single (sSTRIDE) or double (dSTRIDE) strand breaks in individual cells. In addition to detect DNA breaks in cell lines, STRIDE also showed a potential for measuring DNA fragmentation in spermatozoa.

Aim: The main aim of this project was to establish and optimize sSTRIDE and dSTRIDE protocols for measuring DNA fragmentation in spermatozoa. Before that, we aimed to reproduce the STRIDE protocols in a somatic cell line as described in the original publication. At last, we wanted to compare results from STRIDE analyses with DNA fragmentation index values obtained earlier by SCSA in the same semen samples.

Methods and materials: The MCF-7 cell line was used in attempts to reproduce STRIDE in somatic cells. Semen samples for STRIDE establishment and optimization were provided by Fertilitetssenteret in Oslo. In addition, some samples were obtained from an ongoing method-developing project in the research group. Samples from a biobank at OsloMet were used to compare DNA fragmentation analysed by dSTRIDE and DNA fragmentation index by SCSA. Heparin and DTT was used to decondense the chromatin structure in spermatozoa. Induction of DNA damage in the different cell types was performed using different amounts of hydrogen peroxide and UVB-irradiation. Immunofluorescence procedures to detect gamma-H2AX, a marker for DNA double stranded breaks, were performed to confirm the induction of DNA breaks. STRIDE signals were collected by 2-D and 3-D microscopy and analysed using the software ImageJ.

Results: While we tried to make both dSTRIDE and sSTRIDE work in MCF-7 cells, only the dSTRIDE method was reproducible. The sSTRIDE method was then not further investigated. During the optimization of dSTRIDE in spermatozoa, coverslips

were replaced with centrifuge tubes to minimize the un-specific background. A facultative chromatin decondensation step was implemented in the final dSTRIDE protocol and was shown to result in a larger number of positive signals. An increased amount of dSTRIDE foci was observed in the nucleus of spermatozoa after hydrogen peroxide exposure and UVB radiation compared to non-exposed cells. Motile spermatozoa prepared by swim-up harboured less dSTRIDE foci compared to spermatozoa from the whole ejaculate. Finally, no significant correlation was observed between the values obtained by dSTRIDE those generated by previous SCSA analyses in the same samples.

Conclusion: dSTRIDE was established in MCF-7 cells and optimized for a robust protocol in spermatozoa. Unfortunately, the DNA-fragmentation results from dSTRIDE and SCSA did not correlate. Further work is necessary to validate and standardize the method so it can be used routinely.

Sammendrag

Bakgrunn: Det er holdepunkter for at infertile menn har høyere andel spermier med DNA-skade sammenlignet med fertile menn. Det er også vist at spermier med høy DNA-skade er mindre motile. Ulike tester brukes for å måle andelen DNA-skade i spermier, men de måler ulike aspekter ved DNA-skade og fleste er ikke standardiserte. Sperm Chromatin Structure Assay (SCSA) er en standardisert metode som benytter flowcytometri for å detektere fluorescens-signaler, og har en lisensbelagt programvare. I 2020 ble det publisert en ny metode for DNA-fragmenteringsanalyse kalt STRIDE (SensiTive Recognition of Individual DNA Ends). Metoden baseres på fluorescensmikroskopi og kan gjenkjenne både enkelttråd-brudd (single; sSTRIDE) og dobbelttråd-brudd (double; dSTRIDE) i DNA på enkeltcellenivå. I tillegg til å detektere DNA-skade i cellelinjer viste metoden også potensiale til å måle DNA-fragmentering i spermier.

Formål: Hovedformålet med oppgaven var å etablere og optimalisere sSTRIDE og dSTRIDE for å måle DNA fragmentering i spermier. Før dette forsøkte vi å reprodusere STRIDE-protokollene i en cellelinje basert på den originale artikkelen. Til sist ønsket vi å analysere prøver hvor det allerede forelå DNA-fragmenteringsresultater analysert ved hjelp av SCSA og sammenligne disse med resultatene fra STRIDE.

Metoder og materialer: Cellelinjen MCF-7 ble brukt for å reprodusere STRIDE-metoden i somatiske celler. Sædprøvene for STRIDE etablering og optimalisering ble hentet fra Fertilitetssenteret i Oslo. I tillegg ble det brukt prøver samlet i forbindelse med metodeutvikling i forskningsgruppen. Prøver fra en biobank ved OsloMet ble brukt for kunne sammenligne mengde DNA-skade analysert ved hjelp av dSTRIDE-metoden med DNA-fragmenteringsindeks ved SCSA. Heparin og DTT ble benyttet for å åpne kromatinstrukturen. For å indusere DNA-skade ble celler eksponert for ulike mengder hydrogenperoksid og UVB-stråling. Immunofluorescens rettet mot gamma-H2AX, en markør for dobletråd-brudd i DNA, ble utført for å bekrefte DNA skade. Resultater ble visualisert ved bruk av 2-D og 3-D fluorescens mikroskopi og analysert ved bruk av programvaren ImageJ.

Resultater: Både sSTRIDE og dSTRIDE ble forsøkt reprodusert i MCF-7 celler, men det var bare dSTRIDE som lot seg reprodusere. Etter gjentatte forsøk ble det bestemt at sSTRIDE skulle tas ut av prosjektet. Under etableringsprosessen av dSTRIDE-metoden på spermier, ble det funnet ut at deler av protokollen måtte gjøres i sentrifugerør for å minimere uspesifikk bakgrunn ved dSTRIDE. Prosedyre for å åpne

kromatinstrukturen i spermier ble inkludert i dSTRIDE protokollen og resulterte i flere dSTRIDE-signaler sammenlignet med resultater fra spermier med kondensert kromatin. Det ble observert økende dSTRIDE-signal i kjernen i spermiene etter eksponering for hydrogenperoksid og UVB-stråling sammenlignet med ikke-eksponerte celler. I motile spermier isolert ved «swim-up» var det mindre dSTRIDE-signal sammenlignet med spermier fra hele sædprøven. Det var ingen sammenheng mellom mengde DNA-skade detektert ved hjelp av dSTRIDE og DNA fragmenteringsindeks ved hjelp av SCSA.

Konklusjon: dSTRIDE ble etablert i MCF-7 celler og i tillegg optimalisert for en robust protokoll i spermier. Dessverre, var det ingen korrelasjon mellom DNA-fragmenteringsresultatene fra dSTRIDE og SCSA. Videre arbeid er nødvendig for å validere og standardisere metoden slik at den kan bli brukt rutinemessig.

Table of contents

Figures and tables

List of abbreviations

AI Artificial Intelligence

ART Assisted Reproductive Technology

BrdUTP 5-Bromo-2’-deoxyuridine 5’-Triphosphate

BSA Bovin Serum Albumin

DAPI 4’,6-DiAmidino-2-PhenylIndole

DFI DNA Fragmentation Index

DMEM Dulbecco's Modified Eagle Medium

DNA DeoxyriboNucleic Acid

DSB Double Strand Break

DTT Dithiothreitol

dUTP DeoxyUridine TriPhosphate

EAU European Association of Urology

EDTA Ethylene-Diamin eteTraacetic Acid

FBS Fetal Bovine Serum

FS Fertilitetssenteret

H_2O_2 Hydrogen Peroxide

ICSI IntraCytoplasmic Sperm Injection

IVF In Vitro Fertilization

MAR Matrix Attachment Regions

MCF-7 Michigan Cancer Foundation-7

NT Nick Translation

OH HydrOxyl

PBS Phosphate Buffered Saline

PE PolyEthylene

PET	PolyEthylene Terephthalate
PFA	ParaFormAldehyde
PP	PolyPropylene
SCD	Sperm Chromatin Dispersion
SCSA	Sperm Chromatin Structure Assay
SSC	Spermatogonia Stem Cell
STRIDE	SensiTive Recognition of Individual DNA Ends
SSB	Single Strand Break
TdT	Terminal deoxynucleotidyl transferase
TUNEL	Terminal deoxynucleotidyl transferase-mediated fluorescein-dUTP Nick End Labelling
UV	UltraViolet
WHO	World Health Organization

1. Introduction

1.1 Background

The loss of ability to achieve a clinical pregnancy for individuals of fertile age can be challenging for the couple as for the individual own self-esteem. From a societal perspective, it is a matter of self-renewal of the population. Every year Statistics Norway (SSB) publishes a total fertility rate for each woman of fertile age. This rate has decreased since 2009 and reached 1.48 child per woman in 2020, the lowest number ever recorded in Norway (1). The decline of number of children per woman is primarily due to higher parental age, where the mothers age at birth of their first child has increased from 24.3 years old in 1980 to 29.9 in 2020. Corresponding numbers for the fathers are 27.1 and 32.1 years old, respectively (1). It has been known for a long time that maternal age is an important factor for fertility, but the recent growing research on male reproductive factors have shown that the age of the father is by no means irrelevant. And at the same time, the percentage of men who lives alone and stays childless at an age of 45 have increased in Norway from less than 15% in 1985 up to 23% in 2013 (2, 3).

According to the World Health Organization (WHO), infertility is “a disease of the reproductive system defined by the failure to achieve a clinical pregnancy after 12 months or more of regular unprotected sexual intercourse” (4). In 2018, infertility has been estimated to affect around 8-12% of all couples in reproductive age worldwide (5). Male reproductive dysfunctions are estimated to be involved in around 50% of all infertile couples and to be the sole cause of infertility in 30% of them (5). From the male perspective, infertility is a dysfunction of the male reproductive system, which main functions are to produce their reproductive cells, the spermatozoa and to transfer them to the female reproductive tract to fertilize the female gamete, the oocyte. Underlying causes of infertility are diverse and can be divided into congenital, acquired or idiopathic factors (6) (or obstructive and non-obstructive factors), but as a result of the condition, the male reproductive system is unable to fulfil its function.

1.2 Male reproduction

The functional male reproductive system contains seven components divided into external and internal genital. External genital consist of the scrotum and the penis,

while internal genital consist of the testes, the epididymis, the vas deferens, the seminal vesicles and the prostate (7) (Fig. 1).

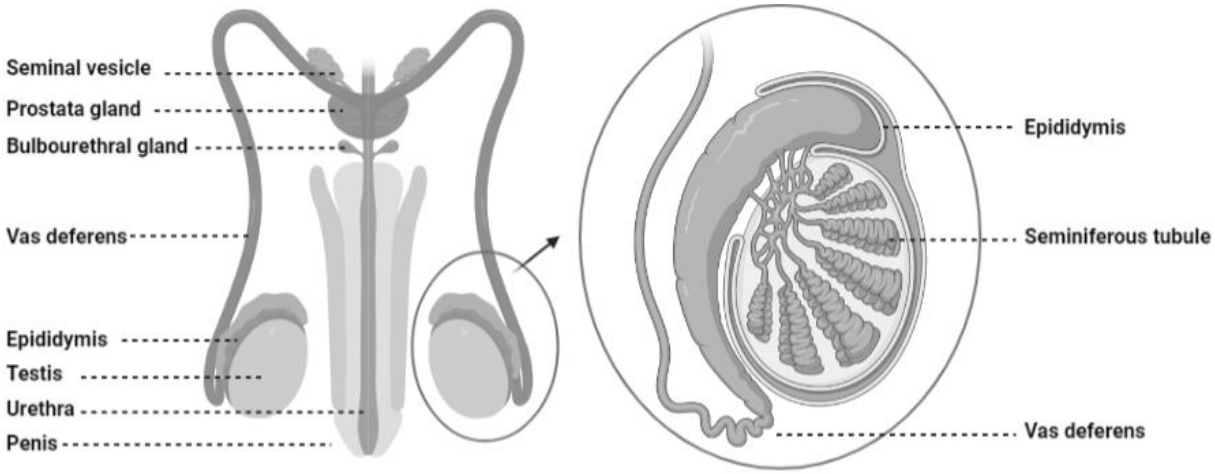

Figure 1 *Male reproductive system with an enlarged sagittal section of a normal testis. The system consists of testes, extra-testicular ducts (epididymis, vas deferens), accessory sex glands (seminal vesicles, prostate and bulbourethral gland), urethra and the penis. The section of seminiferous tubule is where the male gamete cells are produced. Illustration created by the author using Biorender.com.*

The scrotum is the pigmented, muscular sac behind the penis containing the testes surrounded by the epididymis (7). The testes are the male gonads in humans and produce spermatozoa and androgens throughout the reproductive period. The spermatozoon is the male haploid gamete cell which provides the genetic material generated in the testis by spermiogenesis.

1.2.1 Spermatogenesis

Spermatogenesis is the biological process by which fully differentiated spermatozoa are generated from stem cells called spermatogonium. This process takes approximately 74 days in total (8) and takes place in seminiferous tubules located inside the testes (Fig. 1). The first cycle of spermatogenesis start at the beginning of puberty, at the onset of sexual maturity (9). Meiotic spermatocytes are generated and entails two rounds of meiosis. Spermiogenesis is the fulfilling part that maturate cells to fully differentiated, motile spermatozoa (10).

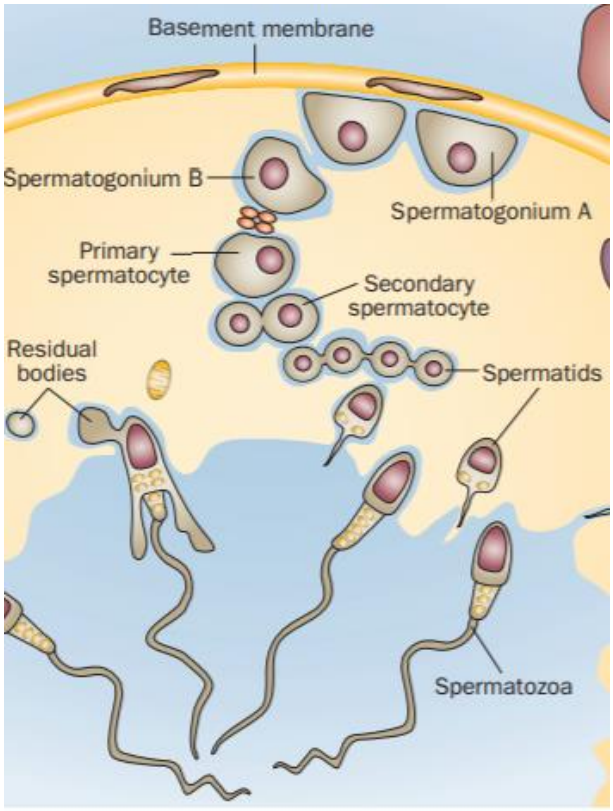

Figure 2 *Spermatogenesis occurs in seminiferous tubules.*
Spermatogonia stem cells, in contact with the basement membrane of the seminiferous tubule, divide into spermatogonia type B. Spermatogenesis is fulfilled after spermiogenesis, when mature spermatozoa are generated from spermatids in the lumen of the seminiferous tubule. The figure is adapted from (11) and used with permission from Nature Reviews Urology.

Located on the basement membranes of the tubules, populations of spermatogonia stem cells (SSCs) proliferate and differentiate. Every male is born with undifferentiated stem cells, spermatogonia type A. The latter exist as reserve and renewing cells. Renewing spermatogonia divide by mitosis and after numerous divisions a more differentiated SSC type A can divide into differentiated SSCs type B.

Each SSC type B undergoes mitosis and differentiates into two primary spermatocytes which further divide to four haploid spermatids by two rounds of meiosis. Meiosis I separate homologous chromosomes, generating haploid secondary spermatocytes. Meiosis II generates four spermatids migrating towards the lumen of seminiferous tubules (Fig. 2) and differentiating into mature spermatozoa during a process called spermiogenesis (Fig. 3).

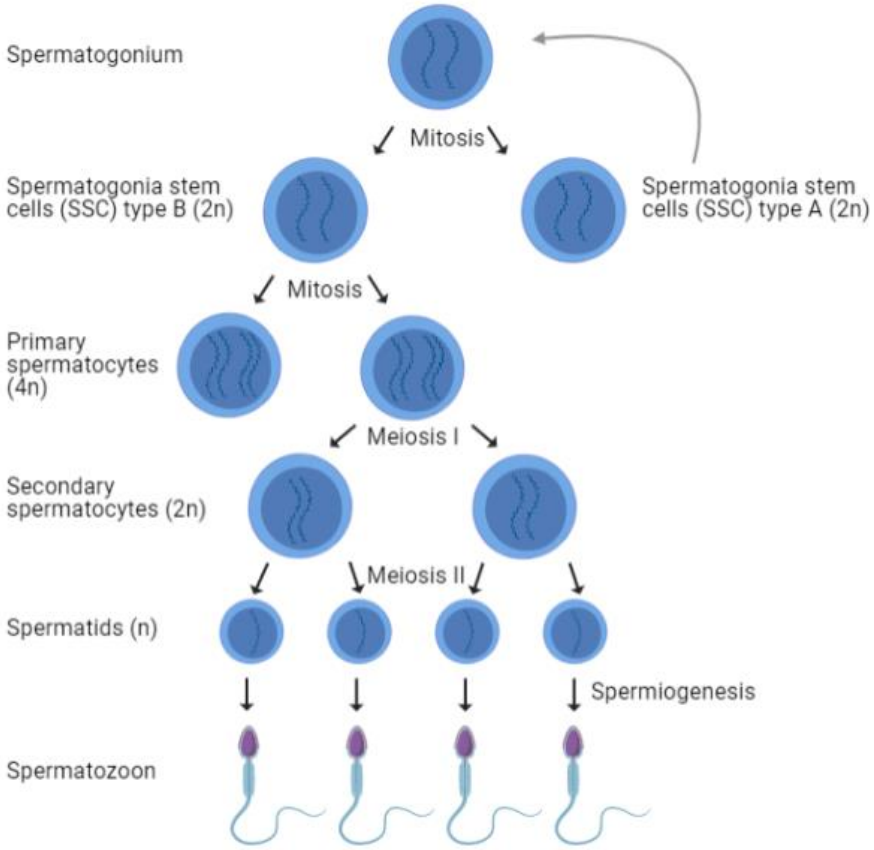

Figure 3 *Generation of mature spermatozoa through spermatogenesis.*
The divisions and differentiation under spermatogenesis generate fully differentiated spermatozoa from spermatogonium stem cells. Spermatogonium stem cells divide into spermatogonia type B that further divide and differentiate into primary spermatocytes. Through meiosis spermatids are generated and further mature into spermatozoa by spermiogenesis. Illustration created by the author using Biorender.com.

Spermiogenesis is the final part of spermatogenesis. In this process, large and round-shaped haploid spermatids differentiate into smaller and line-shaped spermatozoa (Fig. 3). A differentiated spermatozoon consists of a head connected to a midpiece and a tail (Fig. 4).

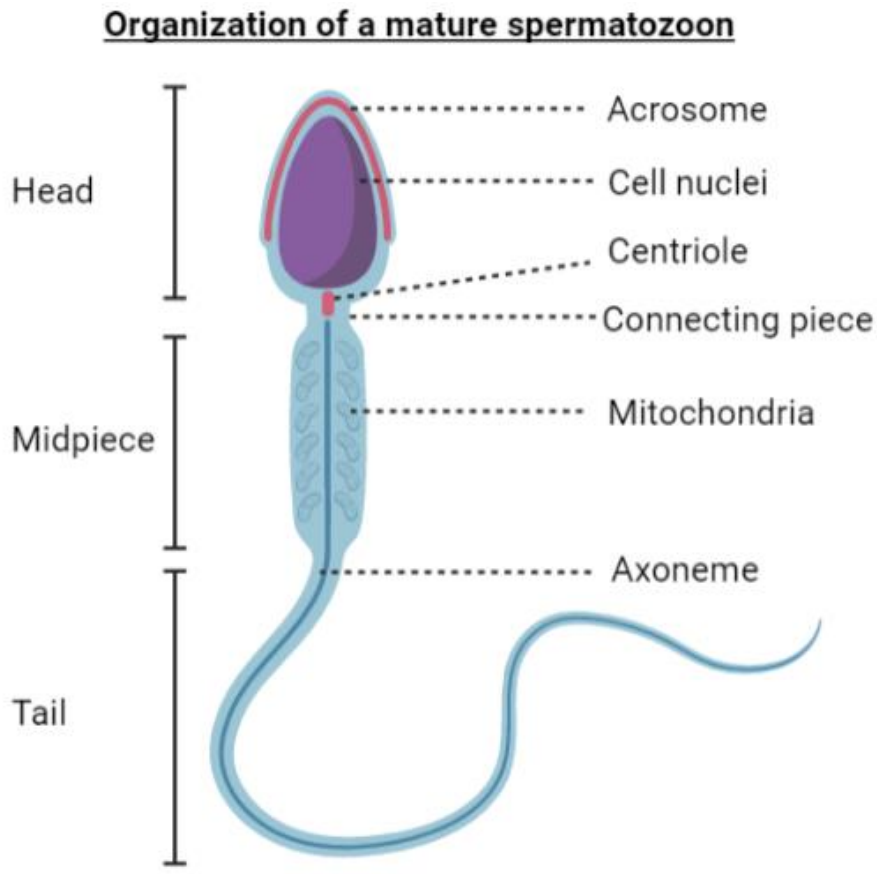

Figure 4 *Mature spermatozoon.*

A simplified figure of a mature spermatozoon consisting of a head, a midpiece and a tail. The head consists of the acrosome, located closely to the cell membrane, and the cell nucleus. The centriole is part of the connecting piece between the head and the midpiece. The midpiece contains mitochondria and the axoneme extending through the tail. Illustration created by the author using Biorender.com.

During spermiogenesis, the spermatids change the organization of their cellular compartments, forming the typical shape of a mature spermatozoon in addition to obtaining proper characteristics to achieve fertilization.

The head undergoes several arrangements. The shape of the nucleus changes, giving the typical oval-shaped head typically measuring between 4-5 µm long and around 3 µm wide (12). The volume of the head is mainly filled with the cell nucleus, containing the male haploid genome. The chromatin in the cell nucleus condensates during spermiogenesis (see below) (13). This chromatin condensation causes genome silencing and important processes for instance DNA repair in the cell are terminated (14).

The acrosome forms during spermiogenesis by lysosome vesicles generated from Golgi apparatus in the spermatid. These lysosome vesicles fuse and generate granules that forms the anterior region of the nucleus of a mature spermatozoon (Fig. 4) (15). The mature acrosome is divided into the inner membrane, the lumen and the outer membrane. The acrosome is important for the fertilization. First, the cell is capacitated so the acrosome and plasma membrane are destabilized. Then, proteins at the zona pellucida (oocyte) interacts with the outer membrane of the acrosome and trigger the acrosome reaction, where enzymatic contents in the acrosome are released to facilitate the penetration of the sperm into the oocyte (16).

Mitochondria in spermatids rearrange their organization, number and location during spermiogenesis, ending as a sheath surrounding the axoneme in the midpiece (Fig. 4). Mitochondria produce the energy for the spermatozoa's movements.

The tail of a mature spermatozoa is built up by a centriole, and an axoneme that performs the physical movement of the cell (Fig. 4). The tail of a spermatozoon is formed during spermiogenesis, by the elongate of the axoneme initiated by the centriole (17). The axoneme structure in the middle of a spermatozoon's tail contain microtubules using dynein to perform movement. The motility is initiated first after transport from seminiferous tubule to epididymis (18).

Mature spermatozoa exit the seminiferous tubules in the testes, and pass through the epididymis where they gain motility and are stored until ejaculation. During coitus, right before ejaculation, mature spermatozoa leave the testes though the contraction of epididymis and further pass through vas deferens where they blend with proteins, enzymes and fructose produced from the seminal vesicles. The mixture continues through the prostatic urethra where it associates with the secretions from the prostate gland before the resulting blending passes the bulbourethral gland to form the final semen. At the end, the semen is ejaculated through the external urethral opening (7).

The chromatin organization within the nucleus changes during spermiogenesis as mentioned above. This rearrangement provides spermatozoa with new characteristics that are important for further functions.

1.2.1.1 Chromatin reorganization during spermiogenesis

The chromatin organization in a mature spermatozoon is fundamentally different comparing to somatic cells. Before spermiogenesis, their deoxyribonucleic acid (DNA) is wrapped around histone proteins, which also are the fundamental proteins that wraps DNA in somatic cells as the first level of chromatin organization. Spermatozoa undergo hyper-compaction during spermiogenesis that enables DNA to be packed in a higher degree by using protamine proteins. A mature human spermatozoon has only around 15% of its DNA packed around histones (19) and failure in the histone to protamine replacement process may result in non-functional spermatozoa (20). The condensed chromatin structure is thought to stabilize the nucleus and to be essential to achieve normal fertilization (21). Protamines enables the DNA to be packed to a higher degree than histones (22). This is mainly due to the fact that histones fold DNA into coils containing approximately 100 bp nucleotides, while protamine proteins are estimated to fold 600 bp of DNA, avoiding supercoiling and therefore increasing the condensation of chromatin (23, 24).

When protamine proteins bind to DNA, intermolecular disulphide bridges are formed linking the protamines together, which stabilizes the whole chromatin structure (20). These bridges are formed by the withdraw of phosphor and the oxidation of cysteine residues occuring when phosphorylated protamine proteins bind to DNA (25).

DNA bound to protamines is further organized in protamine toroids (Fig. 6 A). The exact formation of this structure is unknown, but research indicates that protamine-bound DNA is coiled and generates protamine loop domains (26-28). It is estimated that one toroid can contain up to 60 kb of DNA and each spermatozoon contain up to 50 000 of these toroid's (29).

Each protamine toroid is linked to the spermatozoon's nuclear matrix by matrix attachment regions (MARs) (Fig. 6 B). The specific sequence of DNA attached to MAR is called toroid linker (Fig. 6 C). The knowledge on this linker is limited, but several sequence-specific sites on DNA appears to be frequently attached to the nuclear matrix, suggesting that the structural organization of DNA at these sites has an important function (30, 31). These regions have also a higher sensitivity to nuclease activity, indicating that DNA at these sites could be bound to histones (27).

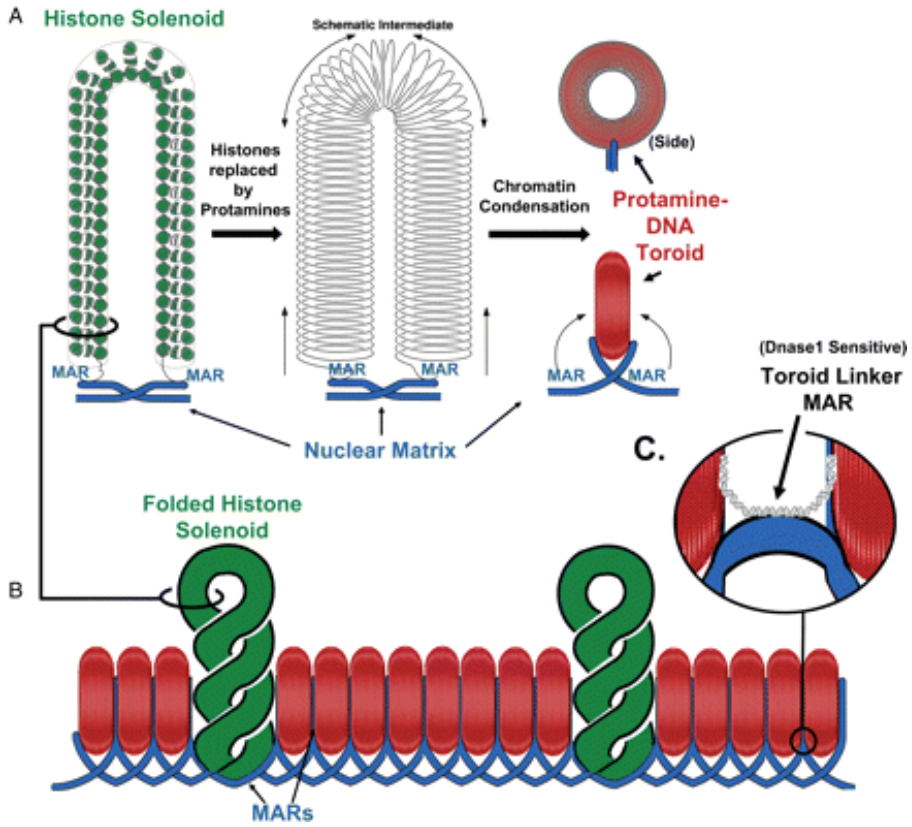

Figure 5 *Different levels of chromatin organization in spermatozoa (27).*
(A) Histone solenoid structures are present in the chromatin organization. The replacement of histones generates an intermediate structure before protamine toroid is established. (B) Potentially organization of protamine toroids and histone solenoid linked to nuclear matrix by matrix attachment regions (MARs). (C) Toroid linker is a DNA sequence that links each protamine toroid and histone solenoid together. Figure are used with permission from Molecular Human Reproduction.

1.2.3 Semen analysis

Semen analysis is a laboratory test performed when evaluating male fertility status. In some conditions, semen analysis can predict fertility, but in the majority of cases fertility is also related to female fertility which are not examined by a semen analysis (32). The standard evaluation of semen is done by examination of different parameters, including the cell concentration, motility, morphology, and vitality. Semen analysis is broadly used in fertility clinics and in research. All parameters are standardized by WHO through their laboratory manual for the examination and processing of human semen (12) (Table 1), making the results reliable, valid and useful for the functional status of the male reproductive organs. The last edition was published in 2010, but the 6th edition

was out for public review until the 9th of April 2021 indicating that a new edition will be published in the near future.

Table 1 *Standard semen parameters from table A1.1.in WHO laboratory manual for the examination and processing of human semen (12).*

Variable	**Lower reference limits**
Semen volume (mL)	1.5 (1.4-1.7)
Total sperm count (10^6/ejaculate)	39 (33-46)
Sperm concentration (10^6/mL)	15 (12-16)
Sperm progressive motility (A + B) (%)	32 (31-34)
Sperm morphology (%)	4 (3-4)
Vitality (% alive)	58 (55-63)

Approximately 15% of infertile patients have semen analysis results within the reference values from the 2010 WHO manual (33), questioning if more specific and optimal predictors of fertility are needed.

Studies show that infertile men have higher levels of DNA fragmentation compared to fertile men (34-38), however standard semen analysis does not include DNA fragmentation tests or assessment of sperm chromatin quality of any kind. The WHO laboratory manual edition from 2010 mention it as a paragraph under section of research procedures, but neither recommend nor acknowledge its utility value. The assessment of DNA fragmentation has been recommended by several profiled research groups when infertile males are examined, especially when deciding which fertility treatment should be proposed (6, 39-41). In that respect, the 2020 edition of the European Association of Urology (EAU) guidelines on sexual and reproductive health (42) recommends to assess the level of DNA fragmentation in sperm, for couples with unexplained infertility and/or experienced repeated pregnancy losses.

1.2.4 Male Infertility

Male infertility is caused by factors divided into congenital, acquired, and idiopathic factors. Congenital factors are genetic causes of male infertility, identified by sequencing or karyotyping of genomic material. Acquired factors make up over 40% (6) of the cases regarding infertility in men, with varicocele as the most recurrent factor (43). Acquired factors also includes tumours, infections, and systemic diseases. Idiopathic factors make up between 30-50% with no female factor involved. Male infertility caused by oxidative stress is one recurrent idiopathic factor affecting 37 million men worldwide (44).

To examine male infertility, semen analysis in addition to physical examination and reproductive and medical history search are performed. It has been notified that semen parameters under WHO lower reference limit alone are not enough to predict infertility, unless in men with highly impaired parameters such as azoospermia (no spermatozoa in the ejaculate) (32). In clinics, an additional semen sample is analysed if some parameters are under the lower reference limits (45, 46) due to natural within-man variation in semen parameters (47, 48). There are also known limitations with the use of WHO manual regarding different ethnic groups, biological variation and the accountability of female factor (49).

1.2.5 Assisted reproductive technology

Despite the reported controversies regarding reduced semen quality, two meta-analysis show a decline in total sperm count and sperm concentration (50, 51). Along with higher maternal (52, 53) and paternal age (54) when attempting to conceive, the demand and use of assisted reproduction technology (ART) have risen and are expected to further grow in the coming years (55-58).

Conventional in vitro fertilization (IVF) and intracytoplasmic sperm injection (ICSI) are among the most widely used ART procedures and both require the quality of the semen to be evaluated. This is especially important when determining which procedure should be performed, since ICSI will be favoured in case of low sperm quality (59).

1.3 DNA fragmentation

1.3.1 DNA fragmentation in spermatozoa

DNA damage is any change in the structure of the DNA, continuously in every cell every day. DNA damage can be induced by cellular or environmental factors (DNA damaging agents) and several types of DNA damages exist, including DNA fragmentation that contains single stranded breaks (SSBs) and double stranded breaks (DSBs). In somatic cells, DNA damage is often repaired by different DNA repair mechanisms. Such mechanisms are not present in differentiated spermatozoa leading to permanent damage if the fragmentation occurs before spermiogenesis and is not repaired, or after DNA replication prior spermiogenesis.

During spermiogenesis, topoisomerase induce nicks in the DNA when replacing histones with protamine proteins (60). These are normally temporary, but if nicks remain, permanent fragmentation will be present in the mature spermatozoa since the repair-machinery is terminated after spermatogenesis when transcription and translation stop. DNA fragmentation occurring after spermiogenesis are permanent and present in the ejaculated spermatozoa, making genomic damage vulnerable. In contrast, oocytes does not have this limitation, and can repair DNA damage in spermatozoa during fertilization (61). It is worth mentioning, that since females of advanced age has lower DNA repair capability in their oocytes, an injection of minimal DNA damaged spermatozoon could be beneficial (62).

The amount of DNA fragmentation in spermatozoa variates through the reproductive active lifespan, with higher incidence with advanced age (63). In spermatozoa, DNA fragmentation can come from intrinsic factors such as protamination failure, oxidative stress or cell apoptosis, extrinsic factors as lifestyle-related factors, varicocele, infections, radiations, or exposure to toxins or caused by several diseases (64). While SSBs are initiated mainly by oxidative damage DSBs are mainly generated from failure during protamination (65).

1.3.2 Sperm DNA fragmentation related to reproductive outcomes and fertility

DNA fragmentation in spermatozoa has been studied for a long time and increased amount of evidence from numerous studies shows that it influences reproductive clinical outcomes (66-69). It has been observed that increased DNA fragmentation in spermatozoa increase risk of prolonged time to pregnancy (34), spontaneous abortions (67, 70-72) and significantly reduced success rates in *in vivo* and *in vitro* fertilizations (35, 73-75). It is worth mentioning that DNA fragmentation is still a controversy, based on articles indicating that DNA fragmentation is not linked to reproductive outcomes (70, 76) – but overall, the connection between sperm DNA fragmentation and infertility in men has been strengthened by extensive research over the years (33, 77).

A review by Ribas-Maynou and Benet presents different reproductive effects depending on the type of sperm DNA fragmentation (65). While natural pregnancy achievement is negatively correlated with extensive SSBs (78), DSBs are suggested to generate lower implantation rates (79). This last study used a population of couples with recurrent miscarriages without female factor and found that the lower implantation rates were caused by delayed embryo development.

Sperm DNA fragmentation is also elevated in couples with unexplained infertility, consisting of approximately 30% of couples struggling with fertility. *Simon et al.* (2013) (80) reported that 84% of the men with unexplained infertility (n=147) had DNA fragmentation above threshold value for the particular method used, *Oleszczuk et. al* (2013) (38) reported 26% of the men with unexplained infertility (n=119) had higher DNA fragmentation than threshold for another method.

Taken these factors in consideration, in addition to the plausible detrimental effect that DNA fragmentation may have on fertilization, embryo development and success rates in ART procedures, the assessment of DNA fragmentation could have valuable insight on the male fertility.

1.3.3 Methods for assessing sperm DNA fragmentation

Several methods for detection of DNA fragmentation have been established in the past 40 years, since the first sperm DNA fragmentation method was published. These methods aim to determine the amount of DNA fragmentation in spermatozoa, presented as ratios, percentage, or events.

Three separate levels of chromatin organization can be detected by DNA fragmentation methods:

i) DNA at the toroid linker region containing MAR.
ii) Fibres of chromatin on the surface of protamines.
iii) Chromatin fibres inside the toroid.

DNA at toroid linker region is not well understood, but studies have shown a positive association between histone-bound DNA and nuclear matrix (31, 81). In animals, DNA at this region is more sensitive to DNase I treatments than DNA bound to protamine (26), supporting association mentioned above. DNA at the surface of protamine is bound completely to the protein, making enzyme-binding difficult. DNA inside the toroid will not be accessible as long the cell maintains a condensed chromatin structure.

The discrepancy in DNA damage results may be due to, at least partially, the use of different methods developed to examine DNA fragmentation in sperm (82, 83). Since several of them detect various regions of the chromatin structure, variation in the results are expected. There is still no clear clinical threshold for several of these methods, making data generated user dependent. Lack of strict standardization make them unreliable for precise and reproductive diagnostics.

Four of the most used DNA fragmentation tests are Sperm Chromatin Structure Assay (SCSA), Terminal deoxynucleotidyl transferase-mediated dUTP Nick End Labelling (TUNEL) assay, COMET assay and Sperm Chromatin Dispersion (SCD) assay. The methods differ in the way DNA damages are assessed (directly or indirectly), technique and strength properties (Table 2). To date, only two methods, SCSA and the TUNEL assay are fully standardized and widely used to assess DNA fragmentation in sperm.

Table 2 *Descriptions of the most common used assays for DNA fragmentation in spermatozoa.*

Assay	***Fragmentation assessment***	**Principle**	***Advantages***	***Disadvantages***

SCSA	Indirect	Measure susceptibility to DNA maturation when exposed to acid by acridine orange staining.	Standardized. Established thresholds. Time-effective. Sensitive. Reproducible. Accuracy.	Need a high number of cells (> 1 million). Expensive due also to a licensed software.
TUNEL assay	Direct	Single and double stranded DNA breaks are labelled with fluorescence dUTPs.	Standardized (flow cytometer based). Commercially kits. Time-effective. Sensitive. Reproducible. Accuracy.	Not established thresholds. Expensive (flow cytometer based).
COMET assay	Direct	Assay based on gel electrophoresis. Damaged DNA moves faster in the gel since the size is lower.	Affordable instrument. Sensitive.	Measure 50-200 cells each sample. Lacks established protocols. Inter-observer variability.
SCD assay	Indirect	Assay based on agarose gel. Nucleus spreads after denaturation, resulting in halos.	Inexpensive. Simple performance.	Measure 50-200 cells each sample. Inter-observer variability.
Abbreviations: SCSA – Sperm Chromatin Structure Assay. TUNEL - Terminal deoxynucleotidyl transferase-mediated fluorescein-dUTP Nick End Labelling. SCD – Sperm Chromatin Dispersion.				

1.3.3.1 SCSA

SCSA is the pioneer method in the field, established in 1980 (84). The method uses flow cytometer and acridine orange staining to distinguish spermatozoa with DNA fragmentation from normal spermatozoa. Only DNA with breaks can be pH- or heat-denatured due to its bounding to protamine proteins. More fragmentation produces

stronger signal. SCSA presents results as DNA fragmentation index (DFI) corresponding to the percentage of fragmented cells in the sample determined from a dot-plot showing fluorescence intensities. This method detects DNA breaks in the toroid linker regions, but research on mice indicates that also some DNA breaks in the protamine toroid can be detected since acridine orange is a small molecule (85).

1.3.3.2 TUNEL

TUNEL assay is based on the incorporation of labelled deoxyuridine triphosphate (dUTP) nucleotides by the DNA polymerase Terminal Deoxynucleotidyl Transferase (TdT) enzyme, which identifies free 3'hydroxyl (OH) groups. In theory, several modified dUTPs can be used, but 5-Bromo-2'-deoxyuridine 5'-Triphosphate (BrdUTP) is the most widely used. When BrdU is used as a tag, the newly incorporated dUTPs are further recognized by anti-BrdU antibody. The whole DNA is stained using PI and the results are presented by DFI, as in SCSA.

Compared to SCSA that is an indirect method, the TUNEL method labels directly the DNA break sites in the chromatin of a spermatozoon and the results can be obtained by using flow cytometer or fluorescence microscopy. Standard TUNEL assays do not open the chromatin structure, and the accessible DNA is therefore limited to DNA in the toroid linker region and regions accessible to TdT-enzyme. It is discussed that TdT may bind DNA at the surface of the toroids since it adds to free 3'OH ends only, but this is not determined (20). Discrepancies are found when comparing TUNEL with SCSA. Research by Chohan *et al.* (2006) (86) has found a strong correlation between these two methods, while *Henkel et al.* (2010) (87) argue that the methods reveal different types of damage making them incomparable.

Several TUNEL protocols and kits are available, thus thresholds allowing the separation between normal semen samples and samples with DNA damage correlated to male infertility are fluctuating. The new 6th edition of WHO manual for the examination and processing of human semen recommends that each laboratory set their own thresholds indicating that the inter-variability is high.

1.3.3.3 A new possible DNA fragmentation test: SensiTive Recognition of Individual DNA Ends (STRIDE)

Within male reproductive medicine, a more versatile method for direct, sensitive and specific detection of DNA fragmentation is needed. A recent study published in Nucleic Acids from *Kordon et al.* (2020) (88) present a new quantitively, *in situ* method which detects DNA breaks in a highly specific and sensitive manner that potentially could be optimized for assessment in spermatozoa: SensiTive Recognition of Individual DNA Ends (STRIDE).

STRIDE is based on the incorporation of labelled nucleotides at DNA break sites (Fig. 6). Proximity ligation assay (PLA) are further used to enhance signals that are visible under a fluorescence microscope. PLA yields a high sensitivity and specificity, and a fluorescence microscope is cheaper than a flow cytometer.

PLA reaction uses two PLA probes (plus and minus) that binds labelled primary antibodies that are specific for the incorporated nucleotides at break sites. As both probes must bind nearby nucleotides to achieve further signals, unspecific background is theoretically eliminated. The oligonucleotides from nearby probes are further ligated, and hybridize, and PCR is performed to amplify circular DNA. Fluorescence-labelled oligonucleotide probes binds to amplified circular DNA, resulting in clear bright spots in microscope (89).

Depending on the type of DNA break site to detect, two different approaches are used. Double strand breaks are detected by dSTRIDE using TdT enzyme like the TUNEL assay but are assumed to have a higher sensitivity thanks to the PLA procedure (88). dSTRIDE will detect free 3'OH-ends suited for double-strand DNA breaks. Single strand breaks are detected by sSTRIDE using the principle of *in situ* nick translation (NT). Here, DNA polymerase I from *E. coli* incorporate biotinylated nucleotides for detecting both 3'-5' and 5'-3' single stranded nicks on the DNA strand.

Overall, STRIDE aim to detect individual DNA breaks and visualize them with a fluorescence microscope, yielding a high sensitivity. While other methods present results by % of DNA fragmented cells, STRIDE has the possibility to evaluate individual events single cells.

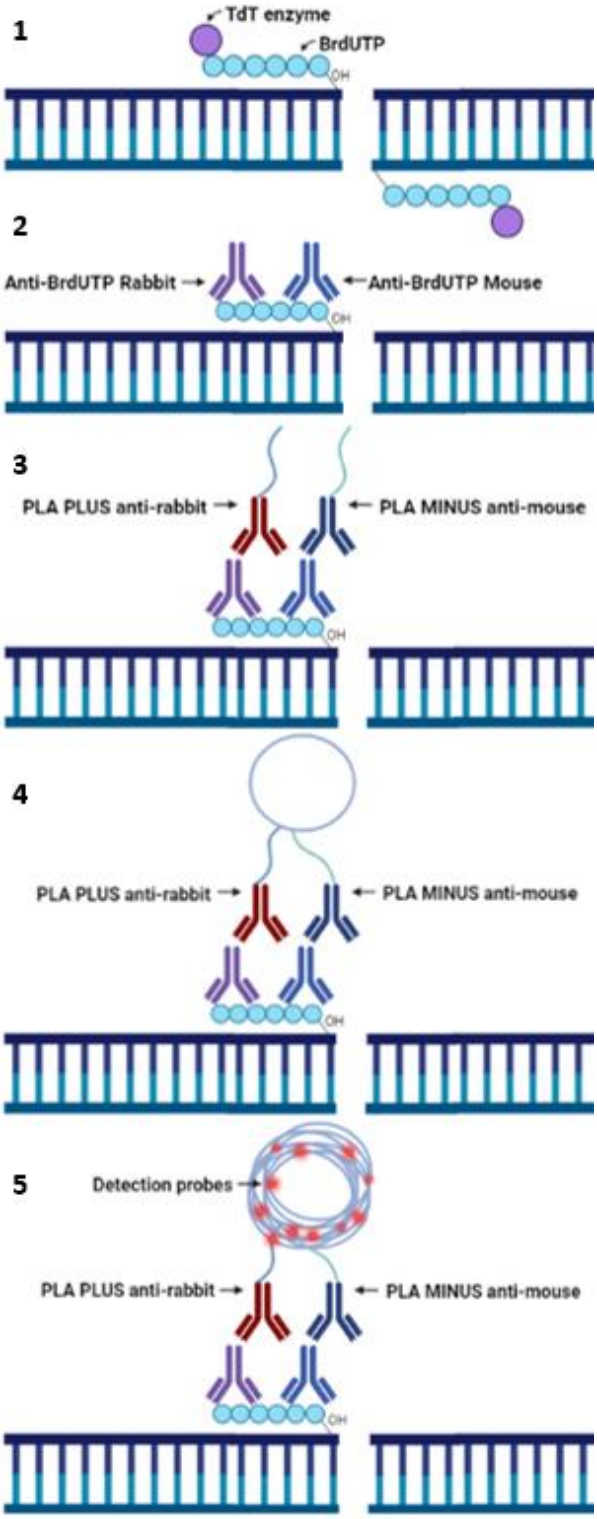

Figure 6 *Principle of dSTRIDE.*

(1) Incorporation of BrdUTP into DSBs generated by TdT-enzyme. (2) Cells are incubated with anti-BrdU antibodies from two different hosts, rabbit and mouse. (3) PLA probes, anti-rabbit and anti-mouse with conjugated nucleotides are then added to cells. (4) PLA probes that bound antibodies in near distance hybridize and ligate. (5) Amplification of the sequence are initiated by DNA polymerase I and detection probes are added. Fluorescence signals are made by detection probes and visualized in fluorescence microscopy. Illustration created by the author using Biorender.com.

1.4 Aim of study

The role of DNA fragmentation in male fertility is increasingly accepted but remains source of controversy. This can, at least partially, be explained by a major lack of standardisation in methods used for measuring DNA fragmentation in spermatozoa. STRIDE is a microscopy-based method that was recently developed to detect double strand (dSTRIDE) and single strand (sSTRIDE) DNA breaks *in situ* (88). Its high sensitivity and specificity make STRIDE a promising, reliable, and powerful alternative to the current methods to assess DNA fragmentation in spermatozoa. However, its establishment and optimization for this cell type has not been achieved yet, and therefore the overall aim is to establish dSTRIDE and sSTRIDE protocols suited for the male gametes. The first goal is to reproduce sSTRIDE and dSTRIDE in a cell line. Another aim of this project is to compare STRIDE results in semen samples with known DNA fragmentation. It is expected that the new protocols emerging from this work will be used to answer critical and yet unanswered questions about male fertility.

2. Methods and materials

Before establishing dSTRIDE and sSTRIDE protocols in spermatozoa, the method was verified using a somatic cell line in preliminary experiments to test if results were similar to what was published by *Kordon et al*. (2020) (88). The protocol where then tried out in spermatozoa before optimization especially for these cells.

All instruments, reagents and solutions used in these methods are listed in appendix A3. Materials and solutions.

2.1 MCF-7 cell line

Michigan Cancer Foundation-7 (MCF-7) human adenocarcinoma cells were cultured in Nunc™ EasYFlask™ 75 cm^2 flasks (Thermo Scientific) as monolayers, in Dulbecco's Modified Eagle Medium (DMEM) (Sigma-Aldrich) supplemented with 10% (v/v) fetal bovine serum (FBS) (Sigma-Aldrich) and 1% (v/v) PenStrep containing penicillin and streptomycin (Gibco) at 37°C in a humidified incubator with 5% CO_2. The medium was changed every 2-3 days and cells were passaged when reaching approximately 90% confluence. For each passage, cells were washed with 10 mL of room temperature

1XPhosphate Buffered Saline (PBS) (Sigma-Aldrich) before incubation with 1.5 mL of pre-warmed 0.25% Trypsin-Ethylenediaminetetraacetic acid (EDTA) (Gibco) at 37°C for 3-4 minutes until they detach. Detachment of the cells was monitored using an inverted phase-contrast microscope (Motic AE31 with ELWD condenser N.A 0.30), and the action of trypsin-EDTA was neutralized by adding 8.5 mL of complete growth media prewarmed at 37°C. For regular maintenance, 2 mL (1/5) of the 10 mL cell suspension was transferred into a new flask containing 11 mL of complete growth medium. Cell maintenance was performed in laminar flow cabinet.

2.1.1 Cell counting and seeding

For STRIDE and immunofluorescence experiments, cells were counted using an Invitrogen ™ Countess ™ Automated Cell Counter (Invitrogen). This automated cell counter use cell-uptake of trypan blue to differentiate between live and dead cells (90). Trypan blue diffuses through membranes of dead cells due to their permeability showing a uniform blue colour, while alive cells do not take up the dye and is bright with only dark edges in the outer circle of the cells. The instrument automatically counts four (1 mm^2, 0.1mm^3) squares in a manual haemocytometer (90).

For this, 15 µL of cell suspension after detachment by trypsinization was mixed with the same volume of 0.4% trypan blue (Invitrogen) staining solution in a 1.5 mL tube. 10 µL of the resulting solution was loaded onto a Countess ™ cell counting chamber slide (Invitrogen) before insertion in the instrument. As a result, the main screen presents the total, live and dead concentration and viability (%). A volume equivalent to 1x10^5 live cells were seeded onto 12 mm diameter, round glass coverslips (VWR) placed in 24-well plates (Nunclon ™ Delta Surface, Thermo Fisher) with 500 µL culture medium 24 hours before further experiments at 37°C in a cell culture incubator with 5% CO_2.

2.1.2 Cell thawing

MCF-7 cells were earlier cryopreserved at OsloMet and stored in nitrogen tank. The thawing protocol was executed in laminar flow cabinet. MCF-7 cells were quickly thawed in a 37°C water bath and transferred to a 15 mL tube (Sarstedt) with 8 mL pre-warmed growth medium and centrifuged at 1000 rpm for 5 minutes (Rotofix 32, Hettich

Zentrifugen). After centrifugation, the supernatant was removed, and 2 mL of growth medium was added to resuspend the cell pellet. Resuspended solution was transferred to a Nunc™ EasYFlask™ 25 cm^2 flask with additional 3 mL growth medium and placed at 37°C in a cell culture incubator with 5% CO_2.

2.1.3 Cryopreservation

Cryopreservation of MCF-7 was performed after the cells had achieved a stable phenotype and the procedure was executed in laminar flow cabinet. Growth medium was removed from Nunc™ EasYFlask™ 75cm^2 flask (Thermo Scientific) and cells were rinsed with 5 mL PBS. To detach cells, 1.5 mL of pre-warmed trypsin-EDTA was added to the cells and placed in incubator at 37°C with 5% CO_2 for 3-4 minutes. Detachment was observed under the inverted contrast-phase microscope. 5 mL of growth medium was applied into the flask to stop trypsinization and the whole suspension was transferred to a 15 mL tube (Sarstedt) and centrifugated at 1000 rpm for 5 minutes. After centrifugation, supernatant was removed, and cell pellet resuspended in 3.6 mL growth medium to achieve desired dilution, here approximately 2x10^6 cell/900 µL. Four cryo-tubes (VWR) were prepared and 900 µL of suspension was added to each tube before 100 µL of dimethyl sulfoxide (DMSO) (Merck Life Science) was added dropwise. Each cryotube was turned repeatedly upside down for mixing before placing them into a Styrofoam box with ice. Cells were transferred to a Cool Cell box and placed in freezer at -80°C. By placing cells in a Cool Cell box, cells are frozen at a controlled rate. After two days, cells were transferred from the freezer to a nitrogen tank at -196°C.

2.2 Semen sample collection

Approximately 30 semen samples obtained from FS were used for method establishment and optimization. Semen samples were produced for semen analysis after 3-5 days of sexual abstinence. Samples were stored at room temperature before analysis and transported in 15 mL tubes (Falcon) within a few hours after ejaculation. Results from the semen analysis were above and below the lower reference limit defined by WHO. Severe oligozoospermia samples (0-5x10^6 cells/mL) were excluded.

Two semen samples were submitted by anonymous participants after 3 days of sexual abstinence in relation to an undergoing method developing project. The samples were used for dSTRIDE and γH2AX immunofluorescence performance.

Semen samples were also obtained from biobank at OsloMet, related to an earlier project (91). Samples with known DFI (%) by SCSA (N=11) were chosen by supervisor and aliquots with cell concentration closely to $5x10^6$ cells were thawed.

2.3 Sperm preparation

Sperm preparation was performed to isolate spermatozoa from seminal plasma.

Liquefaction of the collected semen samples were achieved before further preparations by incubation for 30-60 minutes at 37°C (with and without rocker). This proteolytic process transforms gel-like coagulum to liquefied semen by components from seminal vesicle and prostatic fluid (92). Samples obtained from FS were usually liquefied upon arrival to OsloMet. For samples with delayed liquefaction, the tube was either repeatedly turned upside down or alternatively, an equal volume of room-tempered Sperm Preparation Medium™ (Origio) or PBS was added to the sample followed by pipetting to induce liquefying. For highly viscous samples, a 0.80 mm needle attached to a syringe was used by gently drawing up and down the sample 6-10 times as described in WHO laboratory manual under section 2.3.1.1 Delayed liquefaction (12).

The quality of each ejaculate was roughly assed by estimating the cell density and motility with a 40x objective (400x final magnification) mounted on a phase-contrast microscope (OLYMPUS CX31), using 5 µL of the liquefied sample onto a microscope slide. For semen samples with spermatozoa of high motility (swimming progressively straight-forward) and high density, swim-up protocol was performed.

2.3.1 Measurement of semen concentration

By assessing quality of each ejaculate, dilution rate was determined to measure the sperm concentration using an improved Neubauer haemocytometer. Dilution rate of 1:20 or 1:5 with trypan blue was in most cases sufficient.

The semen sample was mixed by vortex before aspirated by a positive displacement pipette and added into a 1.5 mL tube with trypan blue to achieve the appropriate dilution. The tubes were mixed by vortex for 15 seconds before 10 µL was applied under cover glass on the haemocytometer. The chamber was placed in a petri dish with a dampened filter paper functioning as a humidity chamber for 10 minutes before counting (Fig. 7).

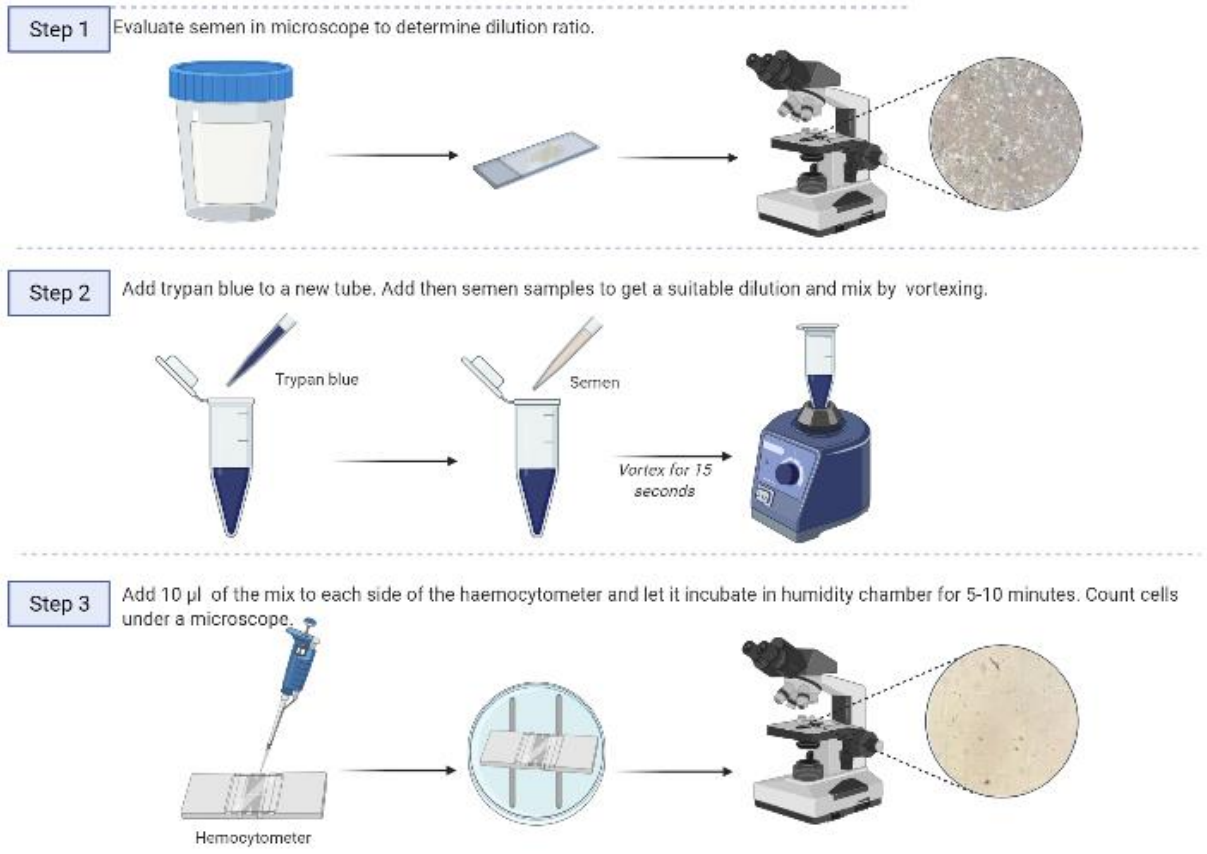

Figure 7 *Approach for cell concentration of spermatozoa in semen sample.*

Density of spermatozoa in semen was first evaluated to indicate a dilution rate, before trypan blue and semen were mixed by vortex for 15 seconds. 10 µL of mix was placed under the coverslip of each side in a haemocytometer for cell counting. Illustration created by the author using Biorender.com.

Spermatozoa were analysed at 200x or 400x magnification using microscope (OLYMPUS CX31). Counting procedure was performed following WHO Guidelines (12). A minimum of 200 spermatozoa or five squares (one row) of the central grid in the haemocytometer were counted in each slide for the calculation of concentration. If the number of cells in the central grid was too low, a lower dilution rate was used.

Alternatively, grid 4 and 6 could be counted. The differences between the two counting's shall not overcome 5% of the sum, if so, the counting was repeated.

To calculate the sperm concentration, the total number of cells counted on both sides *(N)* was divided by the total number of rows (*n*) used for counting the cells and multiplied with the *dilution factor*. The equation is listed below (1) and taken from WHO's manual (12). The sperm concentration is presented as 10^6/mL.

$$C = \frac{N}{n} * \frac{1}{20} * dilution\ factor \qquad (1)$$

2.3.2 Thawing and cryopreservation of spermatozoa

Frozen semen samples with known concentration were removed from -80°C freezer and thawed on ice for approximately 30 minutes before transferring volume corresponding to approximately 5x10^6 cells to a 15 mL conical tube (Falcon).

Cryopreservation of spermatozoa from leftover aliquots in samples received from FS was performed to preserve spermatozoa in cases cells were needed but could not be received. Spermatozoa were stored in liquid nitrogen (N_2) at -196°C. For this, a simple protocol using Sperm Freezing Medium™ (Origio) was performed (93).

Sperm Freezing Medium™ was brought to room temperature and added 1:1 (v/v) dropwise to a tube containing room-tempered semen sample. The tube was mixed carefully by vortex at speed 0.5 on a scale of 10 units after each drop of medium added. After the last drop, the tube was left on the bench for 20 minutes before aliquoted into cryo-tubes (VWR). The tubes were placed approximately 5-10 cm above the surface of liquid nitrogen inside a Styrofoam box with two reagent racks in it. After 30 minutes, the tubes were placed into the nitrogen tank at -196°C for storage.

For samples related to ongoing method-development project, a volume corresponding to 5x10^6 cells were placed in 1.5 mL tubes and immediately placed on ice before transferring samples to freezer at -80°C for storage.

2.3.3 Swim-up method for accumulation of motile sperm

Swim-up was performed to isolate motile sperm from immature and dead spermatozoa, non-sperm elements and seminal plasma in the ejaculate. Swim-up was performed by adding 1 mL of semen sample to a 15 mL tube, before gently adding 2

mL of Sperm Preparation Medium on top by holding the tube tilted. The tube was then placed tilted in a humidified environment at 37˚C for 1 hour. Sperm Preparation medium contains bicarbonate and resemble in vivo conditions, suitable for stimulation of motility. Motile spermatozoa swim up to the Sperm Preparation Medium, while immotile and dead sperm cells were left at the bottom of the tube. After 1 hour, the upper layer was pipetted from the tube hold with a ca. 45° angle and transferred into a new tube. 15 µL was used for cell counting while the rest was centrifuged at 400 x $\boldsymbol{g}$ for 10 minutes at 22°C. The supernatant was discarded, and the cell pellet resuspended in PBS.

For separating spermatozoa not prepared by swim-up, volume equivalent to $5x10^6$ cells were placed in a 15 mL conical bottom tube (Falcon) and mixed with 500 µL PBS (or Sperm Preparation Medium™). The tube was centrifuged using a swing-out rotor centrifuge (Eppendorf Centrifuge 5810 R) to avoid the cell pellet to be spread over a large area of the tube. Centrifugations were performed at 400 x $\boldsymbol{g}$ for 10 minutes, at 4°C. This was repeated two times as washing steps to remove seminal fluid. A low centrifugation force is preferred so as less damage to the cells are generated (94), while 10 minutes were used to achieve well-defined pellets and to minimize cell loss from each centrifugation.

2.3.4 Decondensation of sperm chromatin

To get access to the highly condensed chromatin-structure in spermatozoa, cells were treated to mimic decondensation as in fertilization. The decondensation protocol was based on *Antonucci, N et. al* (2013) (95) with adjustment due to cell concentration and timeframe. Decondensation was performed both in tubes and on coverslips.

Cells in tubes (following from 2.3.3) were washed once with 500 µL 0.5% bovine serum albumin (BSA) (Sigma-Aldrich) in PBS at 400 x $\boldsymbol{g}$ for 10 minutes at 4°C. Pre-fixation was achieved by resuspending the cell pellet with 500 µL 0.5% paraformaldehyde (PFA) (Thermo Scientific) and placing the 15 mL Falcon tube on ice in the dark at orbital shaker. After 10 minutes, 500 µL 0.5% BSA was added to the tube and centrifuged. This was repeated once to remove all fixation reagent. A decondensation solution for $4x10^6$ cells were made containing 1182 µL 0.1% Tx-100 (Sigma-Aldrich) in PBS, 12 µL of heparin (Merck Life Science) corresponding to 60 Units (10 000 U/mL) and 6 µL of 1 M dithiothreitol (DTT) (Merck Life Science) to achieve 5 mM concentration

in solution. Cell pellet was resuspended in 1200 µL of decondensation solution and placed in a humidified environment at 25°C for 20 minutes in the dark. After incubation with decondensation solution, tubes where centrifuged three times with 500 µL PBS to remove all reagents.

Spermatozoa attached to coverslips were rinsed for 5 minutes with 1 mL 0.5% BSA in PBS before decondensation treatment. For the experiment, spermatozoa were stabilized with 400 µL 0.5% PFA in PBS on ice in the dark at orbital shaker, followed by two washes with 1 mL 0.5 % BSA for 5 minutes each at orbital shaker. The decondensation-solution was made of 197 µL 0.1% Tx-100, 2 µL heparin and 1 µL of 1 M DTT for each well and spermatozoa were incubated at 25 ˚C for 15 minutes in the dark. Decondensed cells on coverslips were rinsed in 1 mL PBS for 2 minutes.

2.3.5 Fixation

After last wash with PBS, the pellet was resuspended well in 30% (v/v) PBS, before adding 70% (v/v) of pure ethanol (-20°C) dropwise while the tube was placed on vortex (Vortex Genie 2) at speed 0.5 on a scale of 10 units. This was done carefully since possible agglutination of spermatozoa which is difficult to work with later, could occur. The fixation was performed within minutes on ice or stored at -20°C for longer period if feasible.

For spermatozoa attached to coverslips, 1 mL of 70% ethanol (-20°C) was added in the wells and stored at -20°C freezer overnight.

2.4 Attachment of spermatozoa on poly-L-lysine coated coverslips

For analysis of DNA breaks in spermatozoa, sperm cells were attached to coverslips pre-coated with poly-L-lysine. A variety of cell concentrations for applying cells on coverslips were evaluated for optimization (see Table 3 in result section 3.2.1).

For pre-coating, a volume of 300 µL 0.1% (w/v) poly-L-lysine solution in H_2O (Sigma-Aldrich) was added to round coverslips in 24-well plates (Nunclon ™ Delta Surface, Thermo Fisher). Right before applying spermatozoa, coverslips were sequentially dipped in water and PBS for one second and placed on parafilm.

For immunofluorescence experiments, 15 µL of spermatozoa ($1x10^6$) resuspended in PBS were applied onto pre-coated wet coverslips. For dSTRIDE experiments, after the last rinse after BrdU-incorporation, cells were resuspended in 15 µL PBS, added onto pre-coated wet coverslips and let to dry out completely.

2.5 Induction of DNA fragmentation in MCF-7 cells and spermatozoa

To induce DNA breaks, cells were exposed to ultraviolet (UV) light or hydrogen peroxide (H_2O_2).

For MCF-7 cells, $1x10^5$ cells were seeded 24 hours prior exposure to DNA-damaging agents onto 12mm diameter, round glass coverslips (VWR) placed in a 24-well plate with 500 µL growth medium at 37°C in a humidified environment with 5% CO_2.

2.5.1 Exposure to UV

MCF-7 cells growing on coverslips on 24-well plates were placed inside a laminar flow cabinet. Right before UV exposure, the culture medium was replaced with 500 µL of PBS and the lid from the plate was removed. Irradiation of the cells was performed in the laminar flow cabinet using the UV lamp inside the latter. The plate containing the cells was placed approximately 54 cm from the lamp, and the cells were irradiated for one or three minutes. Cells were then fixated with fixative. For STRIDE, cells were fixed with 70% ethanol at -20˚C overnight. For immunofluorescence experiments, three different fixatives were used: ethanol as for dSTRIDE, methanol at -20˚C for approximately six minutes or 3% PFA for 13 minutes at room temperature.

For spermatozoa, two approaches were used. First, spermatozoa applied onto pre-coated coverslips were placed on top of a plate and exposed to UV for 2, 5 or 10 minutes in the same manner as for MCF-7 cells. The coverslips were then put on parafilm to dry before further treatment. In the second approach, a volume corresponding to $5x10^6$ cells were washed with PBS as described in section 2.3.3, dissolved in PBS to a total volume of 1 mL and placed in a petri dish. The petri dish was placed under the UV-lamp for 10 minutes before further preparation and fixation.

2.5.2 Incubation with H_2O_2

MCF-7 cells growing on coverslips in 24-well plates were placed inside a laminar flow cabinet. Immediately before exposure to H_2O_2, cell media was removed and replaced with DMEM without FBS and antibiotics for a quick wash. Cells were then incubated 30 or 60 minutes at 37°C with DMEM supplied with 4 mM or 20 mM of H_2O_2 diluted from a 30% (v/v) solution (Apotektjenesten AS). After incubation, cells were quickly washed with PBS before fixation with -20°C 70% ethanol overnight.

For spermatozoa, H_2O_2 diluted in Sperm Preparation Medium™ in a total volume of 1 mL was added to the cell pellet containing $5x10^6$ cells for 2 hours at 37°C in a humidified environment. Concentrations of H_2O_2 used in these experiments were 0, 10, 40, 100 and 200 mM diluted from the 30% (v/v) solution. After incubation, cells were centrifuged at 400 x ***g*** for 10 minutes at 4°C before decondensation protocol and further experiments.

2.6 Immunofluorescence

Immunofluorescence experiments to detect and visualize phosphorylated (Ser139) H2AX in MCF-7 cells and spermatozoa were performed to confirm the presence of DNA breaks. Nearby molecules of H2AX become phosphorylated at Ser139 when DSBs occurs (96), making γH2AX complex one of the first protein accumulating at DSB sites during the DNA damage repair process in somatic cells.

For MCF-7 cells, $1x10^5$ cells were seeded 24 hours prior experiment onto coverslips placed in a 24-well plate with 500 µL growth medium at 37°C in a humidified environment with 5% CO_2. Right before fixation, the plate was taken out from the incubator and placed in a laminar flow cabinet. Growth medium was replaced with 500 µL pre-warmed PBS (37°C) to remove reagents. Plate was immediately transferred on bench, PBS removed and 1 mL of 70% ethanol (- 20°C) was added to the wells and placed at - 20°C overnight. After fixation, cells on coverslips were washed three times with 1 mL PBS for 5 minutes on orbital shaker.

For spermatozoa, cells were either attached to pre-coated poly-L-lysine coverslips after isolating cells from seminal fluid (see section 2.3.3), after decondensation (see section 2.3.4) or after washes following fixation (see section 2.3.5).

Spermatozoa on coverslips were incubated in 1 mL of the blocking solution containing 2 % BSA, 0.01 % Tween 20 and 0.1 % Triton X-100 in PBS (PBST-BSA-Tx100) for 30 minutes. For immunodetection, cells were sequentially labelled with 35 µL anti-phospho-histone (Ser139) H2AX (1:100, Millipore) as primary antibody and 35 µL Cy3-conjugated AffiniPure Donkey Anti-Mouse IgG (H+L) (1:200, Jackson ImmunoResearch) as secondary antibody. Antibodies were diluted in PBS containing 2% BSA and 0.01% Tween 20 (PBST-BSA). For each antibody, coverslips with cells were incubated upside-down on parafilm for 45 minutes. Between antibody incubations, cells were washed 3 times with PBST-BSA for 5 minutes. After incubation with the secondary antibodies, cells were washed 3 times in PBS for 5 minutes each before DNA was labelled for 5 minutes with 500 µL 4',6-Diamidino-2-Phenylindole (DAPI) (50mg/mL) diluted in PBS. The coverslips were further mounted on glass slides (Thermo Scientific) using a Mowiol 4-88 (Sigma-Aldrich) based mounting medium.

2.7 dSTRIDE

The dSTRIDE protocol is based on direct targeting at DSB sites and contains two major parts: incorporation of nucleotides with immunodetection and PLA for enhancement of signals.

Incorporation of nucleotides are initiated by TdT-enzyme, and nucleotides incorporated are conjugated to 5-Bromo-2'-deoxyuridine (BrdU). The kit used for BrdUTP incorporation are APO-BrdU™ TUNEL Assay Kit (Thermo Fisher). Since this initial step is performed different by two approaches, they will be described separated.

2.7.1 BrdU incorporation into MCF-7 and spermatozoa growing on coverslips

Cells in 70% ethanol (kept at -20°C) were washed two times with 1 mL of PBS containing 10 mM EDTA (PBS-EDTA), then once with 1 mL of washing buffer from the same APO-BrdU™ TUNEL Assay Kit for 5 minutes at room temperature. BrdU was incorporated at DSB sites by TdT enzyme for 1 hour at 37 °C in a humidified environment following the manufacturer's instructions. TdT was added to BrdU-solution right before use. The volume of the reaction solution was adjusted to 35 µL for each coverslip, placed upside-down on a parafilm for incubation. After two washes under hard shaking on an orbital shaker with 1 mL of rinsing buffer from the kit, cells

were incubated in 1 mL PBST-BSA for 30 minutes at room temperature for blocking. Hard shaking was implemented to remove excess BrdU from the coverslips.

2.7.2 BrdU incorporation into spermatozoa in tubes

After fixation, 500 µL of PBS were added to the tubes containing spermatozoa in 70% ethanol (kept at-20°C). The tubes were centrifuged at 800 x ***g*** for 5 min at 4°C and the spermatozoa washed one time with 500 µL of PBS following the same centrifugation procedure. Another wash was performed in the same way using 500 µL of washing buffer from the kit.

Spermatozoa were resuspended in 50 µL of the BrdU-solution and incubated at 37°C for 1 hour. The reaction solution was made following the manufacturer's instructions. After incubation, two washes with 500 µL rinse buffer from the kit were performed using centrifugations at 800 x ***g*** for 5 min, at 22°C. Following the last wash, cells were resuspended in 15 µL PBS and transferred onto coverslips. Air-dried coverslips where placed in a 24-well plate containing 1 mL PBST-BSA and incubated overnight at 4°C.

2.7.3 Immunodetection and signal amplification

For detection of BrdUTP, cells were first incubated with 35 µL of a primary antibody solution containing anti-BrdU antibodies (Abcam) produced in mouse (ab8039, 1:500) and rabbit (ab152095, 1:200) diluted in PBST-BSA, for 45 minutes at room temperature. Coverslips were put upside-down on a parafilm for incubation.

Enhanced fluorescence labelling of BrdU was further achieved following a PLA protocol, using Duolink™ In Situ Orange Starter Kit Mouse/Rabbit (Sigma-Aldrich) containing anti-mouse and anti-rabbit, oligonucleotide-labelled secondary antibodies (PLA probes). The procedure was performed according to the manufacturer's instructions. Specifically, all washes were performed at room temperature in 1 mL volume, and incubations with PLA probes, ligation and amplification were performed in 35 µL volume at 37°C in a humidified environment. Ligase and polymerase were added to the ligation- and amplification-solutions right before use. At the end, DNA was labelled with DAPI (50 mg/mL) diluted in washing buffer B from the kit for 5 minutes at room temperature. Coverslips were then mounted on glass slides with Mowiol-488 as for immunofluorescence (section 2.6).

2.8 sSTRIDE

The sSTRIDE protocol from *Kordon et al.* (2020) (88) was tested and optimized for in situ detection of SSBs in MCF-7 cells. sSTRIDE is based on incorporation of nucleotides at SSB sites and is divided into two major parts: incorporation of nucleotides conjugated to biotin with immunodetection and PLA. Incorporation is generated by DNA polymase I, with both 3'-5' and 5'-3' exonuclease activity, which enables nick-translation.

Briefly, after cell fixation with 70% ethanol (-20°C) cells were incubated sequentially with streptavidin and biotin using Endogenous Biotin-Blocking Kit (Invitrogen) to block biotin naturally present in cells. One drop of streptavidin was added on parafilm before coverslips were placed upside down on top and incubated at 37°C in a humidified environment for 30 minutes. Before incubation with biotin, cells were washed three times with PBS-EDTA for 30 seconds each. After 30 minutes incubation with biotin, cells were washed three times for 5 minutes each.

After three washes with PBS-EDTA, biotinylated and native nucleotides (Jena Bioscience, N6-(6-amino)hexyl-2'-deoxyadenosine-5'-triphosphate – Biotin (Biotin-7-dATP): NU-835BIO-S, Biotin-16-propargylamino-dCTP: NU-809-BIO16, biotin-16-5-aminoallyl-dUTP: NU-803-BIO16, dGTP. NU-1003) were incorporated in SSB sites using *E. coli* DNA polymerase I (BioLabs, M0209S) in NEBuffer (BioLabs, B7002S) for 15 minutes, at 37°C. A total volume of 38 µL solution was made for each coverslip (27.75 µL MQ H_2O, 4 µL reaction buffer, 2 µL each nucleotide and 0.25 µL DNA polymase I), and 35 µL used. Cells were subsequently washed twice with 500 µL PBS for 5 minutes, then placed in PBST-BSA and incubated for 30 minutes at room temperature.

For immunodetection of biotinylated nucleotides, monoclonal and polyclonal anti-biotin primary antibodies (abcam) from mouse (ab201341, 1:200) and rabbit (ab53494, 1:100) diluted in PBST-BSA were incubated with the cells at 37°C for 45 minutes in a humidified environment.

Enhanced fluorescence labelling of biotin was further achieved following the same PLA procedure as for dSTRIDE (section 2.7.3), with the same kit.

2.9 Evaluation of DNA fragmentation by microscopy

Two microscopes were used for the purpose of this master thesis. For all experiments related to method-development, a 2-D fluorescence microscope was used. Biased characteristics by images obtained from 2-D fluorescence microscopy can be fluorophores in out-of-focus planes that are registered at the detector plane, generating false positives. The total lateral resolution is reduced in this microscopy. To obtain reliable data for quantitative analyses, a 3-D fluorescence microscope with deconvolution from Department of Molecular Medicine, University of Oslo was used. By using this microscope, certain planes were extracted minimising false positives and the deconvolution improves resolution of images obtained.

2.9.1 2-D microscopy

Images taken in method-developing experiments were acquired with a 100x objective mounted on a widefield fluorescence microscope OLYMPUS BX40, equipped with a CMOS DP74 (Olympus) camera driven by the CellSens software (Olympus).

Cells were located by using the coarse wheel and focused by the fine wheel. The first image for each region was taken with DAPI filter (emits blue), then the same region was pictured by A594 filter (emits red). Images were stored in grayscale, 8-bit with pixel values from 0 – 255, where 0 is black and 255 is white. Every spot of the images has a value representing brightness of the pixel.

2.9.2 3-D microscopy

Images for quantification of DSBs obtained by dSTRIDE were taken with a 100x objective mounted on the widefield fluorescence microscope OLYMPUS IX71 fitted with a DeltaVision imaging station (GE Healthcare) driven by the SoftWoRx 6.5.2 software (GE Healthcare). Immersol^{TM} 518 F (Zeiss) was used as a mounting medium.

Within SoftWoRx 6.5.2, Resolve3D was used and parameters for acquisition were made. Excitation and emission wavelengths for BrdU/γH2AX (A594) and DAPI were selected. Percent of transmission was sat at 32% for A594 and 5 or 10% for DAPI. Exposure time was determined as close to 0.100 seconds (fluorescence intensity 2000

for A594 and 1000 for DAPI). Cell thickness (µm) (Z plane) was sat by determining the top (dX) and bottom (dY) of the cells.

Auxiliary magnification (1.6X) was used for some experiments to increase magnification and decrease working distance but is not essential for obtaining useful results. Since the field diameter for receiving images are highly decreased, auxiliary magnification was not further used.

For imaging, excitation shutter was opened, and a joystick at slow or medium speed was used to locate cells. Fine Z Focus wheel was used to move the objective to focus cells. Images were acquired into a series of images along the Z axis set by cell thickness and stored in grayscale at 16-bit with pixel values from 0 – 4096, where 0 is black and 4096 is white. Every spot of the images has a value representing brightness of the pixel.

2.10 Image processing program ImageJ

Image processing and analyses were performed using the free, open-source software Image J (National Institutes of Health).

Image J was used for cropping images, drawing scale bars and measuring the number of foci presenting DSBs in each nucleus. Number of DSBs in the nucleus of each cell were obtained by using the plugin Object Counter3D downloaded from ImageJ.net following the plugin's instructions (97).

The Deltavision workstation generates 16-bit images, but since we only wanted to detect a number of bright foci, images were transformed into 8-bit.

Z-projections were performed using maximum intensities across the z-stack to generate so called MAX projections. The resulting projections are 2-D images made from images originally obtained in 3-D (stacks).

For STRIDE analyses, we used hyperstacks allowing the visualisation of the z-stacks for the different fluorophores in sperate channel. For our experiments, two channels were chosen to visualise signals corresponding to BrdU and DAPI staining. Composite images were made to see both fluorophores at the same time, with DAPI in blue and BrdU in red. For each nucleus present in the hyperstack, cropped images corresponding to the red channel were extracted as squares and Object Counter3D was used to count the number of objects (foci). The intensity threshold was manually

set to make each foci recognized as an object and was always around the same value for all analysis (intensity level 135). After running the Object Counter3D a result table with intensity and other parameters was presented in addition to a particle window showing all objects counted presented as dots with numbers for quality check. The composite images were used to determine if any counted objects were outside the nucleus. The total number of objects in each nucleus was further written into an excel sheet.

2.11 Statistical analysis using SPSS and Prism

Image analysis that included identification and counting the number of DSBs in individual nuclei was performed using ImageJ '3D Objects Counter' plugin. Shapiro-Wilk was used to assess the normality of the distribution. Since the distribution of signals representing DSBs was skewed (≥ 2 x standard error and Shapiro-Wilk test, $p < .01$) data were presented as median and quartiles, IQ_3 and IQ_1. Tukey's fence method was used for outlier detection, which are values below $Q_1 – 1.5xIQR$ or above $Q_3 + 1.5xIQR$.

To visualize the distribution and the differences between experiments and treatments, scatter dot plots were used. Due to the skewed data, nonparametric Mann-Whitney U test was used to compare differences between treated and not treated cells, while Kruskal Wallis test between more than two different treatments/exposures. The level of statistical significance was set at .05. Simple regression analysis was performed to observe any relation between results obtained by dSTRIDE and SCSA, with a statistically significant level at .05. Statistical analyses were performed using IBM SPSS Statistics for Windows, version 26 (IBM Corp., Armonk, N.Y., USA) and GraphPad Prism Version 9.0.1 for Windows (GraphPad Software, San Diego, California USA).

2.12 Ethical considerations

This thesis was performed in compliance with all applicable laws relevant to this project: The Health Research Act (98), the Biotechnology Act (99) and the Act on ethics and integrity in Research (100). MCF-7 cells and spermatozoa were stored according to the Act relating to Biobanks (101) .

Guidelines from OsloMet – Oslo Metropolitan University (102), and the policy statement by the World Medical Association (WMA), the Declaration from Helsinki (103) were followed.

Semen samples for the establishment of the STRIDE method were anonymous and obtained from FS or by the research group. No personal data were processed and there was no risk, benefit, or consequences for the patients, hence there was no need of reporting the project to Data Protection Officer at OsloMet nor approval from REK.

Semen samples used for the assessing DNA breaks by the STRIDE method and comparing them with DNA fragmentation values obtained earlier by SCSA (91), were from the biobank established for the project “Betydningen av lipidmetabolisme for manlig reproduksjonsfunksjon” with REC no. 2010/2721 s-08220b. Data and samples from this project were anonymized in December 2017. Approval from The Regional Committees for Medical and Health Research Ethics (REC) and The Norwegian Directorate of Health are submitted in appendix A4. (Fig. 33 and 34).

3. Results

The result section is divided in three main parts: 1) preliminary results performed in the human breast cancer cell line MCF-7, 2) establishment and optimization of the STRIDE method in spermatozoa and 3) comparison of results obtained from dSTRIDE as a DNA fragmentation test.

STRIDE is a quantitative technique for *in situ* detection of DNA breaks. According to the authors of the original article presenting this method, the latter should result in “strong signal amplification and near-zero signal background in microscopy images where even individual DNA breaks are represented by bright, readily detectable fluorescence signals” (88). Before establishing the STRIDE method in male germ cells, the protocol from (88) was first verified and optimized in MCF-7 cells. Method descriptions was not precise nor reproducible and consequently, several experiments had to be done to accomplice suitable results.

3.1 Preliminary experiments with MCF-7 cells to verify STRIDE

In a first series of experiments, we wanted to test the STRIDE protocols as described in the original publication (88). Cell cultures offer a continuous refill of cells with similar characteristics over a long period of time (usually several weeks) so numerous experiments can be performed. The MCF-7 cell line was available at OsloMet in addition to be easy to work with, and is expected to contain DNA fragmentation, considering that they are cancer cells (104).

When following the original protocol for dSTRIDE (88), the first experiments resulted in unexpected background in MCF-7 cells (Fig 8). Speed on the orbital shaker was increased by two-fold during washing steps and implemented in the protocol to reduce background. The hard shaking led to less unspecific background around cell nuclei and signals in the nucleus were bright with high intensity (Fig. 8).

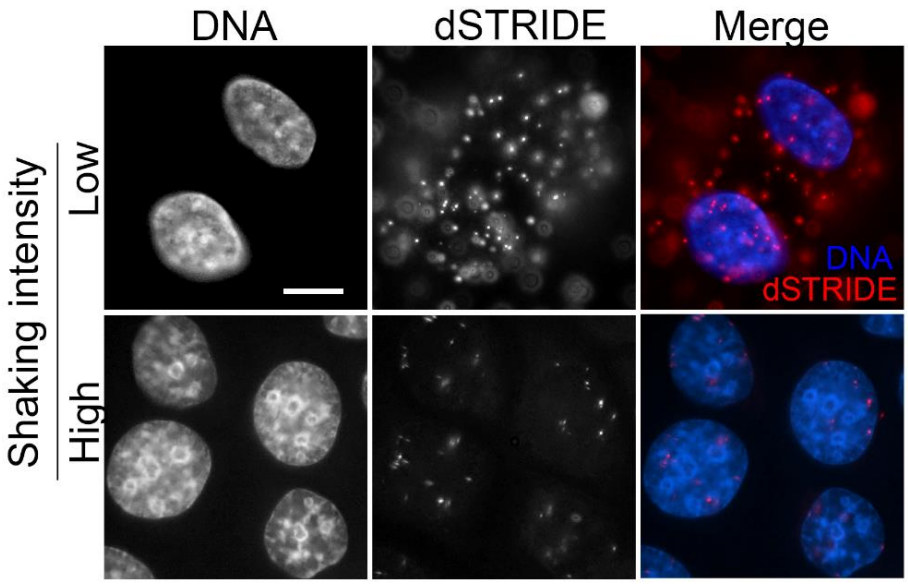

Figure 8 *dSTRIDE experiments in MCF-7 cells with low or high intensity of speed on orbital shaker during washing steps visualised by 2-D fluorescence microscopy.*
Nuclear DNA was counterstained with DAPI. Scale bar, 10 µm.

Initial experiments showed sSTRIDE signals within the nucleus and low background around the cell (Fig. 9 a). Signals were detected in close vicinity to but outside the nucleus, possibly due to primary antibody binding to biotin and not related to DNA breaks.

To evaluate the reliability of the method, an experiment with negative control, having no biotinylated nucleotides nor nucleotides applied to the biotin-incorporation step, was

performed. No difference between sSTRIDE signals in sample using biotinylated nucleotides (control) and sample without was observed (Fig. 9 b), suggesting that biotin naturally occurring in cells were detected, and that both blocking step and biotin-incorporation in these experiments were inadequate. In an attempt to reduce the unspecific binding of primary antibodies to biotin, we increased drop-size of streptavidin and biotin applied from the blocking kit and decided to change the reagent setup for biotin-incorporation. The incubation time was prolonged to 30 minutes, instead of 15 minutes described in the original article (88). No differences were observed (Fig. 9 c).

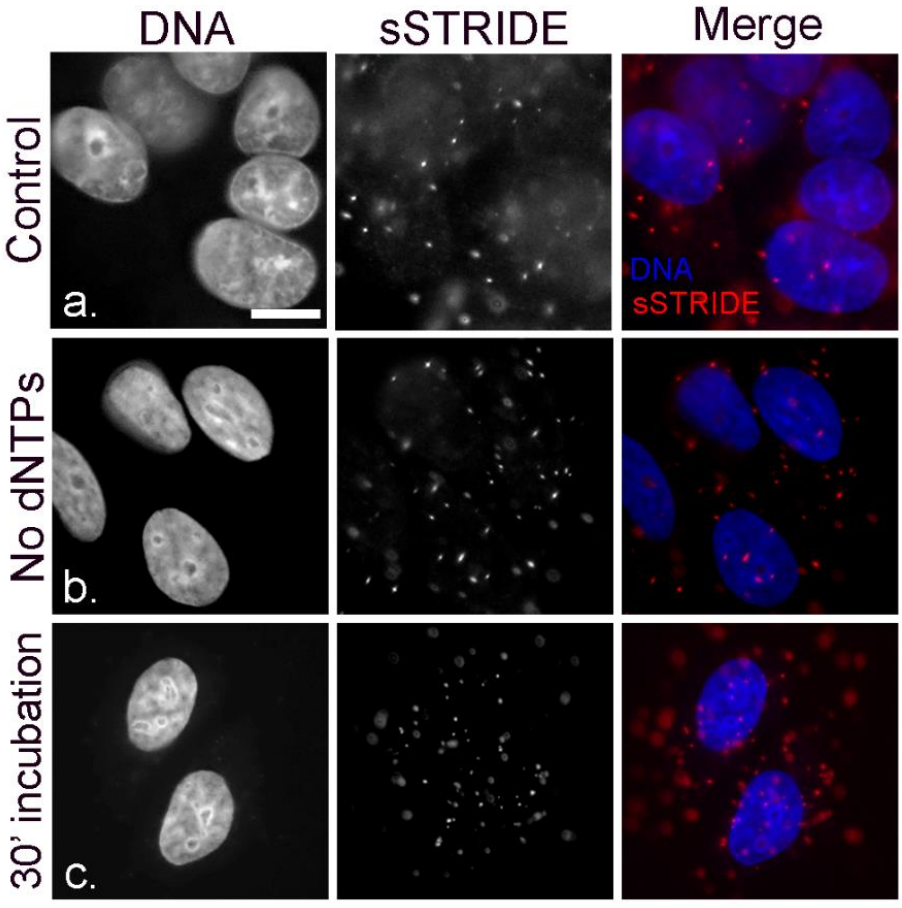

Figure 9 *Initial experiments of sSTRIDE in MCF-7 cells using 2-D fluorescence microscopy. MCF-7 cells were incubated with biotin for 15 min as described in original publication (88) (a) in the absence of biotinylated dNTPs (b) or 30 min (c) and single-stranded DNA breaks were detected by sSTRIDE. Nuclear DNA was counterstained with DAPI. Scale bar, 10 µm*

3.1.1 UVB irradiation showed more DNA breaks by dSTRIDE

Experimental data collected after performing a new method must be compared with acquainted, controlled and manipulated variable to evaluate its validity. In this context,

we used UVB and H_2O_2 as DNA damaging agents to induce DNA lesions and verify, indirectly, that the STRIDE signals detected in our previous experiments did actually correspond to DNA breaks. We reasoned that if signals corresponding to DNA breaks detected before treatment with DNA damaging agents, an increasing number of this signals should be detected after treatment.

To confirm the presence of DNA fragmentation, immunofluorescence experiments were performed using primary antibody against phosphorylated (Ser139) H2AX (γH2AX). γH2AX is an indirect biomarker for DSBs.

We observed more signals in MCF-7 cells exposed to UVB irradiation compared to non-irradiated cells (controls) by dSTRIDE (Fig. 10 a). Experiments were performed in triplicate with UVB irradiation for 1 minute or 3 minutes exposure time. Signals increased in a time-dependent manner and were observed by 2-D fluorescence microscopy. Each condition (1 or 3 minutes) had a waiting time before fixation of either 1 minute or 3 minutes and did not give differences in case of signals by visual evaluation in the microscope.

It was not detected an increased number of signals in cells exposed to irradiation when performing sSTRIDE experiment (Fig. 10 b). Signals were observed similar to control cells and to earlier experiments (Fig. 9), with bright signals inside and around nucleus.

An increased number of γH2AX signals were also observed in irradiated MCF-7 cells by immunofluorescence (Fig. 11). Results were similar to dSTRIDE, as anticipated since γH2AX and BrdU detect same type of DNA fragmentation.

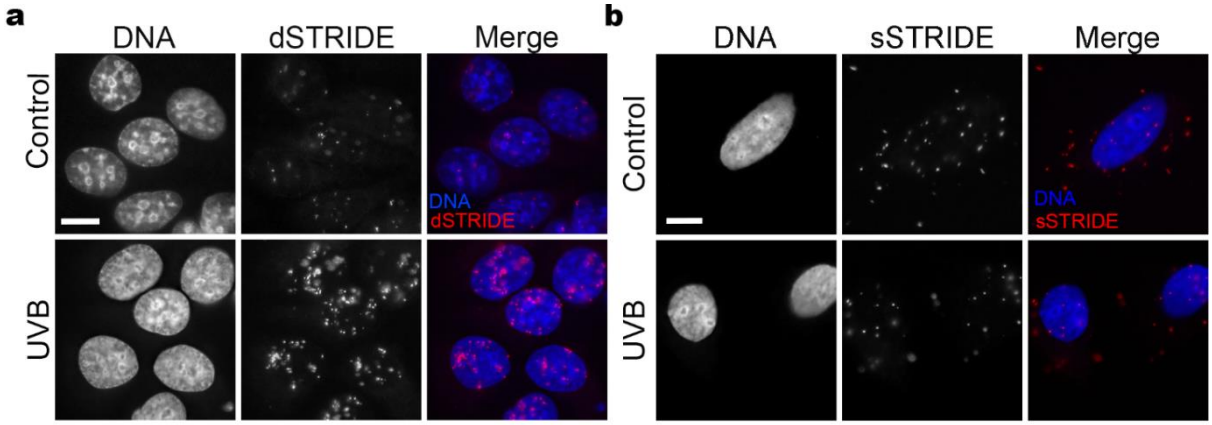

Figure 10 *DNA breaks induced by UVB irradiation of MCF-7 cells resulted in increased dSTRIDE but not sSTRIDE signals.*

MCF-7 cells were irradiated for 3 min and DNA breaks were detected by dSTRIDE (a) or sSTRIDE (b) using 2-D fluorescence microscopy. Non-irradiated cells were used as controls. Nuclear DNA was counterstained with DAPI. Scale bar, 10 µm.

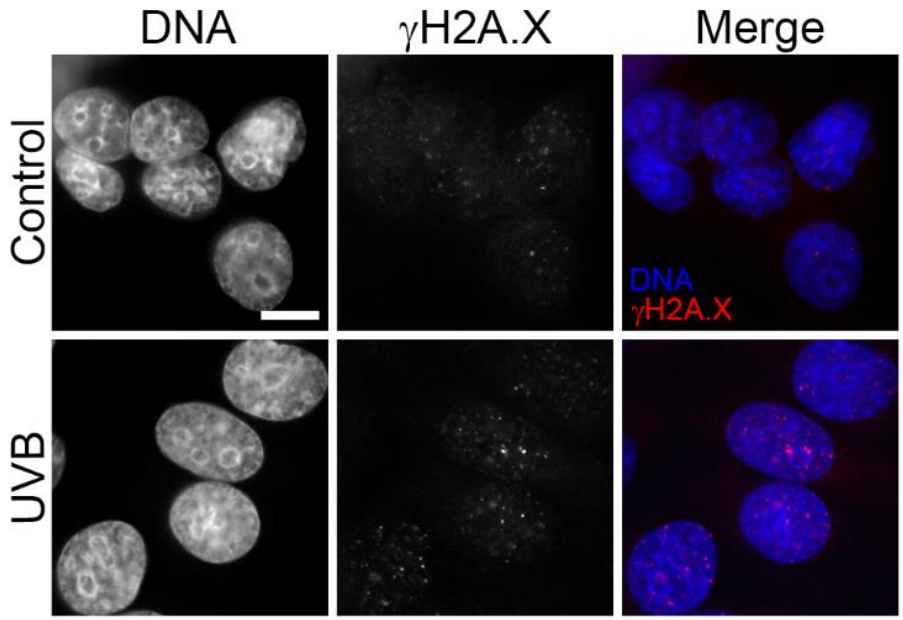

Figure 11 *Increased levels of γH2AX observed in MCF-7 cells by 2-D fluorescence microscopy after exposure to irradiation.*
MCF-7 cells were exposed to UVB irradiation for 3 minutes. Non-irradiated cells were used as control. Nuclear DNA was counterstained with DAPI. Scale bar, 10 µm.

Altogether, these results show that the protocol for dSTRIDE are valid and reliable for performance in MCF-7 cells. On the other hand, when testing our sSTRIDE protocol in these cells after irradiation, it was not observed any differences compared to control cells (Fig. 10 b), and the amount of alleged specific SSBs was not as anticipated. As a conclusion, the sSTRIDE protocol we followed according to descriptions from original article (88) did not work and it was decided to not continue with it.

3.1.2 Hydrogen peroxide induced DNA fragmentation in MCF-7 cells

To confirm the specificity of the dSTRIDE signals and evaluate the sensitivity of the method, we induced DNA breaks in MCF-7 cells using H_2O_2, reagent known to induce DNA fragmentation by initiating oxidative stress (105).

MCF-7 cells were incubated with 4 mM H_2O_2 for 30 minutes or 20 mM H_2O_2 for either 30 minutes or 60 minutes. The experiment was performed in triplicate but only one obtained quantitative result with 3-D microscopy. Cells treated with H_2O_2 and control cells were then submitted to immunofluorescence to detect γH2AX and by optimized dSTRIDE protocol.

As expected, H_2O_2 treated cells showed an increased number of signals compared to control cells (Fig. 12, Fig. 13 a). There was a clear difference between each condition. The highest number of dSTRIDE and γH2AX foci was observed in cells treated with 20 mM H_2O_2 for 60 minutes and an intermediate level of signals was observed in cells treated with 20 mM H_2O_2 for 30 minutes. An increased number of foci was roughly observed in 4 mM H_2O_2 with some variations (Fig. 12, 13 a) compared to the lowest number of dSTRIDE and γH2AX signals observed in control cells. For the cells treated with 20 mM H_2O_2, a visible amount of cell loss was observed under the microscope, indicating that cells detach after such damaging treatment.

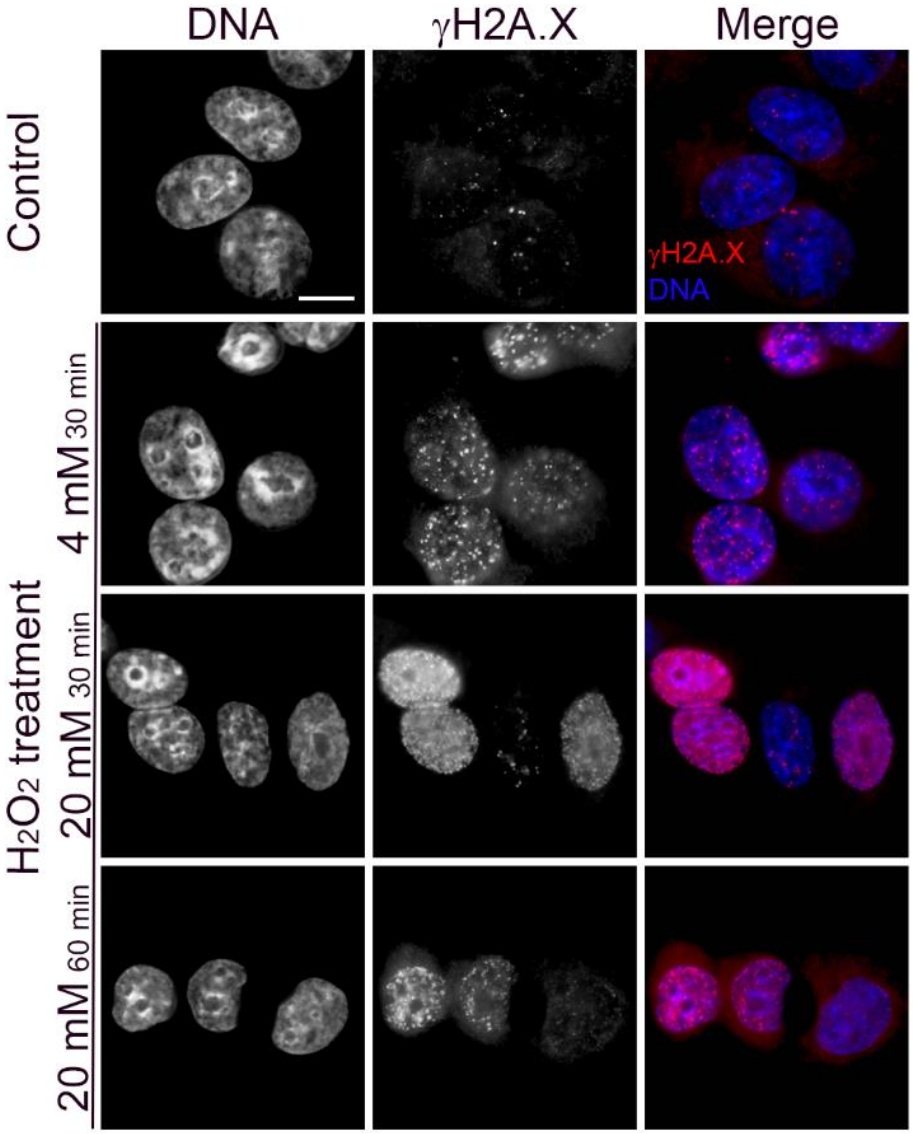

Figure 12 *Increased levels of γH2AX* observed *in MCF-7 cells by 2-D fluorescence microscopy after treatment with hydrogen peroxide.*

Immunofluorescence of MCF-7 cells treated with 4 mM or 20 mM H_2O_2 for 30 or 60 min and stained for γH2AX to visualized double-stranded DNA breaks. Control cells were not exposed to H_2O_2. Nuclear DNA was counterstained with DAPI. Scale bar, 10 µm.

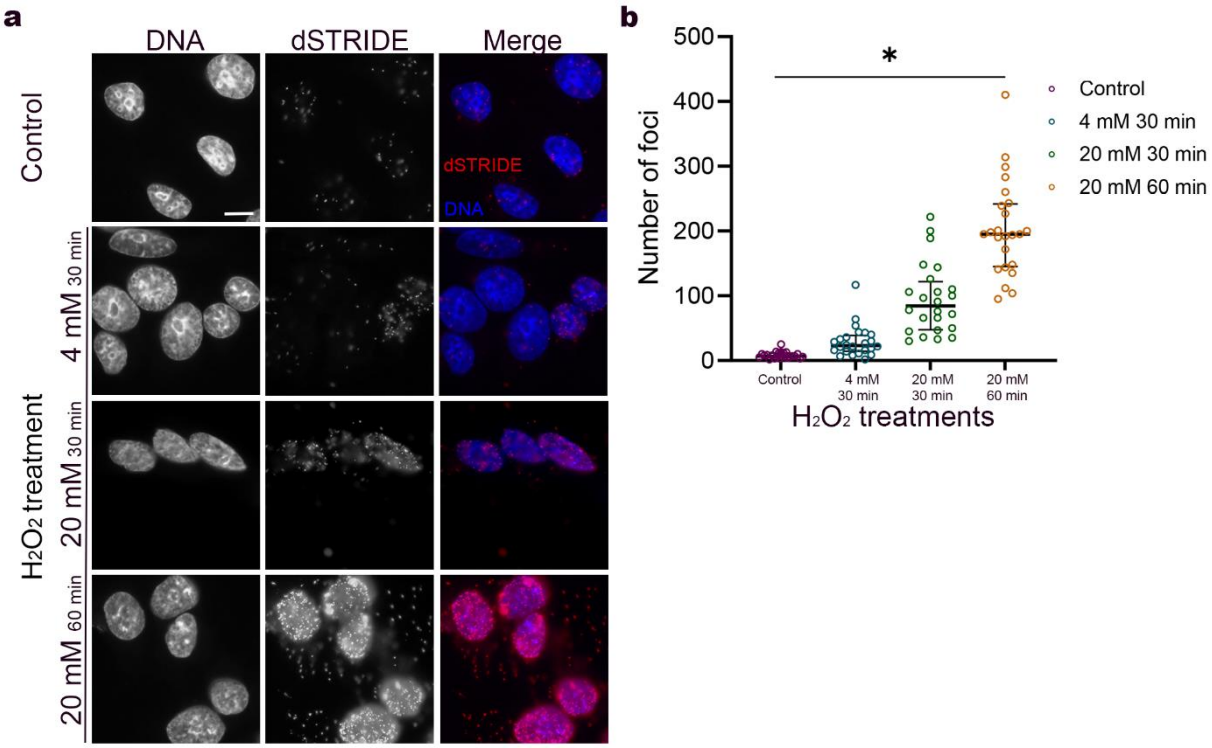

Figure 13 *Hydrogen peroxide increased DNA fragmentation in MCF-7 cells detected by dSTRIDE and 2-D fluorescence microscopy.*

*MCF-7 cells were treated with 4 mM or 20 mM H_2O_2 for 30 or 60 min and double-strand breaks were detected by dSTRIDE. Control cells were not exposed to H_2O_2. Nuclear DNA was counterstained with DAPI. Scale bar, 10 µm. b) Scatter dot plot showing distribution of foci observed by dSTRIDE for each condition as in a). Plots are shown with median (bold horizontal line) and whiskers representing lower and upper quartiles. Each dot represents number of breaks in a single cell. * significant difference, p < .0001 obtained by Kruskal-Wallis test between the different conditions.*

For quantifications, dSTRIDE on MCF-7 cells treated with H_2O_2 were repeated and images of cells were obtained with 3-D microscope. The number of foci corresponding to dSTRIDE signals, hence DSBs were measured using Object Counter3D plugin in ImageJ.

A total number of 24 cells (N=24) from each treatment was used to perform non-parametric statistics. Raw data are presented in table 8 in appendix (A2 Raw Data, A2.1). Scatter dot plot (Fig. 12 b) was made to represent the number of signals counted in each cell from every condition. All values were included in further tests. Most of the values from each condition are located near the median and IQ_1-IQ_3 (Control = 7 (5.0-11.5), 4 mM 30 min = 23 (14.5-39.0), 20 mM 30 min = 84 (47.8-122.0), 20 mM 60 min = 195 (145.0-242.0) (Table 3).

To assess whether it was a significant difference between exposures, Kruskal-Wallis non-parametric test was performed. The test compares the variations in the medians for DNA fragmentation foci in the groups. A significant variation in the rank of distributions for the treatments (p <.0001) were reported (Figure 13 b). Follow-up Mann-Whitney U test was performed in addition to examine which treatment that differed significantly from others. A statistically significant difference was found between all treatments when compared to control value (p <.0001), and when comparing exposures to each other (p <.0001) (Table 3).

Table 3 *Comparison of different hydrogen peroxide exposures and the effect on DNA fragmentation in MCF-7 cells.*

H_2O_2 exposure concentration and time	**Cells counted in each H_2O_2 treatment**	**DNA fragmentation foci**		**Differences between exposures**
	N	**Median**	**$IQ_1 – IQ_3$**	**p-value**
0 mM (Control)	24	7	5.0-11.5	
4 mM 30 min	24	23	14.5-39.0	<.0001 [ab]
20 mM 30 min	24	85	47.8-122.0	<.0001 [ac]
20 mM 60 min	24	184	145.0-242.0	<.0001 [a]

Mann-Whitney U test was performed to examine the differences between the exposures.
[a] compared to control
[b] compared to conditions 20 mM H_2O_2 for 30 or 60 min.
[c] compared to condition 20 mM H_2O_2 for 60 min

Altogether, our data show that signals representing DSBs in MCF-7 cells increase both in a dose-dependent and time-dependent manner after H_2O_2 treatment (Fig. 13 b). Results are consistent with UVB experiment data, where exposed cells had higher number of DSBs. dSTRIDE are observed to be reliable, sensitive, and specific method for performance in MCF-7.

3.2 Setting up and optimization of dSTRIDE method in spermatozoa

Results of dSTRIDE in spermatozoa was published in the original article (88) but precautions and critical steps were not described. The protocol for dSTRIDE had to be tested and validated in spermatozoa.

To test the method, we used semen samples obtained from FS. The samples contained a broad spectrum of concentrations spanning from 2 million to 200 million cells/mL. In this process, all collected samples were used regardless of cell motility, morphology, and vitality.

Three main challenges were faced during the setup of dSTRIDE method in spermatozoa.

1. To make the spermatozoa attach on coverslips for dSTRIDE to be performed and analysed
2. To make the dSTRIDE procedure work specifically in spermatozoa
3. To make the sperm chromatin accessible to the different components of the dSTRIDE protocol

3.2.1 Attachment of spermatozoa onto poly-L-lysine coated coverslips

The dSTRIDE method, as for other immunofluorescence-based procedures, requires the cells to be attached to a coverslip (88). Since spermatozoa are non-adherent cells, coverslips had to be coated with an attachment factor so the cells could firmly stick to it. In *Kordon et al.* (2020) (88) the authors used poly-L-lysine as a chemically synthesized extracellular matrix to coat the coverslips for spermatozoa attachment. Poly-L-lysine is a positively charged polymeric form of the amino acid L-lysine that link efficiently to negative charged ions of the cell membrane (106). Coating coverslips with poly-L-lysine is a cheap, easy to perform and fast procedure so we decided to use it in our dSTRIDE protocol. However, as for the rest of the procedure, the conditions used to make the coating and let the spermatozoa attached to the coverslips were not fully described.

Different volumes of poly-L-lysine (300 µL – 1000 µL) and different incubation times (from 10 minutes to 48 hours) were tested for attachment of spermatozoa. We found that 10 minutes were enough for the coverslip to be coated efficiently and that an

incubation in 300 µL of poly-L-lysine (enough to cover the entire surface of the coverslip) into wells of 24-well plates was a practical and cost-effective procedure.

For attaching spermatozoa to the coated coverslips, different volumes of semen samples, different incubation times and cell numbers were tested (Table 3). We found that the most important factor was the incubation time, and that none of the incubation times tried out (Table 3) were long enough for the spermatozoa to firmly attach to the coverslips no matter the other parameters. The sample needed to dry out to prevent a wash-out effect.

Table 3 *Conditions tested for attachment of spermatozoa in semen to poly-L-lysine coated coverslips.*

Semen volume (µL)	**Time (min)**	**Cells (total, in $1x10^5$)**	**Attachment**
200	5, 10, 15, 20	Not counted	No
150	10, 15	Not counted	No
100	5, 10	Not counted	No
50	5, 10, 15	Not counted	No
35	5, 10, 15, 20	Not counted	No
20	Until complete drying	1, 2, 3.5, 5, 10	Yes
15	Until complete drying	3.5, 5, 7.5	Yes
5	Until complete drying	2	Yes

The way the semen sample is loaded onto the coverslip is also a parameter that we found to be critical, especially for further investigations under a microscope. For example, four spots of 5 µL spermatozoa diluted in PBS were added directly on an air-dried coverslip and were totally dried out before further experiments, as in *Du et al.* (2016) (107) with boar spermatozoa. This approach worked well, and the cells were not lost undergoing further washing steps, immunofluorescence or dSTRIDE. However, when looking at the coverslip under a microscope a heterogeneous cell distribution was observed. As shown in figure 14, the cells at the centre of each spot were observed to be spread, but the cell density at the edge of the spot was too high

with aggregation of overlapping spermatozoa. This setup could not be used further for analysing as it was difficult to isolate single nuclei for quantification of DNA breaks in the nucleus of spermatozoa.

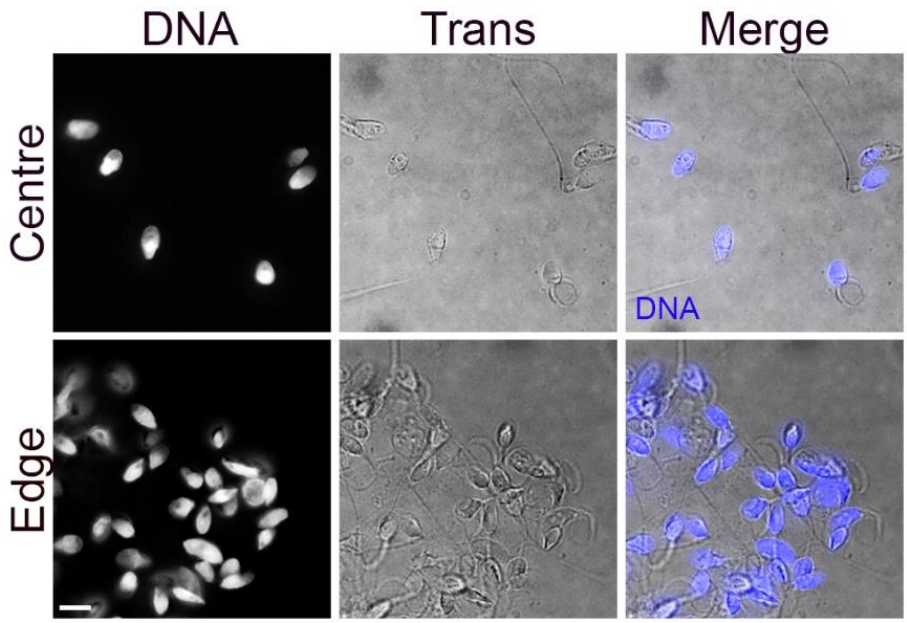

Figure 14 *Cell density differences between the centre and the edge of spotted and attached spermatozoa on air-dried coverslips.*
Spermatozoa in semen samples were applied onto coverslips by drops of 5 µL, fixed and washed three times before nuclear DNA was stained with DAPI to observe cell density and cell loss by 2-D fluorescence and transmission light microscopy (Trans). Scale bar, 5 µm.

Therefore, we aimed to optimize the loading of the semen sample on the coverslip to obtain a greater spreading of the cells. We observed an overall more homogeneous cell distribution when 15 µL of semen sample were added to the coated coverslips. However, the drop did not spread much at the surface of the coverslip and the cell density remained high. As we thought that the drop was too small to be able to cover the entire surface of a dry coverslip, we tested the same approach on wet coverslips by immersing coverslips in distilled H_2O followed by PBS right before spermatozoa were applied. This provided the opportunity to spread the drop over the whole surface, as we also observed under a phase-contrast microscope. For further experiments, a volume of 15 µL semen sample was applied onto wet pre-coated poly-L-lysine coverslips to achieve spreading of cells on coverslips.

3.2.2 Setting up a dSTRIDE protocol in human spermatozoa

After solving the problem with attachment of spermatozoa onto poly-L-lysine coated coverslips, dSTRIDE could be verified in spermatozoa.

3.2.2.1 Performing the BrdU incorporation step in tubes instead of on coverslips strongly reduces the background

We first tried to reproduce the original dSTRIDE protocol on spermatozoa on coverslips, as indicated by *Kordon et al.* (2020) (88). For this, we attached spermatozoa onto coverslips as described above, fixed them in ethanol overnight and submitted them to the dSTRIDE procedure as for MCF-7 cells. To our surprise, a strong background, was present all over the coverslip, making further analyses of specific signals nearly impossible. Moreover, when a chromatin decondensation step was performed before the dSTRIDE procedure (see below), we observed multiple fluorescence signals along the tail of the spermatozoa, where there should not be any detectable DNA in the first place (Fig. 15 a). Performing the cell fixation with ethanol in tubes as in a regular flow-cytometry-based TUNEL assay decreased substantially the overall background around the cells (Fig. 15 b). However, a large amount of discrete fluorescence signals (foci) was still present outside the nucleus (same figure), indicating that a significant part of the dSTRIDE signals may not be specific.

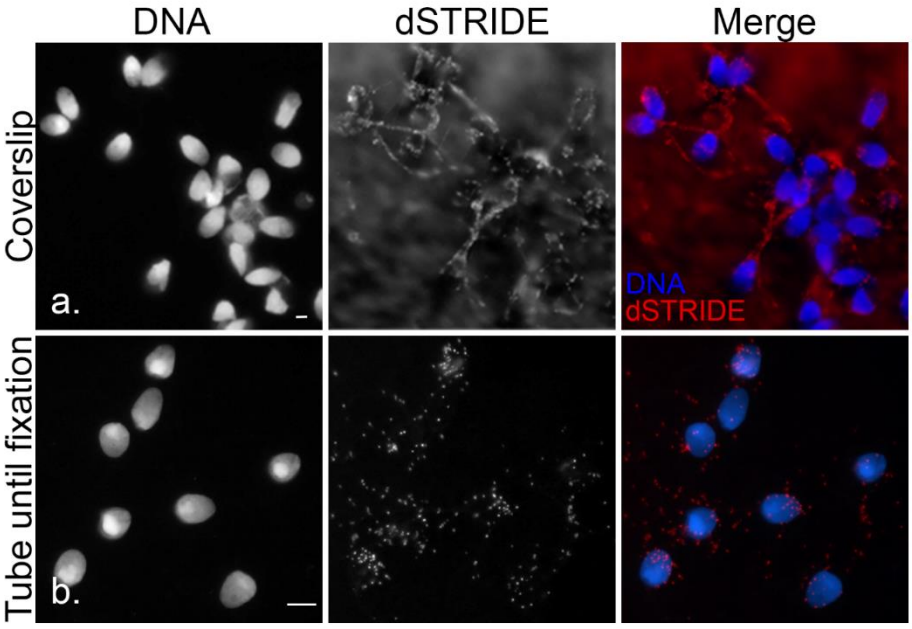

Figure 15 *dSTRIDE experiment in spermatozoa on coverslips and in tubes.*

(a) STRIDE experiment in decondensed cells performed after applying spermatozoa onto coverslip. Scalebar, 5 µm. (b) dSTRIDE experiment in decondensed cells when spermatozoa were applied onto coverslip right before fixation. Scalebar, 5 µm.

dSTRIDE were performed by excluding reagents and/or part(s) to get a clearer overview of where the background was coming from during the performance of dSTRIDE. Different conditions were set; without TdT and BrdUTP nucleotides during BrdU-incorporation, dSTRIDE without BrdU-incorporation and dSTRIDE excluding incubation with primary antibodies in addition to BrdU-incorporation (Table 4). Results showed no signals nor background for the different conditions (Fig. 16, Table 4), indicating that during the BrdU-incorporation step, non-incorporated BrdU stuck to the coverslip due to the poly-L-lysine coating.

Table 4 *dSTRIDE experiment with decondensed spermatozoa excluding reagents to detect origin of background signals.*

Coverslips	**Excluding reagents and/or part(s) during dSTRIDE**			
	TdT and BrdUTP in BrdU-incorporation	BrdU-incorporation	BrdU-incorporation and incubation with primary antibodies	dSTRIDE signals
Positive control	+	+	+	Yes
Test 1	-	+	+	No
Test 2	-	-	+	No
Test 3	-	-	-	No

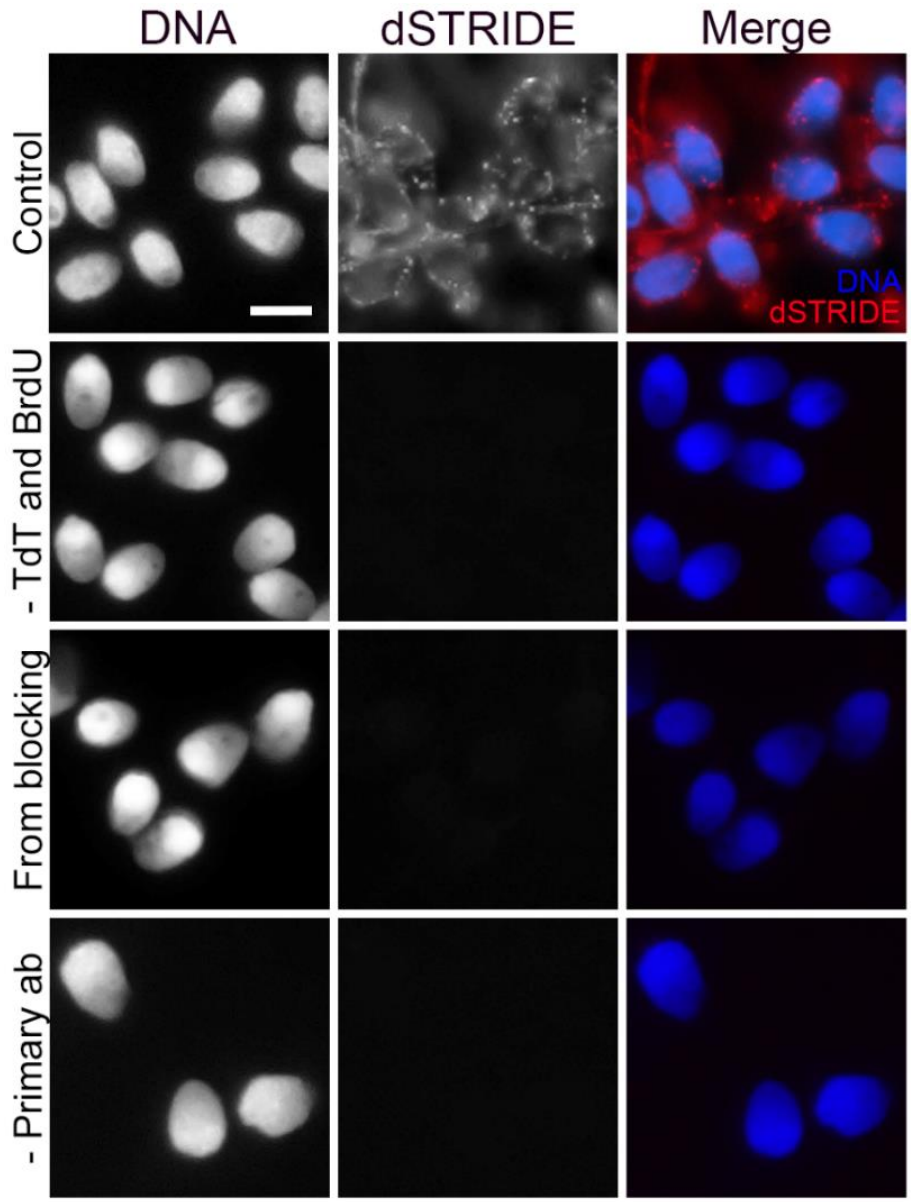

Figure 16 *dSTRIDE experiment on decondensed spermatozoa with different conditions visualized by 2-D fluorescence microscopy.*
dSTRIDE was performed according to method-section with variated conditions excluding TdT enzyme and BrdUTPs, BrdUTP-incorporation step or BrdUTP-incorporation step and without incubation with primary antibodies. Nuclear DNA were counterstained with DAPI. Scale bar, 5 µm.

To circumvent the background obstacle, we tested the possibility to perform all the steps from semen sample preparation until BrdU-incorporation into tubes and to attach the labelled spermatozoa afterwards. For this, we first used 1.5 mL tubes (PET) and a fixed angle centrifuge to pellet the spermatozoa after each reaction and for the washing steps (Fig. 17). In order to preserve the cell integrity and to not further damage the

DNA, centrifugations were performed at 400 *x* ***g*** for 10 minutes before and 800 *x* ***g*** for 5 minutes after fixation. A centrifugation force at 800 *x* ***g*** reduces the time necessary to pellet the cells and should not harm fixed cells. To minimize DNA damages caused by oxidative stress, the centrifuge was set at until the BrdU-incorporation step. Since the latter is performed at 37°C and to avoid a thermal shock, the final washing steps were performed at 22°C. Unfortunately, the spermatozoa were spread alongside the tubes after each centrifugation and were progressively lost during the procedure. Therefore, we replaced the 1.5 mL tubes with 15 mL polystyrene (PS) or polypropylene (PP) tubes and used a swing-out rotor centrifuge to ensure the formation of a strong and compact cell pellet (Fig. 17). Spermatozoa successfully formed visible pellets after each centrifugation steps and were further attached onto coverslips after the final washing step, as described above. The rest of the dSTRIDE protocol was followed as for the MCF-7 cells. As shown in figure 18, the overall background was strongly reduced, and the vast majority of the signals was located within or at the edge of the nucleus. This observation is consistent with the hypothesis that the background observed in our previous "all on coverslip" protocol was due to unspecific binding of BrdU to poly-L-lysine.

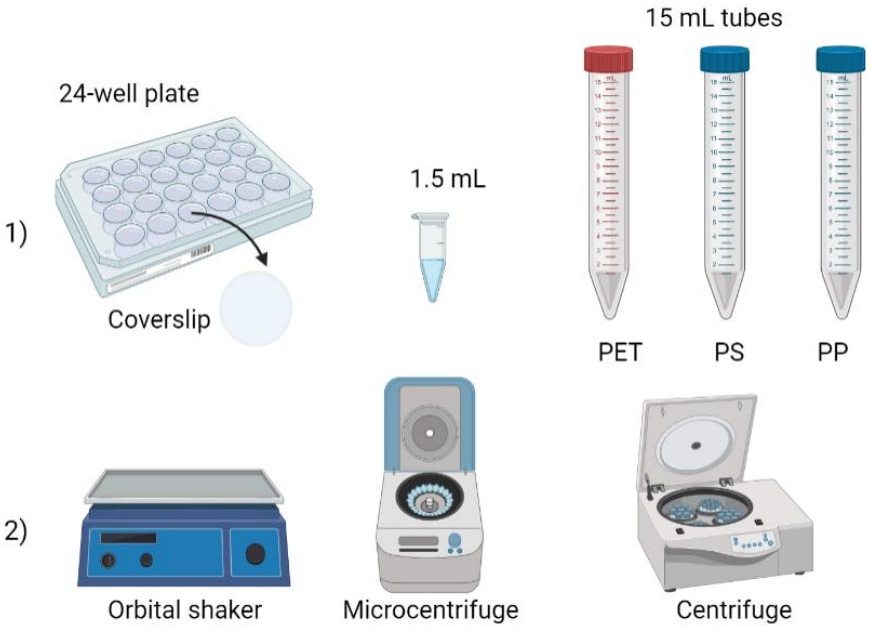

Figure 17 *Lab equipment tested to achieve minimal non-specific background by dSTRIDE in spermatozoa.*

Cells were either prepared onto coverslips placed in 24-well plates, in 1.5 mL tubes or in 15 mL tubes (1). The variation of 15 mL tubes tested are Sarstedt polyethylene terephthalate (PET) tubes, Falcon polystyrene (PS) and Falcon polypropylene (PP) tubes. Associated

instruments used were orbital shaker, fixed-angle microcentrifuge, and swing-out rotor centrifuge (2). For established protocol, 15 mL PS or PP with swing-out rotor centrifuge were preferred. Illustration created by author using Biorender.com.

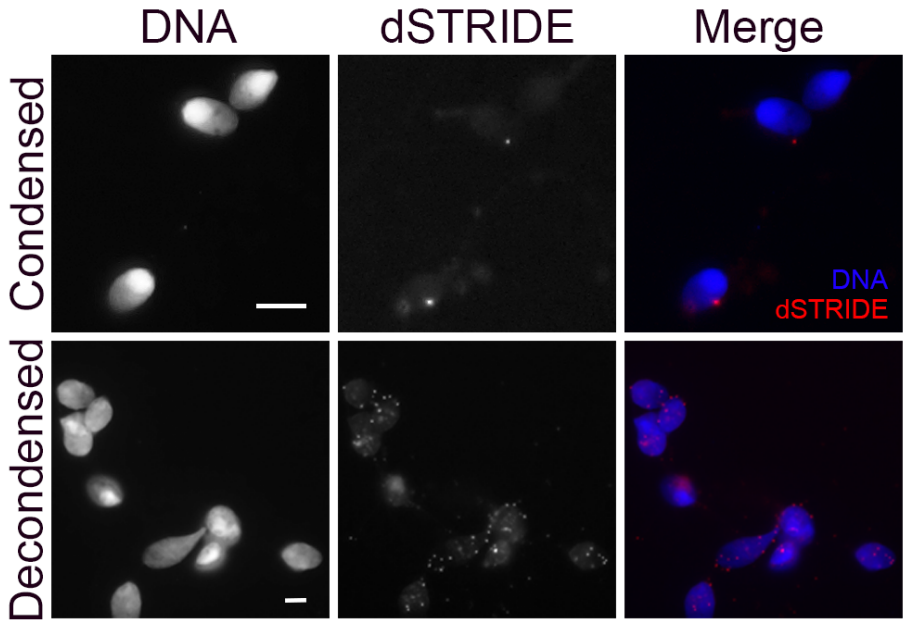

Figure 18 *dSTRIDE experiment with and without decondensation where spermatozoa were applied onto coverslips after BrdU-incorporation.*
Nuclear DNA were counterstained with DAPI. Scalebar, 5 µm.

To confirm that the signal detected in the nucleus resulted from the TdT-enzyme activity, we performed two experiments in parallel from the same sample with or without TdT-enzyme during the BrdU-incorporation step. Our results showed no detectable signals in the spermatozoa in absence of the TdT enzyme while several signals were observed in the control cells (Fig. 19). These data strongly suggest that the signals detected in spermatozoa after the optimized dSTRIDE procedure correspond to DSBs.

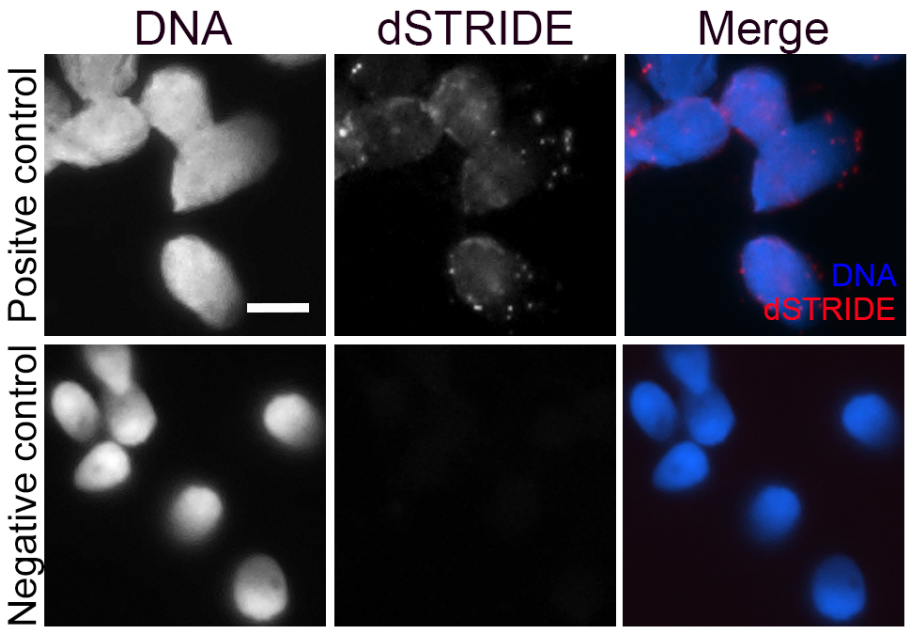

Figure 19 *dSTRIDE experiment performed on spermatozoa with and without TdT in the BrdU-incorporation step visualized by 2-D fluorescence microscopy.*
dSTRIDE was performed according to method-section with TdT (positive control) or without (negative control). Nuclear DNA was counterstained with DAPI. Scale bar, 5 µm.

From our results, we can conclude that dSTRIDE in spermatozoa has to be performed in tubes to reduce unspecific background observed when performing dSTRIDE on coverslips. Centrifugations lead to cell loss, and to preserve a majority of cells, swing-out rotor centrifuges were preferred compared to fixed-angle centrifuges. Tubes of 15 mL composed of PS or PP were preferred compared to 1.5 mL PET tubes.

3.2.2.2 Performing dSTRIDE protocol in human spermatozoa

Initial experiments of dSTRIDE in human spermatozoa resulted in loss of cells and lot of background. The loss of cells was improved by solving the attachment difficulties (section 3.2.1), while the background was determined to be due to BrdU incorporation at unspecific sites on poly-L-lysine coated coverslips and was solved by replacing coverslips with tubes until after this step (section 3.2.2.1).

The important optimization by dSTRIDE in spermatozoa was to change the instruments used, replacing coverslip-based methodology to implement the protocol for performance in tubes (Fig. 17). Protocol is illustrated in figure 20.

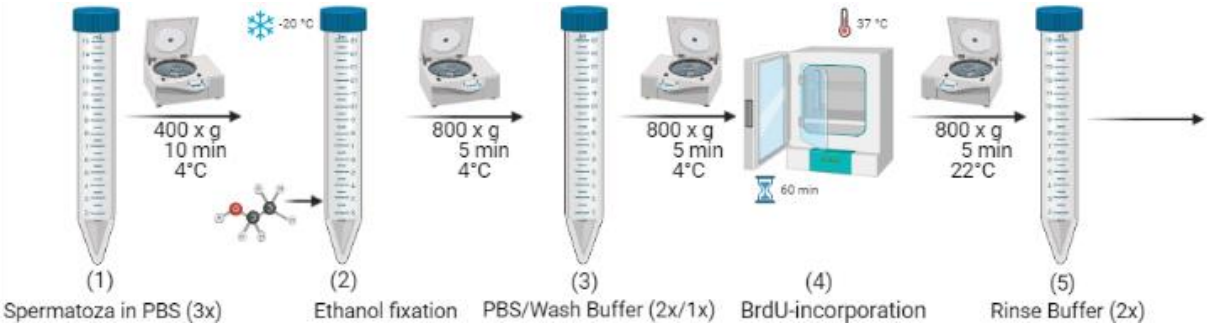

Figure 20 *Sperm preparation in tubes for dSTRIDE performance in spermatozoa. Spermatozoa were placed in 15 mL tubes and washed three times with PBS with centrifugation in a swing-out rotor centrifuge at 400 x* ***g*** *for 10 minutes at 4ºC (1) before fixated in 70% ethanol and placed at -20ºC (2). The day after, cells were washed twice with PBS and once with Washing Buffer from the kit used for BrdU-incorporation with centrifugation at 800 x* ***g*** *for 5 minutes at 4ºC (3). BrdU-solution was applied to the cells and placed in a humidified environment for 60 minutes at 37ºC (4). Cells were then washed twice with Rinse Buffer from the kit, temperature adjusted to 22ºC (5). Cells were applied onto pre-coated coverslips, let dried and further dSTRIDE protocol were followed with cells attached onto coverslips. Illustration was made by author using Biorender.com.*

3.2.3 Additional steps to decondense the chromatin to facilitate the incorporation of BrdU at double strand break sites

The decondensation solution contains 0.1% Tx-100 in PBS (permeabilise cell membrane (108)), 100 U/mL heparin (deplete protamines from chromatin (109)) and 5 mM DTT (reduce disulphide bonds (110)) and was performed after stabilization of the cells with 0.5% PFA in PBS. Opening chromatin could be damaging for the cell, and they are therefore stabilized in advance. Several decondensation protocols are published (111-114), but the protocol by *Antonucci et al.* (2013) (95) includes washing steps, pre-fixation and incubation. The protocol is carefully examined and optimized, so every step has a specific function to access DNA content. It is also mentioned the opportunity the protocol provides to improve TUNEL assay (95).

Results from the sperm chromatin decondensation were a visible enlargement in size of the nucleus while intact nuclear morphology (115) in addition to their reduced light refractivity compared to untreated cells (Fig. 21). As dSTRIDE was performed on coverslips, time of incubation in decondensation solution was evaluated and optimized. Cells were observed under an inverted phase-contrast microscope each 5 minutes until 30 minutes of incubation. Swelling of the nuclei was observed after incubation for

10 minutes (most cells), but some samples needed 15 minutes before all cells received same physical swelling and therefore, 15 minutes incubation was favoured. Cells stained with DAPI after 10 and 30 minutes of incubation with decondensation solution are shown below and have same physical appearance (Fig. 21).

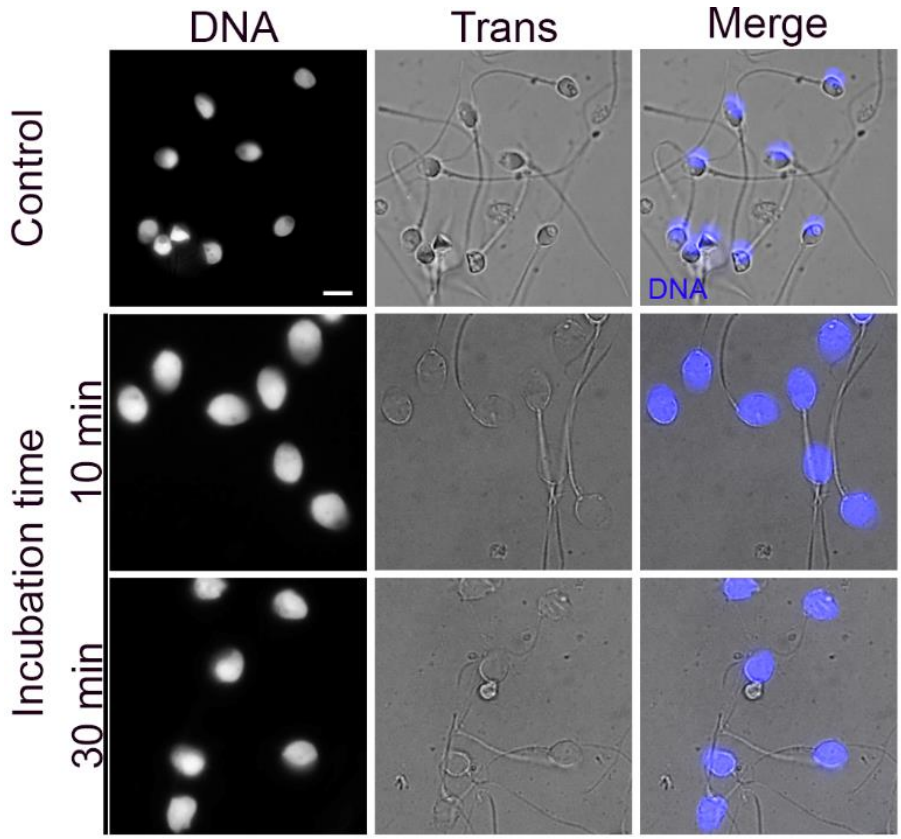

Figure 21 *Optimization of decondensation for spermatozoa applied onto coverslips. Spermatozoa from the same semen sample were subjected to chromatin decondensation (decondensation procedure) or not (control) before ethanol fixation and further DNA staining with DAPI. Two incubation times (10 min and 30 min) are shown and the size of the nuclei for each experiment was compared between the different conditions by 2-D fluorescence microscopy. Scale bar, 5 µm.*

When decondensed cells followed dSTRIDE procedure on coverslips, strong background signals were observed in addition to signals in the tails for some of the cells. Background was not removed regardless multiplied washing steps (Fig. 15 a), and dSTRIDE procedure was optimized for use in tubes. Decondensation procedure was then performed accordingly to the use of tubes, customized to fit cell concentration used in dSTRIDE experiments.

While published protocol uses 30 minutes incubation at 25ºC in the dark, we observed some altered cell nucleus in some samples using this incubation time (Fig. 22), and therefore, protocol was altered to 20 minutes prior 10 minutes centrifugation to pellet the cells.

In total, decondensation with Tx-100, heparin and DTT increases the volume of the nuclei, open chromatin structure and entail more signals when performing dSTRIDE protocol, as anticipated (Fig. 22).

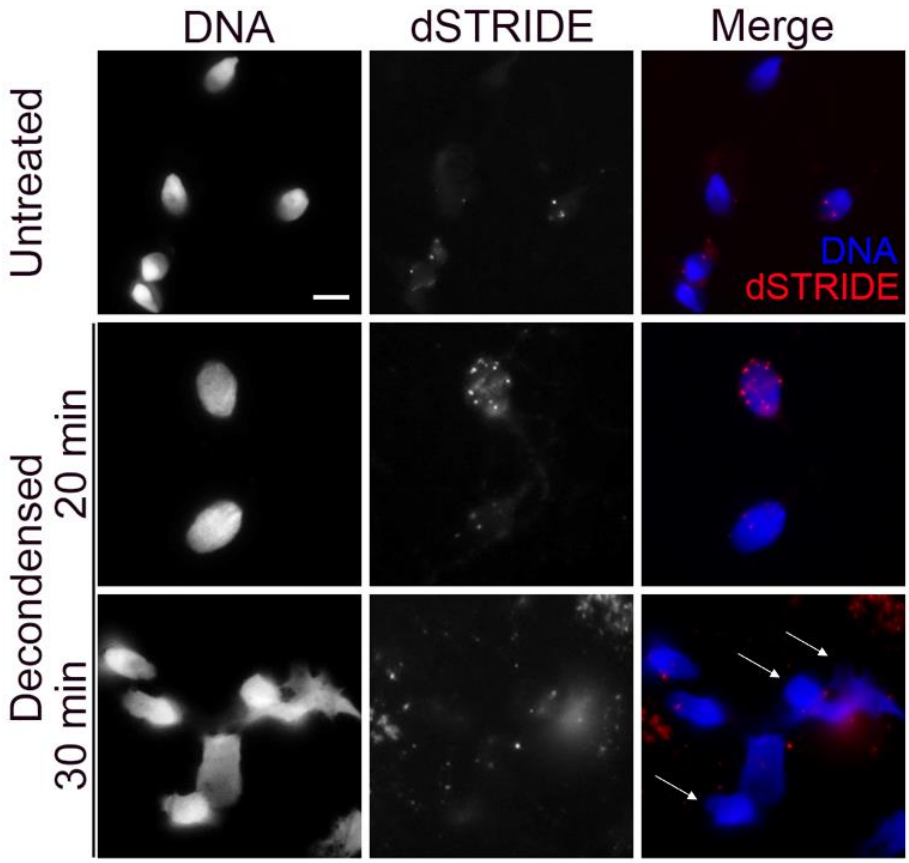

Figure 22 *dSTRIDE experiment with and without chromatin decondensation visualized by 2-D fluorescence microscopy.*

Spermatozoa were subjected to chromatin decondensation for either 20 minutes or 30 minutes, or not (untreated) before fixation and further dSTRIDE procedure. Nuclear DNA was counterstained with DAPI. Nuclear shape was compared between the conditions of decondensed spermatozoa. Arrows indicate deformed nuclear shape. Scale bar, 5 µm.

3.2.3.1 Performing dSTRIDE protocol in human spermatozoa with opened chromatin structure

Human spermatozoa have a higher degree of chromatin compaction than somatic cells due to the packaging of their DNA by protamines. The use of TdT to incorporate BrdU at DSB sites supposes that these sites are accessible to the enzyme. The high degree of chromatin compaction and the resulting inaccessibility of the DNA is often discussed in studies focusing on DNA fragmentation and several of them recommend opening the chromatin (95, 114). For this, disulphide bridges between protamines must be disrupted and protamines depleted.

In our dSTRIDE protocol, an addition step can be implemented to decondense chromatin structure. Below is optimized protocol for dSTRIDE with decondensation protocol that results in low-to-none background and bright, individual dSTRIDE signals observed in fluorescence microscopes.

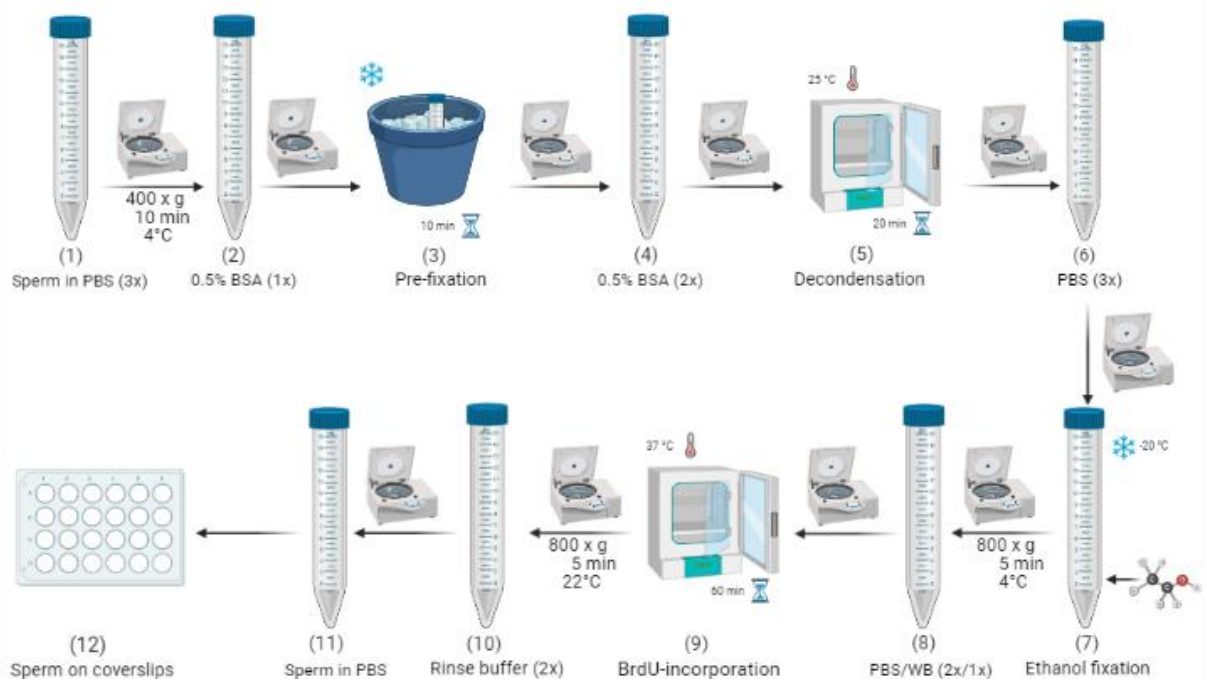

Figure 23 *Sperm preparation for dSTRIDE including BrdU-incorporation step in Falcon tubes. Spermatozoa were placed in 15 mL tubes and washed three times with PBS (1) before one additional wash with 500 µL 0.5% BSA with centrifugation in a swing-out rotor centrifuge at 400 x **g** for 10 minutes at 4ºC (2). Cells were added 500 µL 0.5% PFA for 10 minutes on ice for pre-fixation (3), then washed twice with 500 µL 0.5% BSA with centrifugation (4). A decondensation solution was added and cells were incubated at 25°C in the dark for 20 minutes (5). Cells were then washed three times with PBS by centrifugation (6), before fixated*

*in 70% ethanol and placed at -20ºC (7). The day after, cells were washed twice with PBS and once with Washing Buffer from the kit used for BrdU-incorporation with centrifugation at 800 x **g** for 5 minutes at 4ºC (8). BrdU-solution was applied to the cells and placed in a humidified environment for 60 minutes at 37ºC (9). Cells were then washed twice with Rinse Buffer from the kit, temperature adjusted to 22ºC (10), diluted in PBS (11), and applied onto pre-coated coverslips, let dried and further dSTRIDE protocol were followed with cells attached onto coverslips (12). Illustration was made by author using Biorender.com.*

3.2.3.2 Spermatozoa with decondensed chromatin detected more dSTRIDE signals

To evaluate if decondensation procedure decondense chromatin in spermatozoa and increases the access of TdT enzyme to DSB sites in the DNA for incorporation of BrdU, dSTRIDE with and without decondensation was performed. For this, we divided a fresh semen sample in two fractions, one of which was subjected to our chromatin decondensation using our optimized protocol. Control fraction containing spermatozoa with condensed chromatin was fixated after three washes with PBS by centrifugation. dSTRIDE was performed the day after fixation as described in method section 2.7.2 and 2.7.3.

After the first wash following decondensation protocol, decondensed fraction was assessed with a light microscope to observe an increased size of nucleus and reduced light refractivity.

Spermatozoa from the two fractions were observed by 3-D fluorescence microscopy and more dSTRIDE signals were seen in nucleus of spermatozoa with decondensed chromatin structure compared to spermatozoa with condensed chromatin (Fig. 24 a). This difference was visualized by scatter dot plot and confirmed by Mann-Whitney U test ($p < .0001$) (Fig 24 b). Number of cells with decondensed chromatin counted were lower due to fewer attached sperm on the coverslip (Fig 24 c). Raw data are listed in table 9 in appendix (A2 Raw Data, Section A2.2).

Altogether, this indicates that the protocol functioned as intended.

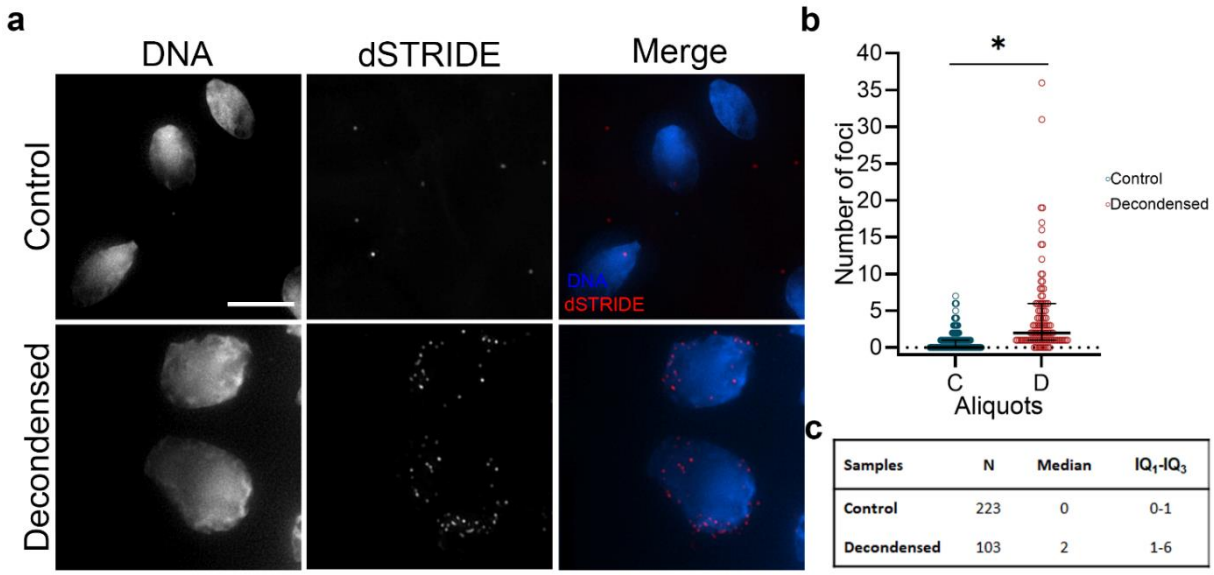

Figure 24 *Spermatozoa with decondensed chromatin structure had more dSTRIDE signals than spermatozoa with condensed chromatin structure.*
*(a) dSTRIDE was performed in control, untreated spermatozoa with condensed chromatin structure and in spermatozoa from same sample with decondensed chromatin structure by decondensation procedure. Images are MAX projections obtained from 3-D images. Nuclear DNA was counterstained with DAPI. Scale, 5 µm. (b) Scatter dot plot showing distribution of foci observed by dSTRIDE in spermatozoa from both fractions, with and without decondensed chromatin structure. Bold horizontal line present median, while whiskers shows the lower and upper quartiles. * significant difference, p < .0001 obtained by Mann-Whitney U test between spermatozoa from the two fractions. (c)Table containing cells counted (n) for each fraction of sample, median and IQ_1-IQ_3.*

When chromatin in spermatozoa decondenses, disulphide bonds are reduced and protamines depleted. TdT enzyme will allegedly get better access to the chromatin in spermatozoa and a higher number of DNA breaks can be detected (95, 116). It is therefore expected to observe an increased number of detected DSBs in spermatozoa with decondensed chromatin structure. In this experiment, a significantly higher number of dSTRIDE signals, hence DSBs were detected in these spermatozoa compared to cells with condensed chromatin structure.

3.2.4 DNA damaging agents increase number of dSTRIDE signals in spermatozoa

Spermatozoa were exposed to DNA damaging agents (UVB or H_2O_2) to further evaluate dSTRIDE procedure.

In a first series of experiments, cells were exposed to UVB irradiation for 2, 5 and 10 minutes, then compared to signals from non-irradiated cells. Irradiation for 10 minutes was the only condition that resulted in an increased number of signals in irradiated cells compared to non-irradiated cells when assessed by 2-D fluorescence microscopy. The experiment with UVB irradiation for 10 minutes where repeated and compared to non-irradiated cells by evaluation with 3-D microscopy. A visible difference between irradiated and non-irradiated where confirmed (Fig. 25).

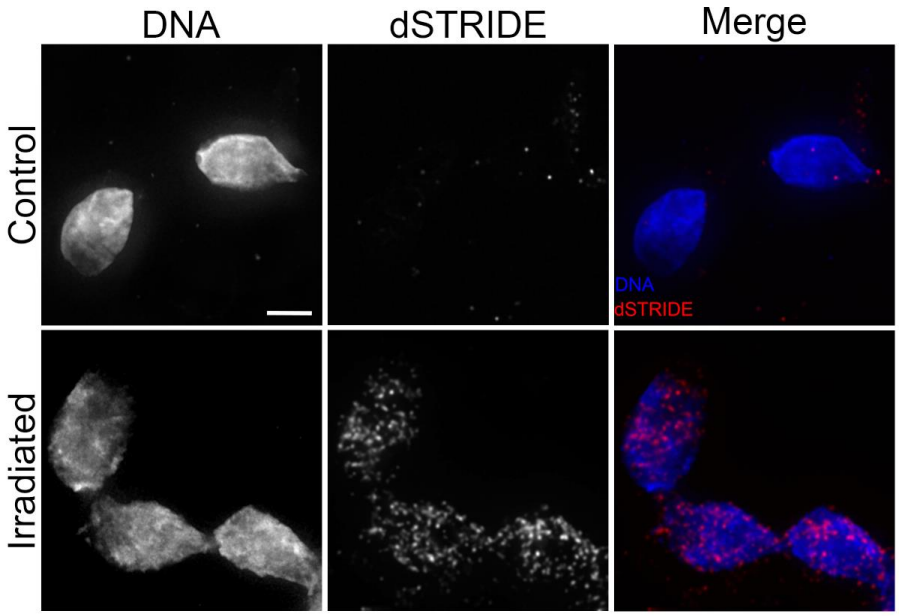

Figure 25 *More dSTRIDE signals in spermatozoa after irradiation with UVB visualised by 3-D microscopy.*
Spermatozoa was exposed for 10 minutes to UVB irradiation or not prior dSTRIDE. Nuclear DNA was counterstained with DAPI. Images are MAX projections from 3-D images. Of note, not all irradiated spermatozoa harboured as much dSTRIDE signals as those showed in this figure. Scale bar, 5 µm.

In a second series of experiments, spermatozoa from the same semen sample were incubated with 0 mM (control),10 mM, 40 mM, 100 mM, or 200 mM H_2O_2 diluted in Sperm Preparation Medium™ for 2 hours at 37°C prior dSTRIDE. Untreated

spermatozoa showed fewer dSTRIDE signals than those incubated with H_2O_2, with some variations, when evaluating by 2-D fluorescence microscope. The experiment was repeated to perform quantifications, and images were obtained for 0 mM, 40 mM and 200 mM by 3D-fluorescence microscopy. A higher number of foci was observed with an increased concentration of H_2O_2, consistent with a higher level of DNA fragmentation induced by H_2O_2 in spermatozoa (Fig. 26 a).

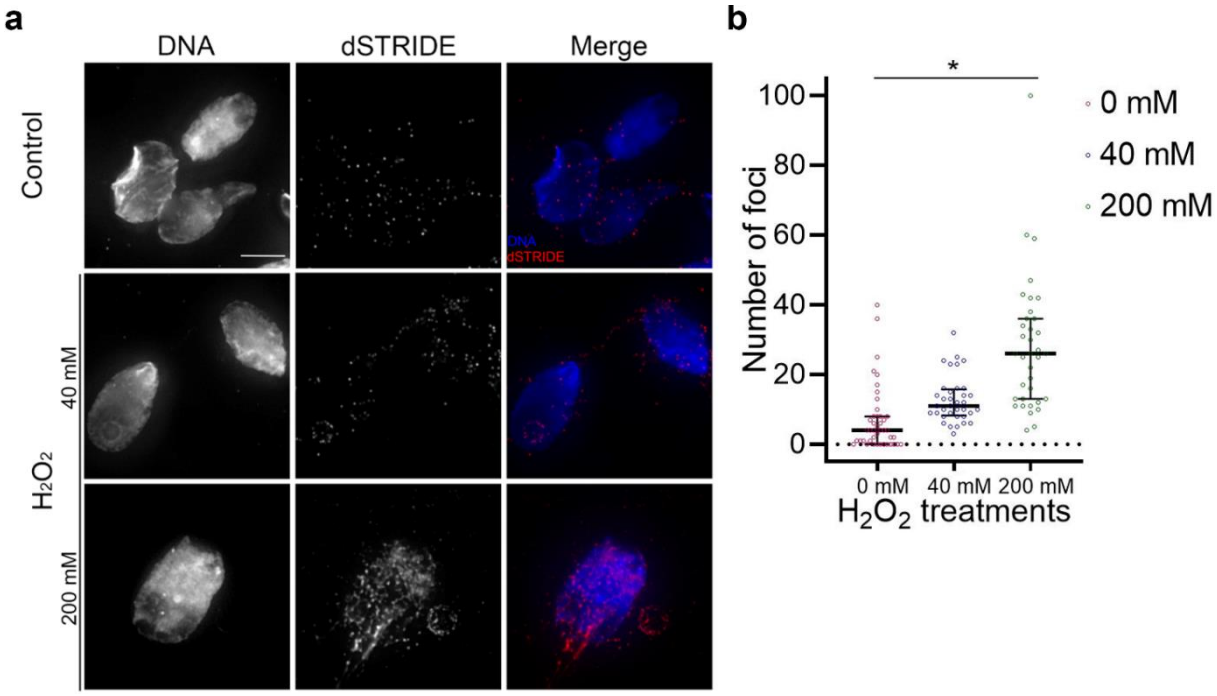

Figure 26 *Hydrogen peroxide increased DNA fragmentation in spermatozoa detected by dSTRIDE and visualized by 3-D fluorescence microscopy.*

*a) Spermatozoa were treated with 40 mM or 200 mM H_2O_2 for 2 hours and DSBs were detected by dSTRIDE. Control cells were not exposed to H_2O_2. Nuclear DNA was counterstained with DAPI. Images are MAX projections. Scale bar, 5 µm. b) Scatter plot showing distribution of foci observed by dSTRIDE for each condition as in a). Plots show median (bold horizontal line) and whiskers representing lower and upper quartiles. Each dot represents number of breaks in a single cell. * significant difference, p < .0001 obtained by Kruskal-Wallis test between the different conditions.*

To assess whether it was a significant difference between treatments with H_2O_2, Kruskal-Wallis non-parametric test was performed. A significant variation in the number of foci after the different treatments (* = p <.0001) were reported (Figure 26 b). Follow-up Mann-Whitney U test was performed in addition to examine which treatment that differed significantly from others. A statistically significant difference was

found between treatments when compared to control value (p <.0001), and when comparing 40 mM H_2O_2 treatment to 200 mM H_2O_2 treatment (p <.0001) (Table 5). Raw data are presented in table 10 in appendix (A2 Raw Data, A2.2).

Table 5 *Comparison of different hydrogen peroxide exposures and the effect on DNA fragmentation in spermatozoa.*

H_2O_2 exposure concentration	**Cells counted in each H_2O_2 treatment**	**DNA fragmentation foci**		**Differences between exposures**
	n	**Median**	**$IQ_1 – IQ_3$**	**p-value**
0 mM (Control)	43	4	0.0-8.0	
40 mM	36	11	8.3-15.8	<.0001 [a]
200 mM	36	26	13.0-36.0	<.0001 [ab]

Mann-Whitney U test was performed to examine the differences between the exposures.
[a] compared to control
[b] compared to conditions 40mM H_20_2.

Overall, our data show that signals representing DSBs in spermatozoa increases in a dose-dependent manner after H_2O_2 treatment (Fig. 26). dSTRIDE is observed to be reliable, sensitive, and specific method for performance in spermatozoa.

3.3 dSTRIDE used as a DNA fragmentation test

Once optimized, our dSTRIDE protocol was used to measure sperm DNA fragmentation under different conditions. The protocol was tested in experiments where expectations for the results were established. In this chapter, dSTRIDE protocol was first performed to compare different parameters of the preparation in the same semen samples by swim-up and decondensation, before the dSTRIDE protocol was performed in semen samples with known DNA fragmentation earlier obtained by SCSA (91).

3.3.1 Spermatozoa prepared by swim-up show less dSTRIDE signals than non-prepared spermatozoa from the whole ejaculate

The swim-up technique is used to isolate progressive motile spermatozoa from seminal fluid without using centrifugation steps. It functions by incubating semen with a layer of medium with nutrition, so motile spermatozoa can be aspirated and further used. Experiment was performed to test dSTRIDE protocol in progressive motile

spermatozoa and compare to the corresponding spermatozoa from the whole semen sample. To do that, the semen sample was divided in two fractions, control (whole sample) and swim-up. Spermatozoa in control fraction was washed three times by centrifugation with PBS to isolate cells from seminal fluid. Spermatozoa with progressive motility have less DNA fragmentation (117) and therefore, this fraction is expected to have less dSTRIDE signals compared to spermatozoa in control fraction.

The quality of each portion was before fixation assessed with a light microscope and observed that samples with swim-up spermatozoa had an increased motility rate and no occurrence of excess cells compared to control fraction.

After dSTRIDE, cells were observed by 2-D microscopy and both fractions had few dSTRIDE signals in the nuclei, making it difficult to observe an immediate difference (Fig. 27 a). Some cells from the whole sample showed a higher number of dSTRIDE signals (Fig. 27 b), indicating that there could be a difference. Images of cells were later obtained by 3-D fluorescence microscopy for quantitative analysis, and Mann-Whitney U test showed significant difference between the number of dSTRIDE signals counted in the two fractions of the sample ($p < .0001$) (Fig. 27 b). The number of counted foci is listed in table 11 in appendix (A2 Raw Data, Section A2.2).

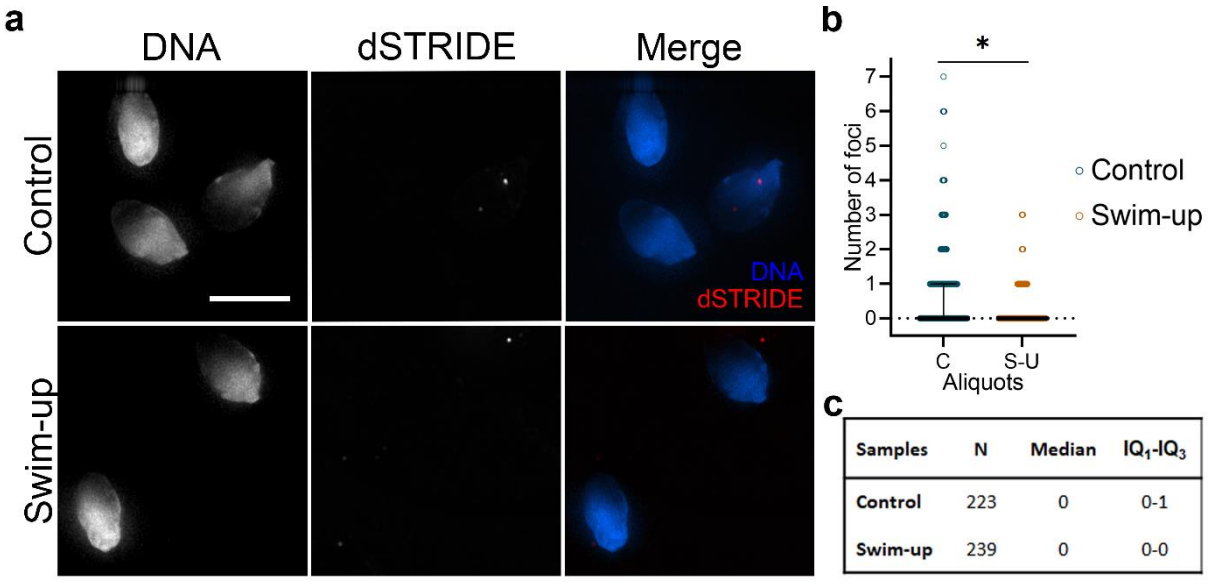

Figure 27 *dSTRIDE experiment with spermatozoa prepared by swim-up or non-prepared spermatozoa from the whole ejaculate.*

(a) dSTRIDE was performed in semen sample divided in two fractions, one containing progressive motile spermatozoa isolated by swim-up and one containing sperm from the whole ejaculate. Nuclear DNA was counterstained with DAPI. Images are MAX projections.

*Scale bar, 5 µm. (b) Scatter dot plot presents the distribution of dSTRIDE foci in spermatozoa present in control (blue) and swim-up (orange) fractions. * significant difference, p < .0001 obtained by Mann-Whitney U test between number of foci in spermatozoa from the two fractions. (c) Table containing cells counted (N) for each fraction, median and IQ_1-IQ_3.*

The use of our dSTRIDE protocol showed more signals in spermatozoa from control fraction, compared to spermatozoa from swim-up preparation from the same semen sample (Fig. 27 b). This was expected due to the observed strong correlation between progressive motility and DNA fragmentation in spermatozoa (117). This result is consistent with earlier experiments with expected outcomes (section 2.3.4) and indicate and strengthen that dSTRIDE presents a sensitive method for detection of DSBs in human spermatozoa.

3.3.2 Measuring double strand breaks in semen samples by dSTRIDE and immunofluorescence with γH2AX

We wanted to briefly compare signals detected by dSTRIDE to signals obtained using γH2AX immunofluorescence in two different samples. The dSTRIDE and γH2AX immunofluorescence were performed in parallel in samples related to an ongoing method-development project. Spermatozoa in the samples were treated with decondensation solution prior to dSTRIDE and γH2AX staining, respectively. Cells were evaluated and signals were compared using a 3-D fluorescence microscopy with deconvolution.

For γH2AX immunofluorescence, no quantification of the number of γH2AX signals was performed. By visual evaluation a difference was seen between the two samples, where sample 1 presented a higher number of bright signals (Fig. 28) Evaluation was primary focused on bright signals, since many diffuse signals were observed in most cells in both samples and was difficult to state as γH2AX signals.

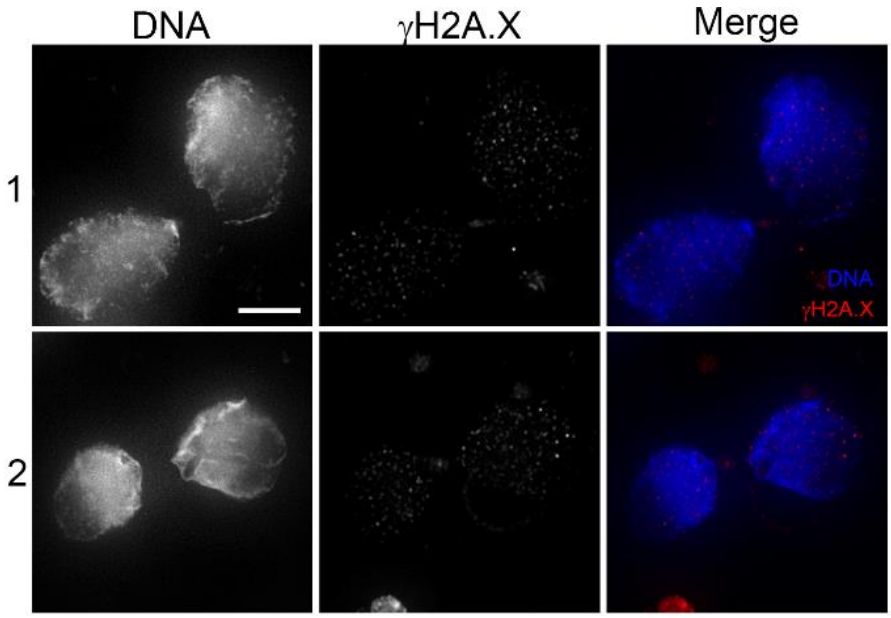

Figure 28 *Immunofluorescence showing γH2AX in spermatozoa from two different samples with decondensed chromatin structure visualised by 3-D fluorescence microscopy with auxiliary magnification.*
Immunofluorescence was performed in parallel to dSTRIDE (Fig. 29) on spermatozoa with decondensed chromatin structure from two semen samples (1 and 2). DNA was counterstained with DAPI. Images are MAX projections. Scale bar, 5 µm.

For dSTRIDE cells were evaluated by microscope and quantifications from the obtained images showed a higher number of dSTRIDE signals in sample 1 compared to sample 2 seen by median and IQ_1-IQ_3 (Fig. 29). This result confirms the previous observation (Fig. 28) where more γH2AX-signals were observed in sample 1.

From this preliminary experiment on two different semen samples, similar DNA fragmentation results were observed using our dSTRIDE protocol and γH2AX immunofluorescence.

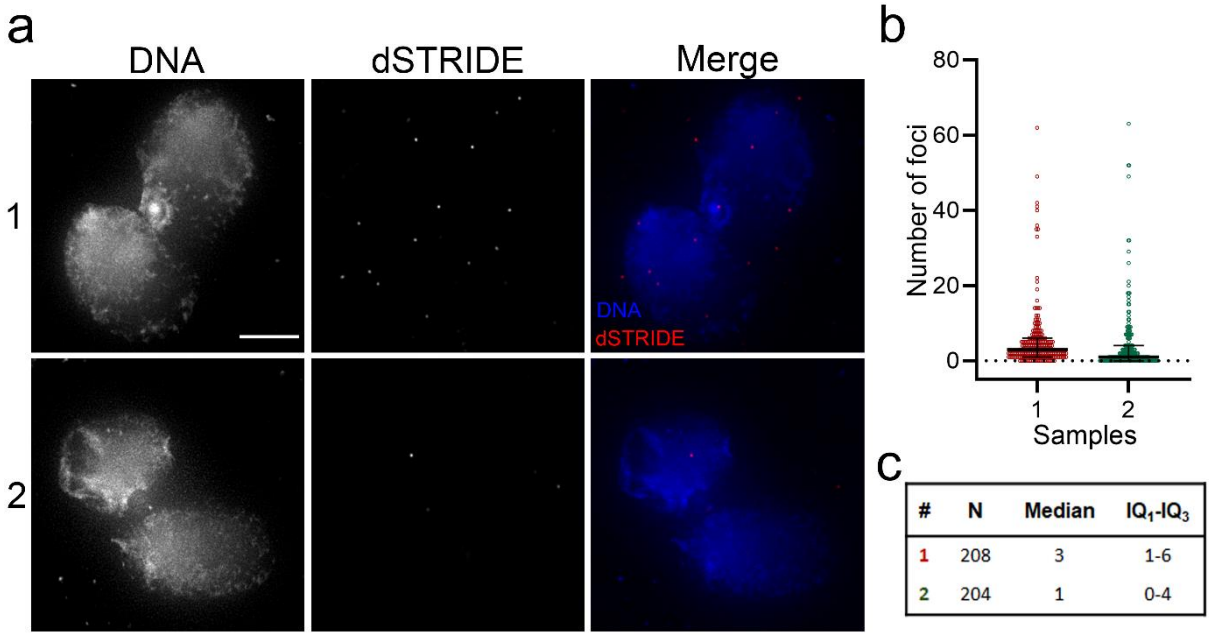

#	N	Median	IQ_1-IQ_3
1	208	3	1-6
2	204	1	0-4

Figure 29 *dSTRIDE experiment in spermatozoa from two different semen samples visualised by 3-D fluorescence microscopy with auxiliary magnification.*
(a) dSTRIDE was performed in two semen samples with decondensation procedure before visualised using 3-D fluorescence microscopy. Nuclear DNA was counterstained with DAPI. Images are MAX projections. Scale bar, 5 µm. (b) Scatter plot show distribution of counted dSTRIDE signals in spermatozoa from the two samples. Median with interquartiles are presented as bold horizontal line and whiskers. Each dot represents number of breaks in a single cell. (c) Number of cells counted (N) in each sample with median for dSTRIDE signals and lower and upper quartiles.

3.3.3 Testing our new protocol against a well-established method: dSTRIDE vs SCSA

Results obtained from experiments comparing different sample parameters have indicated that dSTRIDE is a sensitive and specific method for detection of DSBs in human spermatozoa. To empower and confirm our dSTRIDE protocol as a competitive and alternative method for detection of DNA fragmentation in human spermatozoa, a controlled experiment has to be conducted. The purpose of this experiment was to evaluate if dSTRIDE and SCSA obtained results with same trend across samples.

For this, frozen samples from a biobank containing spermatozoa form a previous project evaluating the relationship between different biological factors and several sperm parameters including DNA fragmentation assessed by SCSA were used. A

total of 11 samples were thawed and further used for dSTRIDE with performance of decondensation in advance.

For all samples, the semen volume and sperm concentration were previously assessed (91) (Table 6).

Table 6 *Semen volume and concentration in samples used to compare STRIDE results with known DNA fragmentation index (DFI).*

Semen sample	**1**	**2**	**3**	**4**	**5**	**6**	**7**	**8**	**9**	**10**	**11**
Semen Volume (mL)	4.2	8.4	4.4	5.8	6.4	3.8	5.4	5.7	5.6	4.5	6.0
Concentration (10^6/mL)	106	134	52	89	104	120	149	122	119	119	106

All samples were evaluated by a 3-D fluorescence microscope and differences between the samples were observed. Images of cells were obtained for quantifications. Number of foci counted in each cell from the samples are listed in table 12 in appendix (A2 Raw Data, Section A2.2). Table 7 shows descriptive statistics obtained from dSTRIDE experiment in addition to SCSA obtained DFI from related in previous project (91).

Table 7 *Table of number of cells (N), median with lower and upper quartiles, minimum and maximum values from dSTRIDE experiment and DFI (%) obtained to earlier project (91) for each sample.*

Samples	**1**	**2**	**3**	**4**	**5**	**6**	**7**	**8**	**9**	**10**	**11**
N	205	206	190	202	204	197	204	204	204	201	204
Median	5	3	1	2	1	0	2	10	1	2	2
IQ_1-IQ_3	2-8	1-6	0-3	1-3	1-3	0-1	1-4	5-16	0-3	1-4	1-5
Minimum	0	0	0	0	0	0	0	0	0	0	0
Maximum	17	13	7	6	6	2	8	32	7	8	11
DFI (%)	58	25	42	80	9	8	9	8	12	39	16

The distribution of number of foci counted in each cell nuclei from the different samples are presented as a scatter dot plot (Fig. 30 a) and presents differences in dSTRIDE signals between samples. Results obtained from the two DNA fragmentation tests showed apparently different results when comparing median of detected dSTRIDE signals with DFI (%) by SCSA. Especially two samples showed high discrepancy between the tests (sample 4 and 8). Simple regression analysis was performed to assess a possible relation between the two methods. The results showed no relation ($r = .36$, $p = .274$), and are also illustrated as a near-horizontal slope in figure 28 b. Interestingly, when the two samples with high discrepancy were removed, a positive relation was found ($r = .686$, $p = .042$) between the two methods (shown in Appendix, A2.3, Figure 32).

Overall results indicated a disparity between the two methods when using the median dSTRIDE foci values obtained from all 11 samples.

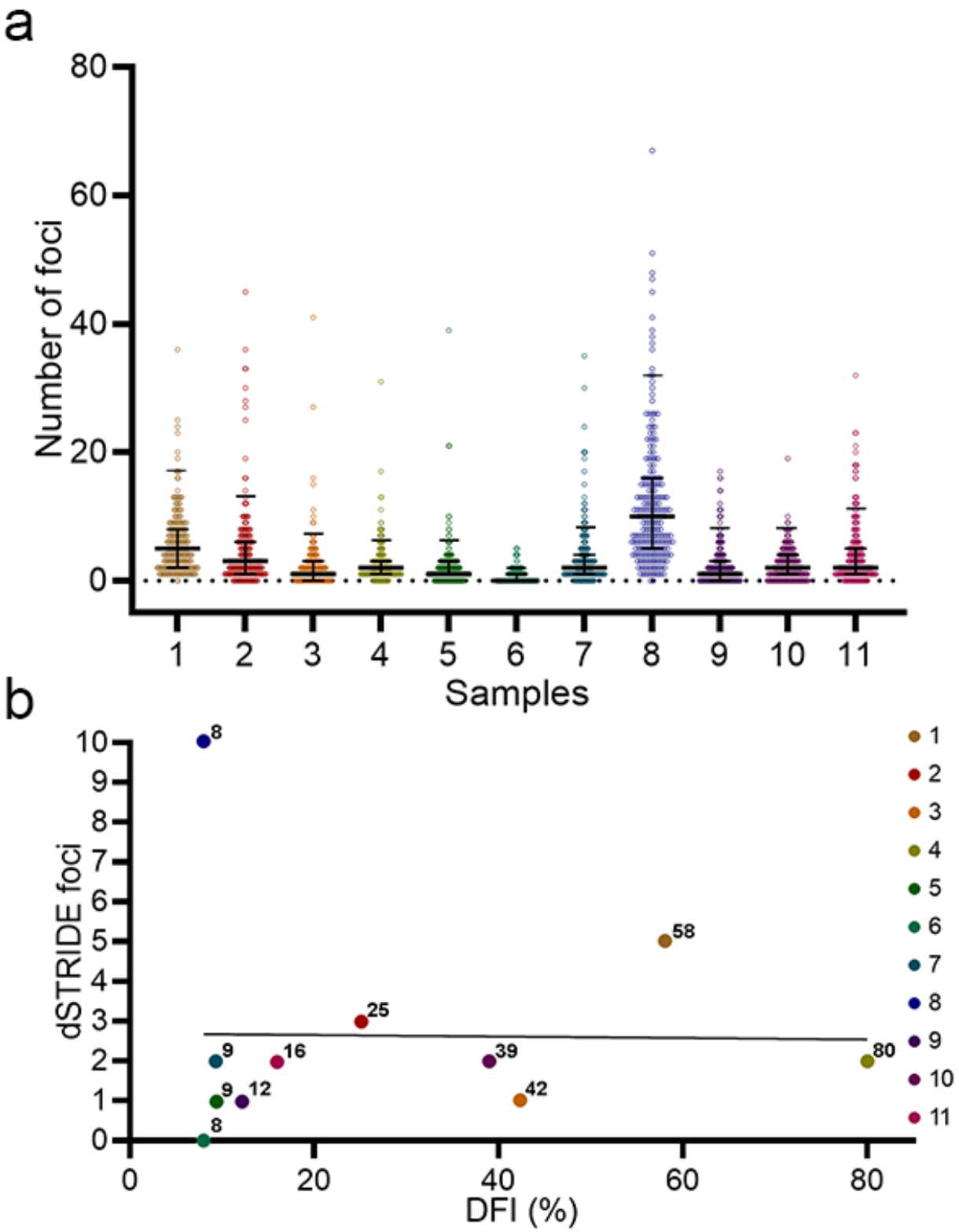

Figure 30 *Number of dSTRIDE foci detected in semen samples and compared with known DNA fragmentation index (DFI).*

(a) Scatter dot plot presenting distribution of dSTRIDE foci across samples. Number of foci in each cell are presented as individual dots. Median with lower and upper quartiles are presented in the scatterplot as horizontal bars in black for all samples. The upper line in each sample indicates the maximum value as defined by Tukey's fences. (b) Simple regression analysis

presenting DNA fragmentation index obtained from SCSA (91) with dSTRIDE signals as median values in the same semen samples. DFI values are written right to each sample.

4. Discussion

In this project, we established and optimized a new protocol for *in situ* detection and quantification of DSBs specifically in spermatozoa. In primary tests, we successfully reproduced and challenged the dSTRIDE method in somatic cells using DNA damaging agents. Afterwards, the dSTRIDE protocol had to be modified to overcome the challenges arising from the sperm cell's characteristics, which include their non adherent nature and a highly compact chromatin structure. In this process, sensitivity and specificity of dSTRIDE were assessed by inducing DSBs and by comparing different sperm preparation methods. Finally, we performed experiments to compare dSTRIDE results with those obtained using other well-established methods to detect DNA fragmentation in spermatozoa, SCSA and γH2AX detection.

4.1 Reproducing and testing the original STRIDE protocols in somatic cells: a challenge

The original s- and dSTRIDE protocols were mainly developed for somatic cells (88). Therefore, in the first series of experiments we aimed to reproduce and test them in the breast cancer cell line MCF-7 since, as the majority of cancer cells, they were expected to harbour a significant level of DNA damage (104, 118). Unfortunately, even though the theory behind each of the two methods was clearly described by the authors, several details were missing in the published protocols.

For the dSTRIDE method, it was unclear how the washes were performed after each reaction and we obtained high levels of background in our first attempts to detect DSBs in MCF-7 (Fig. 8). Preliminary results obtained by Dr. Erwan Delbarre in our lab clearly established a link between the BrdU incorporation step of the protocol and the unspecific signals observed all over the coverslips. Indeed, no fluorescence signals were observed when dSTRIDE was performed without BrdU, indicating that the background was not associated to the PLA procedure (data obtained before the beginning of my project and not shown in this thesis). However, the foci-like appearance of the signals across the coverslips suggested that the remaining, non-

incorporated molecules of BrdU were close enough to each other to be detected during the PLA procedure (119). We drastically reduced the signals outside the nuclei by increasing the intensity of the shaking during the washes following the BrdU incorporation step (Fig. 8). When such hard shaking was applied, the background around the cells were reduced to almost zero in most of our experiments. These results are consistent with the hypothesis that with mild washes, a large amount of BrdU can remain on the coverslip after the labelling of DSBs in the dSTRIDE procedure. The need for reducing the background (also called noise) to a minimal level is a recurrent problem in quantitative analyses relying on fluorescence microscopy (discussed for example in (120)). In methods based on PLA such as STRIDE, the noise may prevent the accuracy of the measurements. Indeed, the quantification of the PLA signals in cells often requires the acquisition of images allowing the visualisation of all of them across the region of interest (for ex. the nucleus). Random foci near this region may be difficult to identify as such and some would undoubtedly be counted as positive signals, potentially distorting the analyses. In our case, it would be difficult to exclude foci located above the nucleus, as the space between the top of the latter and the outer surface of the plasma membrane is very thin when the cells are growing on coverslips (Fig. 31).

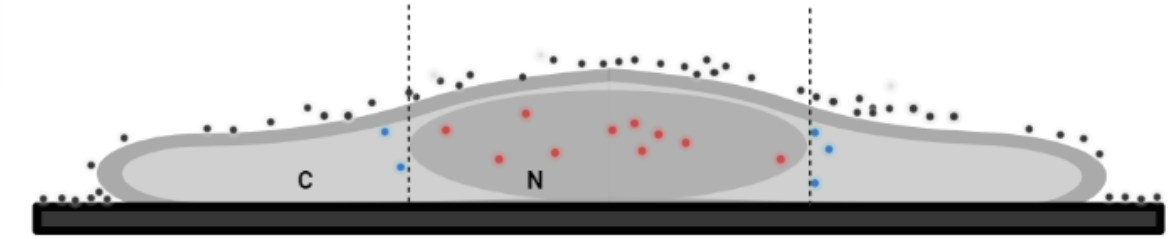

Figure 31 *Schematic representation of an MCF-7 cell showing dSTRIDE signals and a high level of unspecific background.*
The drawing shows a cross section of an MCF-7 cell growing on a glass coverslip, harbouring positive signals of dSTRIDE (red dots) in the nucleus (N). Unspecific signals corresponding to un-incorporated BrdU are represented with black dots when outside the cell and by blue dots inside the cytoplasm (C). While the cytoplasmic signals are easy to recognize on images taken with a fluorescence microscope and hence to remove in quantitative analyses, the unspecific signals right above the nucleus (between the dotted lines) are sometimes difficult to identify as such and may be considered as positive dSTRIDE signals. Illustration created by author using Biorender.com.

Once optimized, we successfully tested the dSTRIDE protocol using UVB exposure and different concentrations of H_2O_2 to induce DNA breaks in MCF-7 cells. For each condition, we observed an increase of the overall amount of dSTRIDE signals in the nucleus of treated cells compared to their respective control cells (Fig. 10 a and Fig. 13). Moreover, the response was dose- and incubation time-dependent with H_2O_2, consistent with the high sensitivity of the dSTRIDE method claimed by the authors (88). These increases were paralleled with higher levels of H2AX phosphorylation (γH2AX) (Fig. 11 and Fig. 12), an early event of the DNA damage response in case of DSBs (121). These data confirm the induction of DSBs in our experiments and strongly suggest that the dSTRIDE signals observed in the cells do specifically correspond to DSB sites. To firmly conclude that dSTRIDE and γH2AX signals are associated with the same DNA structures, an additional experiment could be to incorporate BrdU with the TdT enzyme as in dSTRIDE and to further perform a PLA using primary antibodies against BrdU and γH2AX. Unfortunately, we could not test this within the time frame of this project.

For the sSTRIDE method, the concentrations and/or volumes of the different reagents needed to incorporate labelled nucleotides at SSB sites were not indicated in the original publication (88). In contrast to dSTRIDE, this step was not performed using a commercial kit. Even though we followed the recommendations provided with the Endogenous Biotin-Blocking Kit (Molecular Probes, revised 22.04.2002) and further tested different conditions to block the access to endogenous biotin, we failed to reduce the cytoplasmic background generated by the sSTRIDE procedure in MCF-7 cells. Moreover, sSTRIDE gave similar results when performed with or without labelled dNTPs (Fig. 9 b) and the induction of DNA damage by UVB irradiation did not increase significantly the sSTRIDE signals within the nucleus compared to untreated cells (Fig. 10 b).

These observations strongly suggest that (i) our sSTRIDE procedure failed to label SSBs and (ii) the fluorescence signals detected in our experiments most likely correspond to biotin naturally present in the cell nucleus, mitochondria and cytosol (122). A possible way to confirm this hypothesis, at least partially, would be to stain mitochondria using a mitotracker in addition to the sSTRIDE protocol. It is well known that cells with endogenous biotin should be treated with a blocking solution before any experiment relying on biotin labelling and that this step is critical for quantitative analyses. For further attempts, the blocking step could be performed without the washing steps between streptavidin and biotin incubations, as described in a previous

study (123) mentioned on Thermo Fisher website. On the contrary, another approach could be to wash even more thoroughly between and after incubation with streptavidin and biotin. The protocol we followed included 3 x 30 seconds washing between and 3 x 5 minutes of washing after biotin incubation, while another suggestion from Thermo Fisher (2009) (124) was to use 3 x 10 minutes of washing between and after biotin-incubation. Another group used washes of 3 x 5 minutes both in between and after biotin-incubation (125), indicating that the washing step after streptavidin-incubation could at least be prolonged. However, reducing the overall background in our experiments would not be of any use if we cannot address the dNTPs incorporation issues. And for this, much more work has to be done to test different conditions since we did not find any published studies relying on the incorporation, in fixed cells, of dNTPs by DNA polymerase I (*E. coli*).

4.2 Establishing and optimising dSTRIDE for spermatozoa

4.2.1 Dealing with the non-adherent nature of spermatozoa

Spermatozoa are non-adherent cells and their attachment onto glass coverslips relies commonly on the coating of the latter by poly-L-lysine (106). We found only few publications where the method used for attachment of spermatozoa to coverslips was fully described and it seemed that each lab had their own protocol. Therefore, we performed several tests to optimize the coating conditions and the number of spermatozoa, as well as the volume of sperm preparation to be used in this process. The two major challenges we had to face were (i) the loss of spermatozoa after the attachment procedure, and (ii) the heterogeneity of the cell distribution across the coverslip with very dense area making measurements in these regions nearly impossible.

The volume of semen as well as how it was added to each coverslip was appeared rapidly to be critical parameters. When coverslips were immersed in semen in 24-well plates (Table 3), a drastic cell loss was observed in every experiment. Adding the semen sample to a coverslip placed on a parafilm at room temperature and let it totally dry successfully minimized the cell loss during the following procedures. This idea was inspired from a study were immunofluorescence on boar semen was performed using spots of only 5 µl of semen suspension onto the coverslips (107). However, when using the same volume (5 µl) of sperm suspension, we noticed an important accumulation of

cells at the edges of the coverslips, with only few in the centre (Fig. 14). This pitfall was circumvented by adding a single, larger drop of semen sample to the centre of a still-wet coated coverslip to spread cells homogeneously, instead of making several small spots across the surface. After this procedure, it was essential to let the coverslip dry completely. Indeed, spermatozoa's primary binding structures are their heads and their tail remain motile for a while if immersed in a buffer such as PBS (126). We observed that the midpiece and tail were ripped off and washed away during the fixation step if the spermatozoa were not dried out before the procedure.

In conclusion, we recommend the following procedure to attach spermatozoa on coverslips in experiments where it is needed: First, add 300 µL of 0.1% poly-L-lysine on top of a coverslip in a 24-well plate. Then, right before applying spermatozoa, use a tweezer and place the coverslip into distilled H_2O then PBS for a second each and place on parafilm. Last, add 15 µL of semen to the wet coverslip and wait to it is totally dried.

4.2.2 Trying to implement the dSTRIDE protocol in spermatozoa brings the background issue to another, more complex level

When trying to optimize the dSTRIDE protocol to make it suitable to detect DSBs in spermatozoa, we used a considerable amount of time to overcome the background obstacle associated to the use of both poly-L-lysin and BrdU. This could have been avoided if the authors of the original article had provided proper descriptions of their protocols and/or if they answered our questions. Nevertheless, while the original protocol assessed DSBs in spermatozoa prepared by density gradient centrifugation (88), wanted to examine cells from the whole ejaculate since the evaluation of DNA fragmentation should mirror the whole semen sample.

When dSTRIDE was performed in spermatozoa attached on coverslips using the same procedure as in MCF-7 cells it resulted in high amounts of unspecific signals all over the coverslips, even with intense shaking during the washing steps (Fig. 15 a). We identified the background to be due to the poly-L-lysine coating of the coverslips, to which BrdU can attach in a non-specific manner. Having spermatozoa on coverslips before starting the dSTRIDE procedure appears then to be something to avoid and we resolved this issue by doing the BrdU incorporation step in Falcon tubes and attaching the sperm cells to the coverslips after that. However, this experimental setup requires

several centrifugations before fixation and since we wanted to measure DNA fragmentation, it was essential to prevent as much as possible additional DNA damage, as well as non-physiological alterations of the sperm cells. To ensure that, the centrifugations were performed at low speed (400 x ***g***) and at 4°C to minimize the generation of DNA fragmentation by ROS (127-129). Unexpectedly, we figured out that the type of tubes and centrifuges used in this optimized protocol played a critical role. Indeed, using 1.5 mL Eppendorf tubes together with a fixed angle centrifuge or PET 15mL tubes led to a gradual and critical loss of cells across the procedure. When the aforementioned steps were performed in PP/PS 15 mL tubes combined with a swing-out rotor centrifuge, a strong cell pellet remained visible until the final wash before cell attachment on coverslip and enough spermatozoa were present to be further processed. We also tried to use 1% BSA in PBS during the washing steps instead of replacing the material of the tubes used, but clusters of cells were generated, and this option was not further investigated. For further optimization, centrifugations with a higher force than 400 x ***g*** but shorter time than 10 minutes could also be tested as the centrifugation time is of more importance than centrifugation force in the formation of ROS (130).

In conclusion, we recommend performing the initial steps of the dSTRIDE procedure until the final washes after BrdU incorporation in tubes as we observed minimal background (Fig. 15 b).

4.2.3 Accessing the highly compacted sperm DNA

A mature spermatozoon has its genetic material condensed by protamines, making the DNA highly compacted compared to a somatic cell (27). So, when the access to DNA is required to address specific questions in sperm cells, procedures allowing to open their chromatin are often included in the experimental setup (131, 132). In the dSTRIDE method, the TdT enzyme must get access to dsDNA breaks to incorporate BrdU at these sites. In this thesis, we worked out a chromatin decondensation protocol to be performed prior to dSTRIDE, based on *Antonucci et. al* (2013) (95). The article stated that DTT alone does not decondense chromatin optimally and showed that the addition of heparin into the decondensation solution greatly increased the accessibility to DNA (95). These reagents are analogues of heparan sulphate (133) and glutathione (134) promoting decondensation of sperm chromatin at time of fertilization.

We obtained more dSTRIDE signals in decondensed spermatozoa than in non-treated ones from the same semen sample, consistent with the higher accessibility to discrete DNA sites after chromatin decompaction (Fig 24). The physical appearance of spermatozoa was also altered after the decondensation procedure with a slight, but obvious swelling of the nucleus, making it easier to evaluate and analyse only the spermatozoa successfully decondensed. It is known that the achievement of decondensed chromatin in spermatozoa can vary based on plasma membrane integrity, and spermatozoa with lower plasma membrane integrity achieve chromatin decondensation faster (135). The observed altered nuclear shape of some spermatozoa after incubation with the decondensation solution (Fig. 22), could therefore be a sign of lower plasma membrane integrity. Since the population of spermatozoa in the whole ejaculate are heterogenous, some differences in the degree of decondensation are likely. Either way, by using this protocol, the shape of nucleus is maintained and successfully decondensed in most of spermatozoa regardless sample used.

The presence of dSTRIDE signals in the tail decondensed spermatozoa in some experiments made us question whether our procedure damages DNA or initiates DNA leakage? A study investigating the plausible increase of sperm DNA fragmentation of 5 mM DTT (136) showed no statistical increase between samples with and without DTT. After implementing addition washes, these signals were substantially decreased but still present in spermatozoa from samples with high DNA fragmentations or in cells from fractions exposed to UVB-irradiation. It did not compromise the counted dSTRIDE foci in the cell nuclei and we determined that is was not a problem in the end.

The issue of the highly compacted structure of sperm chromatin is a recurrent topic in the research field focusing on sperm DNA fragmentation and the approaches used in the different DNA fragmentation tests to detect DNA damage in spermatozoa remain source of intense discussions. These tests measure different aspects of DNA fragmentation and differ remarkably from one to the other. SCSA open chromatin directly at the site of breaks (137), Comet assay denatures the chromatin and relaxes DNA loops domain for a better access to DNA breaks (138) while the original TUNEL assay does not decondense chromatin. This was reported by *Mitchell et al.* (2011) (116) when they stated that TUNEL consistently underestimates DNA damage and further suggest a decondensation procedure using DTT prior to TUNEL assay. In the temporary 6th edition of the WHO laboratory manual for the examination and

processing of human semen, chromatin decondensation is listed as the part of the modified TUNEL assay protocol.

Decondensation of chromatin is not performed in most studies published using TUNEL assay or dSTRIDE, but since we wanted to obtain the number of signals as closely related to the cell's whole amount of DSBs, decondensation was implemented. The decondensation procedure contains a mild fixation step with PFA (0.5%) followed by the opening of chromatin using Tx-100, DTT and heparin. At last, we added three washes to remove all reagents before fixation.

4.3 Evaluation of the dSTRIDE sensitivity

4.3.1 In response to DNA damaging agents

By exposing spermatozoa to different DNA damaging agents with several experimental setups we seek to measure the sensitivity and accuracy of our new method while it was obvious in MCF-7 cells, the effect of UVB irradiation on sperm nucleus was difficult to evaluate by dSTRIDE. Our observations suggested a difference between the levels of dSTRIDE signals in spermatozoa exposed to UVB for 10 minutes and those from non-irradiated spermatozoa. These results were consist with *Mallidis et al.* (2011) (139) who observed an increased DNA damage in cells irradiated by UVB for 10 minutes. Study from *Amaral et. al* (2013) (140) also indicated that UVB irradiation generated ROS in the mitochondria found in the midpiece of a spermatozoon, with a significant accumulated number after 60 seconds of radiation. In conclusion, we observed an expected increase of dSTRIDE signals in spermatozoa exposed to UVB radiation.

To test our protocol further, we wanted to incubate cells with different H_2O_2 concentrations. A significant increase of dSTRIDE signals was however observed in spermatozoa incubated with different concentrations of H_2O_2 (Fig. 26 b, Table 5). We based our approach on the article from *Kemal Duru et al.* (2000) (141). In their experiment, spermatozoa were incubated with different concentrations of H_2O_2 and DNA fragmentation assessed using a TUNNEL assay. Their results showed a significantly higher DNA fragmentation value when spermatozoa were treated with 200 µM for 2 hours at 37°C compared to control (0 µM) cells. In addition, a minimum concentration of 100 µM was necessary to observe a significant difference in DNA fragmentation between treated and control cells. Strikingly, not only we observed a dose-response effect in our experiments, but we also measured a significantly higher

number of dSTRIDE signals in spermatozoa exposed to H_2O_2 with a concentration as low as 40 µM compared to control cells. These data argue for a higher sensitivity of dSTRIDE compared to the classical TUNNEL assay used by *Kemal Duru et al.* in their study and confirm the quantitative aspect of the method. Of note, we did not observe visible increases of dSTRIDE signals when we used 10 µM H_2O_2, consistent with the results obtained for this concentration in the study mentioned above (141). To further confirm our results and better assess the sensitivity of the dSTRIDE method, it could be interesting to repeat the same type of experiment with more conditions, for example using 10 different H_2O_2 concentrations spanning from 10 µM to 200 µM. Of course, the reproducibility of the results would have to be confirmed in several semen samples.

4.3.2 Spermatozoa isolated by swim-up vs spermatozoa from whole ejaculate: dSTRIDE can detect the difference

Swim-up is usually performed to isolate motile spermatozoa, used for fertilization since spermatozoa with poor motility most likely won't reach and penetrate the oocyte (142). Spermatozoa isolated by preparation of swim-up also contain less DNA fragmentation (143) and we used this property to test our protocol.

Using dSTRIDE, we detected significantly less DSBs in swim-up spermatozoa compared to control cells, as expected (Fig. 27). These results are consistent with other studies comparing DNA fragmentation in control and swim-up fractions from semen samples using SCD assay (144, 145) or TUNEL (143). Results published using TUNEL (obtained by fluorescence microscope) show more variability than studies using SCD assay, resulting in contradicting results, with and without significantly less DNA fragmentation in the swim-up fraction (143, 146). It is worth mentioning that swim-up was performed with some variations and that the number of spermatozoa counted varied across the studies.

To conclude, even though the experiments were performed on spermatozoa from only one semen sample, our results show similar trends compared to earlier studies and suggest a functional, sensitive dSTRIDE method that can detect differences in DNA fragmentation between motile spermatozoa and spermatozoa from the whole ejaculate.

4.4 Can dSTRIDE be a new reliable DNA fragmentation test?

The experiments referred to in this section are preliminary and were performed only once.

4.4.1 Comparison of dSTRIDE with γH2AX-detection

Although spermatozoa do not have an active DNA repair machinery, protein-kinases that phosphorylates histone H2AX on Ser139 are present in the nucleus of human spermatozoa (147). When DSBs occur in sperm cells, H2AX are phosphorylated (γH2AX) and accumulates at the site of DNA damage (148, 149). Since DNA repair is terminated in mature spermatozoa, the phosphorylated state remains in the cells (150), and γH2AX can be detected. This characteristic makes γH2AX to a valid biomarker for indirect detection of DSBs in human spermatozoa.

To compare DSBs results between dSTRIDE and γH2AX immunofluorescence we performed the two methods in parallel. We used two different semen samples and expected to have different DNA fragmentation levels. Our results showed similarities between the relative number of signals detected by each method. However, the quantification of the γH2AX signals should have been conducted in the same way as for dSTRIDE to firmly conclude the correlation between dSTRIDE and γH2AX signals obtained by the two methods.

A very interesting study published by *Garolla et al.* from 2015 (151) compared DSBs obtained by γH2AX immunostaining and TUNEL assay in spermatozoa from infertile men. Methods were flow cytometer based. The authors observed a significantly higher percentage of γH2AX positive spermatozoa from males from non-pregnant couples compared to pregnant couples. In addition, the quantification of γH2AX levels was shown to be a more sensitive method to measure the DFI (%) than the TUNEL assay. When evaluating the γH2AX signals in our two samples by microscopy, the signals were diffuse in each nucleus (Fig. 28) compared to the dSTRIDE foci (Fig. 29), consistent with previous studies (150). We based our preliminary conclusions on the evaluation of the bright signals in each cell when comparing samples and methods. If the experiment was quantified, we could compare the levels of γH2AX by measuring the fluorescence intensity corresponding to γH2AX signals in the whole nucleus. However, this way to analyse signals could not allow the comparison between γH2AX immunofluorescence and dSTRIDE but could show the possible difference of γH2AX

signals between the samples analysed by γH2AX immunofluorescence. Another experiment could be to implement PLA protocol after γH2AX primary antibody incubation to obtain signal enhancement and then compare. If the same amount of γH2AX signals were detected but with brighter spots, we could confirm that this method detects a remarkable higher number of DSBs compared to dSTRIDE, and therefore confirm one of the results from *Garolla et al*.

4.4.2 dSTRIDE vs SCSA

In this project, we had access to semen samples previously analysed by SCSA, as well as the DFI measured for each of them. We took this opportunity to test whether we could observe the same differences between 11 samples in terms of amount of DNA damage when using dSTRIDE or SCSA approaches. Indeed, even though we succeeded in optimizing a dSTRIDE protocol for DSBs detection in individual human spermatozoa, how to interpret the results in the context of a cell population remains an open question. On the other hand, SCSA is a standardized, reliable and highly accurate method for measuring sperm DNA fragmentation in a large number of cells (64). As mentioned earlier, comparison between methods is challenging essentially because of differences in performance between the instruments used and in the sperm preparation prior to analysing.

From the dSTRIDE experiments, resulted presented a broad range of foci numbers (Fig. 30 a) between samples. However, and to our disappointment, no relation was found between results of the two methods by simple regression analysis for all samples. When having a closer look at the results, two samples appeared to negatively affect the correlation between the two sets of data. In one of them (sample 8), the number of dSTRIDE foci per cell was clearly in contrast with the other samples, with a median value of 10 (Fig. 30 c). In the other one (sample 4), a low median value (2) was measured with dSTRIDE while the DFI-value was 80% with SCSA. When these two samples were excluded from the statistical analysis, a positive correlation was observed. We hypothesize that something went wrong with the samples during the dSTRIDE experiment rather than in the SCSA analyses, since the latter were performed in triplicate, with a good reproducibility (91). Nevertheless, to be able to draw any conclusions, the experiment must be repeated.

The use of the median may not be the optimal method to assess DNA fragmentation in dSTRIDE experiments. We did use it in this thesis as it is easily obtained, but it is not necessary the best fit. We tried express the DNA fragmentation level by the percentage of sperm with fragmented DNA in each sample, and different definitions of what a positive cell was were tested, ranging from 0 – 5 dSTRIDE foci (this are shown in Appendix, A2.3, Table 13). Despite our expectations, none of these led to a better correlation between the two methods compared to the use of median.

SCSA use acridine orange (AO) that stains low pH- and/or heat-denatured fragmented DNA in red or intact DNA in green after spermatozoa are exposed to acid (34). In flow cytometers, the threshold level of intensity must be determined so low intensity coloured cells are accounted for or evaluated as negative. The distribution of fluorescence intensities could overlap with autofluorescence, presenting false positive or negatives, depending on the threshold settings. Thresholding is also used for counting signals generated by the dSTRIDE procedure using ImageJ. The threshold for determining a signal as a dSTRIDE foci is set manually and must be low enough to detect all bright signals as positives foci and ignore what is thought to be negative. These two methods can cause conflicting results due to the specific differences between the instruments. While microscopy can be affected by subjectivity, settings on the microscope and observation time of the specimen (resulting in fluorescence bleaching), flow cytometers can be affected by threshold settings presenting false positives or negatives (for example if non-sperm elements are recognised) (152, 153). Results from TUNEL assay experiments using fluorescence microscope and flow cytometry have also reported % of TUNEL-positive sperm with conflicting results (154-156). Statistical analysis also favours large sample sizes, a time-exhausting mission if images and counting are obtained manually and semi-automatic as by dSTRIDE.

The experiment itself also had several limitations. First, dSTRIDE was only performed once in each of the 11 samples. On a regular basis, similar experiments are performed in triplicate to validate the results. In addition, only few samples were analysed. Optimally, all semen samples with known DFI measured by SCSA stored at biobank, OsloMet should be analysed. Another aspect that may account for the differences observed in the results of the two methods is that SCSA is supposed to detect both SSBs and DSBs, compared to dSTRIDE which only detect DSBs. The discrepancies between our results may come from the detection of different types of DNA damage. A higher DFI may be due to high level of SSBs, which will not be detected by dSTRIDE. We did not find any study comparing the SSB and DSB ratio, correlation or relationship

in human spermatozoa, but this aspect could bias the basis of comparison between the methods. Also, sperm chromatin was decondensed when dSTRIDE was performed in these samples, suggesting, that the accessibility to DNA in these samples could be higher for dSTRIDE than by SCSA. An interesting experiment would be to re-do the dSTRIDE procedure in these samples without the chromatin decondensation step and to compare again the results with the SCSA data.

4.5 Future possibilities for dSTRIDE

The two standardized methods for measuring DNA fragmentation in spermatozoa are SCSA and TUNEL assay, both assessed by flow cytometry. They remain expensive requiring access to a flow cytometer alongside highly qualified and dedicated personnel. If measuring sperm DNA fragmentation are going to be implemented as a test in regular semen analysis or broader used, a more accessible and clinically useful method with a high degree of sensitivity is needed. In this thesis, dSTRIDE have been optimized for use in spermatozoa, with and without decondensed chromatin. By measuring DNA fragmentation with dSTRIDE, individual events can be detected in a single cell, each corresponding to a DSB. The advantage of this in the context of semen analysis per se unknown, but future experiments can investigate if such benefits exist. It however offers the possibility to visualise where, in the sperm nucleus, DSBs are occurring, something that the other methods cannot do. This will maybe allow to define different types of spermatozoa, based on the distribution of the DSBs within their nucleus.

Compared to other methods listed in table 2 (1.3.3), dSTRIDE is a direct method when measuring DNA fragmentation. It incorporates BrdU-conjugated nucleotides at the site of a DSB and uses PLA to enhance signals for visualising foci in fluorescence microscopy. Today, dSTRIDE remain a method in the preliminary phase without any standardized protocols nor established thresholds. The time for an experiment is long compared to the other methods, especially if swim-up preparation and decondensation are performed prior to cell fixation. The possibility to increase centrifugation force and decrease time of each wash could help the protocol to make it less time-consuming. dSTRIDE procedure itself takes about 7.5 hours but further time using for analysing could be optimized with additional tools. For example, by using automated microscope platforms allowing to take 3-D images of many fields followed by automated analysis

of the signals relying on the development of algorithms allowing the recognition of the nucleus followed by the counting of foci for each cell.

Even though our results comparing dSTRIDE with SCSA showed no correlation between the two methods, our and others data (88) suggest that dSTRIDE is a sensitive method for detecting DSBs, hence DNA fragmentation. Further experiments will be needed to determine sensitivity and specificity by ROC-analyses. The interobserver variability (reproducibility, between-subject variance) and intraobserver variability (repeatability, within-subject variance) should also be determined by the mean coefficient of variation because it is important that these values are low to compare across laboratories and to obtain a reliable result for each sample. The parameters are also evaluated to be important when comparing different DNA fragmentation tests in spermatozoa.

Limitation for dSTRIDE as well as other DNA fragmentation methods in sperm, is that they use cells that cannot be further used. Indeed, the spermatozoa processed by dSTRIDE cannot be further used to fertilise the oocyte, so the direct benefit of such a method for the fertility lab is limited. However, if a high number of DSBs are found within the semen samples, then several known solutions are suggested for helping to reduce the number of breaks. Approaches using spermatozoa from second ejaculates for ART techniques suggest that sperm has lower DNA fragmentation and thus increases the chance for an embryologist to select a morphological normal spermatozoon with intact DNA (157, 158). Another possibility is to use ascorbic acid during swim-up, which was shown to reduce ROS-positive spermatozoa that can swim up to the media (159) and is especially of importance in men with DNA fragmentation due to oxidative stress.

Today, new industrial technologies including robotics and artificial intelligence (AI) emerge. Image analysis for dSTRIDE is time consuming and if such technology could be implemented in this method, it would be highly beneficial. Especially if this technology could detect and count foci with high precision while observing under the microscope. In the future, we hope that DNA fragmentation can be evaluated by looking at live spermatozoa from a camera attached to a microscope, so a cell with known low DNA damage can directly be used in for example ART. This type of research is on a rise and a recent study developed an AI-based method to identify live spermatozoa with high levels of DNA fragmentation based on their morphology (160).

Several interesting articles have also been recently published, focusing on other conventional semen parameters as concentration and motility (161, 162), and perhaps results from dSTRIDE testing could one day participate to the development of such tools.

5. Conclusion

We reproduced dSTRIDE method for performance in MCF-7 cells and tested the protocol by inducing DNA damaging agents. dSTRIDE emerged as a very promising method to visualize and quantify DSBs at the single cell level both in MCF-7 cells and in spermatozoa.

A reproductible protocol for performing sSTRIDE was not obtained in this project. It turned out that an important lack of information made the original protocols difficult to reproduce, especially in spermatozoa.

When compared dSTRIDE to DFI by SCSA in spermatozoa, no relation was seen between the results obtained by these two methods. The discrepancies between the results may come from the fact that the detection of DNA damage is different in these two methods.

Altogether, the dSTRIDE protocol that we develop will undoubtedly be of interest for all the research teams working with immunofluorescence and detection of DNA breaks in spermatozoa.

Bibliography

1. Andersen E. Statistics Norway. Decline in fertility [Internet]. 2020 03 11. Available from: https://www.ssb.no/en/befolkning/artikler-og-publikasjoner/decline-in-fertility--448107.
2. Andersen E. Statistics Norway publications. Flere bor alene [Internet]. 2020 06 25. Available from: https://www.ssb.no/befolkning/artikler-og-publikasjoner/flere-bor-alene.
3. Grasdal AL, Lommerud KE. Barnløshet blant menn i Norge. Tidsskrift for velferdsforskning. 2019.
4. WHO. Sexual and reproductive health - Multiple definitions of infertility2020.
5. Vander Borght M, Wyns C. Fertility and infertility: Definition and epidemiology. Clin Biochem. 2018;62:2-10.
6. Agarwal A, Baskaran S, Parekh N, Cho C-L, Henkel R, Vij S, et al. Male infertility. The Lancet. 2021;397(10271):319-33.
7. Widmaier EP, Raff H, Strang KT. Vander's Human Physiology: The Mechanisms of Body Function. New York, NY: McGraw-Hill Education; 2016.
8. Mäkelä J-A, Toppari J. Spermatogenesis. In: Simoni M, Huhtaniemi IT, editors. Endocrinology of the Testis and Male Reproduction. Cham: Springer International Publishing; 2017. p. 417-55.
9. Geyer CB. Setting the Stage: The First Round of Spermatogenesis. The Biology of Mammalian Spermatogonia. New York, NY: Springer; 2017. p. 39-63.
10. Paniagua R, Nistal M. Morphological and histometric study of human spermatogonia from birth to the onset of puberty. J Anat. 1984;139 (Pt 3):535-52.
11. Rato L, Alves MG, Socorro S, Duarte AI, Cavaco JE, Oliveira PF. Metabolic regulation is important for spermatogenesis. Nat Rev Urol. 2012;9(6):330-8.
12. Organization WH. WHO laboratory manual for the examination and processing of human semen. 2010(Fifth Edition):286.
13. Meistrich ML, Mohapatra B, Shirley CR, Zhao M. Roles of transition nuclear proteins in spermiogenesis. Chromosoma. 2003;111(8):483-8.
14. Marcon L, Boissonneault G. Transient DNA strand breaks during mouse and human spermiogenesis new insights in stage specificity and link to chromatin remodeling. Biol Reprod. 2004;70(4):910-8.
15. Khawar MB, Gao H, Li W. Mechanism of Acrosome Biogenesis in Mammals. Front Cell Dev Biol. 2019;7:195.
16. Hirohashi N, Yanagimachi R. Sperm acrosome reaction: its site and role in fertilization. Biol Reprod. 2018;99(1):127-33.
17. Lehti MS, Sironen A. Formation and function of sperm tail structures in association with sperm motility defects. Biol Reprod. 2017;97(4):522-36.
18. Cornwall GA. New insights into epididymal biology and function. Hum Reprod Update. 2009;15(2):213-27.

19. Barone JG, De Lara J, Cummings KB, Ward WS. DNA organization in human spermatozoa. J Androl. 1994;15(2):139-44.
20. Ward WS, De Jonge CJ, Barratt CLR, Yanagimachi R. Sperm Chromatin Stability and Susceptibility to Damage in Relation to Its Structure. The Sperm Cell2017. p. 21-35.
21. Kosower NS, Katayose H, Yanagimachi R. Thiol-disulfide status and acridine orange fluorescence of mammalian sperm nuclei. J Androl. 1992;13(4):342-8.
22. Hayden RP, Aboukhshaba A, Schlegel PN. DNA Damage in Spermatozoa. Male and Sperm Factors that Maximize IVF Success2020. p. 199-210.
23. Ward WS, Partin AW, Coffey DS. DNA loop domains in mammalian spermatozoa. Chromosoma. 1989;98(3):153-9.
24. Ward WS. Deoxyribonucleic acid loop domain tertiary structure in mammalian spermatozoa. Biol Reprod. 1993;48(6):1193-201.
25. Balhorn R. The protamine family of sperm nuclear proteins. Genome Biol. 2007;8(9):227.
26. Sotolongo B, Lino E, Ward WS. Ability of hamster spermatozoa to digest their own DNA. Biol Reprod. 2003;69(6):2029-35.
27. Ward WS. Function of sperm chromatin structural elements in fertilization and development. Mol Hum Reprod. 2010;16(1):30-6.
28. Hud NV, Milanovich FP, Balhorn R. Evidence of novel secondary structure in DNA-bound protamine is revealed by Raman spectroscopy. Biochemistry. 1994;33(24):7528-35.
29. Hud NV, Allen MJ, Downing KH, Lee J, Balhorn R. Identification of the elemental packing unit of DNA in mammalian sperm cells by atomic force microscopy. Biochem Biophys Res Commun. 1993;193(3):1347-54.
30. Kalandadze AG, Bushara SA, Vassetzky YS, Jr., Razin SV. Characterization of DNA pattern in the site of permanent attachment to the nuclear matrix located in the vicinity of replication origin. Biochem Biophys Res Commun. 1990;168(1):9-15.
31. Martins RP, Ostermeier GC, Krawetz SA. Nuclear matrix interactions at the human protamine domain: a working model of potentiation. J Biol Chem. 2004;279(50):51862-8.
32. Patel AS, Leong JY, Ramasamy R. Prediction of male infertility by the World Health Organization laboratory manual for assessment of semen analysis: A systematic review. Arab J Urol. 2018;16(1):96-102.
33. Agarwal A, Allamaneni SS. Sperm DNA damage assessment: a test whose time has come. Fertil Steril. 2005;84(4):850-3.
34. Evenson DP, Jost LK, Marshall D, Zinamanv MJ, Clegg E, Purvis K, et al. Utility of the sperm chromatin structure assay as a diagnostic and prognostic tool in the human fertility clinic. Hum Reprod. 1999(14):10.
35. Spano M, Bonde JP, Hjollund HI, Kolstad HA, Cordelli E, Leter G. Sperm chromatin damage impairs human fertility. The Danish First Pregnancy Planner Study Team. Fertil Steril. 2000;73(1):43-50.

36. Saleh RA, Agarwal A, Nada EA, El-Tonsy MH, Sharma RK, Meyer A, et al. Negative effects of increased sperm DNA damage in relation to seminal oxidative stress in men with idiopathic and male factor infertility. Fertil Steril. 2003;79 Suppl 3:1597-605.
37. Alkhayal A, San Gabriel M, Zeidan K, Alrabeeah K, Noel D, McGraw R, et al. Sperm DNA and chromatin integrity in semen samples used for intrauterine insemination. J Assist Reprod Genet. 2013;30(11):1519-24.
38. Oleszczuk K, Augustinsson L, Bayat N, Giwercman A, Bungum M. Prevalence of high DNA fragmentation index in male partners of unexplained infertile couples. Andrology. 2013;1(3):357-60.
39. Esteves SC, Sanchez-Martin F, Sanchez-Martin P, Schneider DT, Gosalvez J. Comparison of reproductive outcome in oligozoospermic men with high sperm DNA fragmentation undergoing intracytoplasmic sperm injection with ejaculated and testicular sperm. Fertil Steril. 2015;104(6):1398-405.
40. Zini A. Use of testicular sperm for intracytoplasmic sperm injection in oligozoospermic couples with high levels of sperm deoxyribonucleic acid fragmentation. Fertil Steril. 2015;104(6):1376-7.
41. Pabuccu EG, Caglar GS, Tangal S, Haliloglu AH, Pabuccu R. Testicular versus ejaculated spermatozoa in ICSI cycles of normozoospermic men with high sperm DNA fragmentation and previous ART failures. Andrologia. 2017;49(2).
42. Salonia A, Bettocchi C, Carvalho J, Corona G, Jones TH, Kadioglu A, et al. European Association of Urology. EAU Guidelines on Sexual and Reproductive Health [Internet]. 2020 05 29. Available from: https://uroweb.org/wp-content/uploads/EAU-Guidelines-on-Sexual-and-Reproductive-Health-2020.pdf.
43. Damsgaard J, Joensen UN, Carlsen E, Erenpreiss J, Blomberg Jensen M, Matulevicius V, et al. Varicocele Is Associated with Impaired Semen Quality and Reproductive Hormone Levels: A Study of 7035 Healthy Young Men from Six European Countries. Eur Urol. 2016;70(6):1019-29.
44. Agarwal A, Parekh N, Panner Selvam MK, Henkel R, Shah R, Homa ST, et al. Male Oxidative Stress Infertility (MOSI): Proposed Terminology and Clinical Practice Guidelines for Management of Idiopathic Male Infertility. World J Mens Health. 2019;37(3):296-312.
45. National Institute for Health and Care Excellence. Fertility problems: assessment and treatment [Internet]. 2013 02 20. Available from: https://www.nice.org.uk/guidance/cg156/resources/fertility-problems-assessment-and-treatment-pdf-35109634660549.
46. Practice Committee of the American Society for Reproductive M. Diagnostic evaluation of the infertile male: a committee opinion. Fertil Steril. 2015;103(3):e18-25.
47. Keel BA. Within- and between-subject variation in semen parameters in infertile men and normal semen donors. Fertil Steril. 2006;85(1):128-34.

48. Francavilla F, Barbonetti A, Necozione S, Santucci R, Cordeschi G, Macerola B, et al. Within-subject variation of seminal parameters in men with infertile marriages. Int J Androl. 2007;30(3):174-81.
49. Cooper TG, Noonan E, von Eckardstein S, Auger J, Baker HW, Behre HM, et al. World Health Organization reference values for human semen characteristics. Hum Reprod Update. 2010;16(3):231-45.
50. Carlsen E, Giwercman A, Keiding N, Skakkebaek NE. Evidence for decreasing quality of semen during past 50 years. BMJ. 1992;305(6854):609-13.
51. Levine H, Jorgensen N, Martino-Andrade A, Mendiola J, Weksler-Derri D, Mindlis I, et al. Temporal trends in sperm count: a systematic review and meta-regression analysis. Hum Reprod Update. 2017;23(6):646-59.
52. George K, Kamath MS. Fertility and age. J Hum Reprod Sci. 2010;3(3):121-3.
53. United Nations. World Population Prospects 2019 [Internet]. 2019 12. Available from: https://population.un.org/wpp/Download/Standard/Fertility/.
54. Sharma R, Agarwal A, Rohra VK, Assidi M, Abu-Elmagd M, Turki RF. Effects of increased paternal age on sperm quality, reproductive outcome and associated epigenetic risks to offspring. Reprod Biol Endocrinol. 2015;13:35.
55. Page H. The increasing demand for infertility treatment. Health Trends. 1988;20(4):115-8.
56. De Geyter C, Wyns C, Calhaz-Jorge C, de Mouzon J, Ferraretti AP, Kupka M, et al. 20 years of the European IVF-monitoring Consortium registry: what have we learned? A comparison with registries from two other regions. Hum Reprod. 2020;35(12):2832-49.
57. European IVFmCddftESoHR, Embryology, Wyns C, Bergh C, Calhaz-Jorge C, De Geyter C, et al. ART in Europe, 2016: results generated from European registries by ESHRE. Hum Reprod Open. 2020;2020(3):hoaa032.
58. Helsedirektoratet. Assistert befruktning2020.
59. Sherins RJ, Thorsell LP, Dorfmann A, Dennison-Lagos L, Calvo LP, Krysa L, et al. Intracytoplasmic sperm injection facilitates fertilization even in the most severe forms of male infertility: pregnancy outcome correlates with maternal age and number of eggs available. Fertil Steril. 1995;64(2):369-75.
60. Ward WS. Regulating DNA supercoiling: sperm points the way. Biol Reprod. 2011;84(5):841-3.
61. Garcia-Rodriguez A, Gosalvez J, Agarwal A, Roy R, Johnston S. DNA Damage and Repair in Human Reproductive Cells. Int J Mol Sci. 2018;20(1).
62. Fernandez JL, Muriel L, Goyanes V, Segrelles E, Gosalvez J, Enciso M, et al. Simple determination of human sperm DNA fragmentation with an improved sperm chromatin dispersion test. Fertil Steril. 2005;84(4):833-42.
63. Aitken RJ, De Iuliis GN, Nixon B. The Sins of Our Forefathers: Paternal Impacts on De Novo Mutation Rate and Development. Annu Rev Genet. 2020;54:1-24.

64. Agarwal A, Majzoub A, Baskaran S, Panner Selvam MK, Cho CL, Henkel R, et al. Sperm DNA Fragmentation: A New Guideline for Clinicians. World J Mens Health. 2020;38(4):412-71.
65. Ribas-Maynou J, Benet J. Single and Double Strand Sperm DNA Damage: Different Reproductive Effects on Male Fertility. Genes (Basel). 2019;10(2).
66. Simon L, Murphy K, Shamsi MB, Liu L, Emery B, Aston KI, et al. Paternal influence of sperm DNA integrity on early embryonic development. Hum Reprod. 2014;29(11):2402-12.
67. Virro MR, Larson-Cook KL, Evenson DP. Sperm chromatin structure assay (SCSA) parameters are related to fertilization, blastocyst development, and ongoing pregnancy in in vitro fertilization and intracytoplasmic sperm injection cycles. Fertil Steril. 2004;81(5):1289-95.
68. Haghpanah T, Eslami-Arshaghi T, Afarinesh MR, Salehi M. Decreased Fertilization: Human Sperm DNA Fragmentation and in Vitro Maturation of Oocyte in Stimulated Icsi Cycles. Acta Endocrinol (Buchar). 2017;13(1):23-31.
69. Kim SM, Kim SK, Jee BC, Kim SH. Effect of Sperm DNA Fragmentation on Embryo Quality in Normal Responder Women in In Vitro Fertilization and Intracytoplasmic Sperm Injection. Yonsei Med J. 2019;60(5):461-6.
70. Lin MH, Kuo-Kuang Lee R, Li SH, Lu CH, Sun FJ, Hwu YM. Sperm chromatin structure assay parameters are not related to fertilization rates, embryo quality, and pregnancy rates in in vitro fertilization and intracytoplasmic sperm injection, but might be related to spontaneous abortion rates. Fertil Steril. 2008;90(2):352-9.
71. Zini A, Boman JM, Belzile E, Ciampi A. Sperm DNA damage is associated with an increased risk of pregnancy loss after IVF and ICSI: systematic review and meta-analysis. Hum Reprod. 2008;23(12):2663-8.
72. Kennedy C, Ahlering P, Rodriguez H, Levy S, Sutovsky P. Sperm chromatin structure correlates with spontaneous abortion and multiple pregnancy rates in assisted reproduction. Reprod Biomed Online. 2011;22(3):272-6.
73. Bungum M, Humaidan P, Spano M, Jepson K, Bungum L, Giwercman A. The predictive value of sperm chromatin structure assay (SCSA) parameters for the outcome of intrauterine insemination, IVF and ICSI. Hum Reprod. 2004;19(6):1401-8.
74. Giwercman A, Lindstedt L, Larsson M, Bungum M, Spano M, Levine RJ, et al. Sperm chromatin structure assay as an independent predictor of fertility in vivo: a case-control study. Int J Androl. 2010;33(1):e221-7.
75. Zini A. Are sperm chromatin and DNA defects relevant in the clinic? Syst Biol Reprod Med. 2011;57(1-2):78-85.
76. Green KA, Patounakis G, Dougherty MP, Werner MD, Scott RT, Jr., Franasiak JM. Sperm DNA fragmentation on the day of fertilization is not associated with embryologic or clinical outcomes after IVF/ICSI. J Assist Reprod Genet. 2020;37(1):71-6.

77. Tharakan T, Bettocchi C, Carvalho J, Corona G, Jones TH, Kadioglu A, et al. European Association of Urology Guidelines Panel on Male Sexual and Reproductive Health: A Clinical Consultation Guide on the Indications for Performing Sperm DNA Fragmentation Testing in Men with Infertility and Testicular Sperm Extraction in Nonazoospermic Men. Eur Urol Focus. 2021.
78. Ribas-Maynou J, Garcia-Peiro A, Abad C, Amengual MJ, Navarro J, Benet J. Alkaline and neutral Comet assay profiles of sperm DNA damage in clinical groups. Hum Reprod. 2012;27(3):652-8.
79. Casanovas A, Ribas-Maynou J, Lara-Cerrillo S, Jimenez-Macedo AR, Hortal O, Benet J, et al. Double-stranded sperm DNA damage is a cause of delay in embryo development and can impair implantation rates. Fertil Steril. 2019;111(4):699-707 e1.
80. Simon L, Proutski I, Stevenson M, Jennings D, McManus J, Lutton D, et al. Sperm DNA damage has a negative association with live-birth rates after IVF. Reprod Biomed Online. 2013;26(1):68-78.
81. Wykes SM, Krawetz SA. Conservation of the PRM1 --> PRM2 --> TNP2 domain. DNA Seq. 2003;14(5):359-67.
82. Barratt CL, Aitken RJ, Bjorndahl L, Carrell DT, de Boer P, Kvist U, et al. Sperm DNA: organization, protection and vulnerability: from basic science to clinical applications--a position report. Hum Reprod. 2010;25(4):824-38.
83. Barratt CL, De Jonge CJ. Clinical relevance of sperm DNA assessment: an update. Fertil Steril. 2010;94(6):1958-9.
84. Evenson DP, Darzynkiewicz Z, Melamed MR. Relation of mammalian sperm chromatin heterogeneity to fertility. Science. 1980;210(4474):1131-3.
85. Gawecka JE, Boaz S, Kasperson K, Nguyen H, Evenson DP, Ward WS. Luminal fluid of epididymis and vas deferens contributes to sperm chromatin fragmentation. Hum Reprod. 2015;30(12):2725-36.
86. Chohan KR, Griffin JT, Lafromboise M, De Jonge CJ, Carrell DT. Comparison of chromatin assays for DNA fragmentation evaluation in human sperm. J Androl. 2006;27(1):53-9.
87. Henkel R, Hoogendijk CF, Bouic PJ, Kruger TF. TUNEL assay and SCSA determine different aspects of sperm DNA damage. Andrologia. 2010;42(5):305-13.
88. Kordon MM, Zarebski M, Solarczyk K, Ma H, Pederson T, Dobrucki JW. STRIDE-a fluorescence method for direct, specific in situ detection of individual single- or double-strand DNA breaks in fixed cells. Nucleic Acids Res. 2020;48(3):e14.
89. Alam MS. Proximity Ligation Assay (PLA). Curr Protoc Immunol. 2018;123(1):e58.
90. Invitrogen™ Countess™ Automated Cell Counter Manual. Carlsbad, US: Life Technologies Corporation; 2009.

91. Andersen JM, Herning H, Aschim EL, Hjelmesaeth J, Mala T, Hanevik HI, et al. Body Mass Index Is Associated with Impaired Semen Characteristics and Reduced Levels of Anti-Mullerian Hormone across a Wide Weight Range. PLoS One. 2015;10(6):e0130210.
92. Anamthathmakula P, Winuthayanon W. Mechanism of semen liquefaction and its potential for a novel non-hormonal contraceptiondagger. Biol Reprod. 2020;103(2):411-26.
93. CooperSurgical Company. ORIGIO Sperm Freezing Medium [Internet]. 2019 02 28. Available from: https://coopersurgical.marketport.net/MarketingZone/MZDirect/Source/919c6c53-5e64-4216-8863-070823123fac.
94. Makler A, Jakobi P. Effects of shaking and centrifugation on human sperm motility. Arch Androl. 1981;7(1):21-6.
95. Antonucci N, Manes S, Corradetti B, Manicardi GC, Borini A, Bizzaro D. A novel in vitro sperm head decondensation protocol for rapid flow cytometric measurement of deoxyribonucleic acid content. Fertil Steril. 2013;99(7):1857-61.
96. Nelson DL, Cox MM. Lehninger Principles of Biochemistry. New York: W. H. Freeman and Company; 2017.
97. Cordelières FP. ImageJ The 3D object counter plugin aka 3D-OC [Internet]. 2009 11 12. Available from: https://imagejdocu.tudor.lu/lib/exe/fetch.php?media=plugin:analysis:3d_object_counter:3d-oc.pdf.
98. Lovdata. Lov om medisinsk og helsefaglig forskning (helseforskningsloven) [Internet]. 2018 07 20. Available from: https://lovdata.no/dokument/NL/lov/2008-06-20-44.
99. Lovdata. Lov om humanmedisinsk bruk av bioteknologi mm (bioteknologiloven) [Internet]. 2021 01 01. Available from: https://lovdata.no/dokument/NL/lov/2003-12-05-100?q=bioteknologiloven.
100. Lovdata. Lov om organisering av forskningsetisk arbeid (forskningsetikkloven) [Internet]. 2017 05 01. Available from: https://lovdata.no/dokument/NL/lov/2017-04-28-23.
101. Lovdata. Lov om behandlingsbiobanker (behandlingsbiobankloven) [Internet]. 2018 07 20. Available from: https://lovdata.no/dokument/NL/lov/2003-02-21-12?q=biobank.
102. OsloMet. Acts and regulations2021.
103. WMA World Medical Association. WMA Declaration of Helsinki - Ethical Principles for medical research involving human subjects [Internet]. 2018 07 09. Available from: https://www.wma.net/policies-post/wma-declaration-of-helsinki-ethical-principles-for-medical-research-involving-human-subjects/.
104. Francisco DC, Peddi P, Hair JM, Flood BA, Cecil AM, Kalogerinis PT, et al. Induction and processing of complex DNA damage in human breast cancer cells MCF-7 and nonmalignant MCF-10A cells. Free Radic Biol Med. 2008;44(4):558-69.

105. Nyaga SG, Jaruga P, Lohani A, Dizdaroglu M, Evans MK. Accumulation of oxidatively induced DNA damage in human breast cancer cell lines following treatment with hydrogen peroxide. Cell Cycle. 2007;6(12):1472-8.
106. Reineke TM, Davis ME. Nucleic Acid Delivery via Polymer Vehicles. Polymer Science: A Comprehensive Reference: Elsevier; 2012.
107. Du J, Shen J, Wang Y, Pan C, Pang W, Diao H, et al. Boar seminal plasma exosomes maintain sperm function by infiltrating into the sperm membrane. Oncotarget. 2016;7(37):58832-47.
108. Kuster CE, Hess RA, Althouse GC. Immunofluorescence reveals ubiquitination of retained distal cytoplasmic droplets on ejaculated porcine spermatozoa. J Androl. 2004;25(3):340-7.
109. Julianelli V, Farrando B, Alvarez Sedo C, Calvo L, Romanato M, Calvo JC. Heparin enhances protamine disulfide bond reduction during in vitro decondensation of human spermatozoa. Hum Reprod. 2012;27(7):1930-8.
110. Liu L, Aston KI, Carrell DT. Protamine extraction and analysis of human sperm protamine 1/protamine 2 ratio using Acid gel electrophoresis. Methods Mol Biol. 2013;927:445-50.
111. Emery BR. 15: Sperm Aneuploidy Testing Using Fluorescence In Situ Hybridization. Spermiogenesis. New York: Springer Science+Business Media; 2013.
112. Miller D, Paradowska A. Evaluating the Localization and DNA Binding Complexity of Histones in Mature Sperm. Spermiogenesis. New York: Springer Science+Business Media; 2013.
113. Windt ML, De Beer PM, Franken DR, Rhemrev J, Menkveld R, Lombard CJ, et al. Sperm decondensation and semen parameters: utilization of a simple staining technique for the evaluation of human sperm decondensation. Andrologia. 1994;26(2):67-72.
114. Galotto C, Cambiasso MY, Julianelli VL, Valzacchi GJR, Rolando RN, Rodriguez ML, et al. Human sperm decondensation in vitro is related to cleavage rate and embryo quality in IVF. J Assist Reprod Genet. 2019;36(11):2345-55.
115. Zalensky AO, Breneman JW, Zalenskaya IA, Brinkley BR, Bradbury EM. Organization of centromeres in the decondensed nuclei of mature human sperm. Chromosoma. 1993;102(8):509-18.
116. Mitchell LA, De Iuliis GN, Aitken RJ. The TUNEL assay consistently underestimates DNA damage in human spermatozoa and is influenced by DNA compaction and cell vitality: development of an improved methodology. Int J Androl. 2011;34(1):2-13.
117. Le MT, Nguyen TAT, Nguyen HTT, Nguyen TTT, Nguyen VT, Le DD, et al. Does sperm DNA fragmentation correlate with semen parameters? Reprod Med Biol. 2019;18(4):390-6.
118. Alhmoud JF, Woolley JF, Al Moustafa AE, Malki MI. DNA Damage/Repair Management in Cancers. Cancers (Basel). 2020;12(4).

119. Soderberg O, Gullberg M, Jarvius M, Ridderstrale K, Leuchowius KJ, Jarvius J, et al. Direct observation of individual endogenous protein complexes in situ by proximity ligation. Nat Methods. 2006;3(12):995-1000.
120. Waters JC. Accuracy and precision in quantitative fluorescence microscopy. J Cell Biol. 2009;185(7):1135-48.
121. Mah LJ, El-Osta A, Karagiannis TC. gammaH2AX: a sensitive molecular marker of DNA damage and repair. Leukemia. 2010;24(4):679-86.
122. Zempleni J. Uptake, localization, and noncarboxylase roles of biotin. Annu Rev Nutr. 2005;25:175-96.
123. Wood GS, Warnke R. Suppression of endogenous avidin-binding activity in tissues and its relevance to biotin-avidin detection systems. J Histochem Cytochem. 1981;29(10):1196-204.
124. Thermo Fisher Scientific. Block endogenous biotin [Internet]. 2009. Available from: http://tools.thermofisher.com/content/sfs/brochures/TR0016-Block-endogenous-biotin.pdf.
125. Mishra M, Tiwari S, Gunaseelan A, Li D, Hammock BD, Gomes AV. Improving the sensitivity of traditional Western blotting via Streptavidin containing Poly-horseradish peroxidase (PolyHRP). Electrophoresis. 2019;40(12-13):1731-9.
126. Wennemuth G, Eisoldt S, Bode HP, Renneberg H, Schiemann PJ, Aumuller G. Measurement of calcium influx in surface-fixed single sperm cells - efficiency of different immobilization methods. Andrologia. 1998;30:6.
127. Iwasaki A, Gagnon C. Formation of reactive oxygen species in spermatozoa of infertile patients. Fertil Steril. 1992;57(2):409-16.
128. Agarwal A, Ikemoto I, Loughlin KR. Effect of sperm washing on levels of reactive oxygen species in semen. Arch Androl. 1994;33(3):157-62.
129. Zini A, Finelli A, Phang D, Jarvi K. Influence of semen processing technique on human sperm DNA integrity. Urology. 2000;56(6):1081-4.
130. Shekarriz M, DeWire DM, Thomas AJ, Jr., Agarwal A. A method of human semen centrifugation to minimize the iatrogenic sperm injuries caused by reactive oxygen species. Eur Urol. 1995;28(1):31-5.
131. Singh NP, Danner DB, Tice RR, McCoy MT, Collins GD, Schneider EL. Abundant alkali-sensitive sites in DNA of human and mouse sperm. Exp Cell Res. 1989;184(2):461-70.
132. Duty SM, Singh NP, Silva MJ, Barr DB, Brock JW, Ryan L, et al. The relationship between environmental exposures to phthalates and DNA damage in human sperm using the neutral comet assay. Environ Health Perspect. 2003;111(9):1164-9.
133. Romanato M, Cameo MS, Bertolesi G, Baldini C, Calvo JC, Calvo L. Heparan sulphate: a putative decondensing agent for human spermatozoa in vivo. Hum Reprod. 2003;18(9):1868-73.

134. Sutovsky P, Schatten G. Depletion of glutathione during bovine oocyte maturation reversibly blocks the decondensation of the male pronucleus and pronuclear apposition during fertilization. Biol Reprod. 1997;56(6):1503-12.
135. Ahmadi A, Ng SC. Influence of sperm plasma membrane destruction on human sperm head decondensation and pronuclear formation. Arch Androl. 1999;42(1):1-7.
136. Ribas-Maynou J, Garcia-Peiro A, Martinez-Heredia J, Fernandez-Encinas A, Abad C, Amengual MJ, et al. Nuclear degraded sperm subpopulation is affected by poor chromatin compaction and nuclease activity. Andrologia. 2015;47(3):286-94.
137. Evenson DP. The Sperm Chromatin Structure Assay (SCSA((R))) and other sperm DNA fragmentation tests for evaluation of sperm nuclear DNA integrity as related to fertility. Anim Reprod Sci. 2016;169:56-75.
138. Simon L, Carrell DT. Sperm DNA damage measured by comet assay. Methods Mol Biol. 2013;927:137-46.
139. Mallidis C, Wistuba J, Bleisteiner B, Damm OS, Gross P, Wubbeling F, et al. In situ visualization of damaged DNA in human sperm by Raman microspectroscopy. Hum Reprod. 2011;26(7):1641-9.
140. Amaral S, Redmann K, Sanchez V, Mallidis C, Ramalho-Santos J, Schlatt S. UVB irradiation as a tool to assess ROS-induced damage in human spermatozoa. Andrology. 2013;1(5):707-14.
141. Kemal Duru N, Morshedi M, Oehninger S. Effects of hydrogen peroxide on DNA and plasma membrane integrity of human spermatozoa. Fertil Steril. 2000;74(6):1200-7.
142. Bjorndahl L. The usefulness and significance of assessing rapidly progressive spermatozoa. Asian J Androl. 2010;12(1):33-5.
143. Jayaraman V, Upadhya D, Narayan PK, Adiga SK. Sperm processing by swim-up and density gradient is effective in elimination of sperm with DNA damage. J Assist Reprod Genet. 2012;29(6):557-63.
144. Jackson RE, Bormann CL, Hassun PA, Rocha AM, Motta EL, Serafini PC, et al. Effects of semen storage and separation techniques on sperm DNA fragmentation. Fertil Steril. 2010;94(7):2626-30.
145. Xue X, Wang WS, Shi JZ, Zhang SL, Zhao WQ, Shi WH, et al. Efficacy of swim-up versus density gradient centrifugation in improving sperm deformity rate and DNA fragmentation index in semen samples from teratozoospermic patients. J Assist Reprod Genet. 2014;31(9):1161-6.
146. Younglai EV, Holt D, Brown P, Jurisicova A, Casper RF. Sperm swim-up techniques and DNA fragmentation. Hum Reprod. 2001;16(9):1950-3.
147. Zhong HZ, Lv FT, Deng XL, Hu Y, Xie DN, Lin B, et al. Evaluating gammaH2AX in spermatozoa from male infertility patients. Fertil Steril. 2015;104(3):574-81.

148. Coban O, Serdarogullari M, Yarkiner Z, Serakinci N. Investigating the level of DNA double-strand break in human spermatozoa and its relation to semen characteristics and IVF outcome using phospho-histone H2AX antibody as a biomarker. Andrology. 2020;8(2):421-6.
149. Kinner A, Wu W, Staudt C, Iliakis G. Gamma-H2AX in recognition and signaling of DNA double-strand breaks in the context of chromatin. Nucleic Acids Res. 2008;36(17):5678-94.
150. Li Z, Yang J, Huang H. Oxidative stress induces H2AX phosphorylation in human spermatozoa. FEBS Lett. 2006;580(26):6161-8.
151. Garolla A, Cosci I, Bertoldo A, Sartini B, Boudjema E, Foresta C. DNA double strand breaks in human spermatozoa can be predictive for assisted reproductive outcome. Reprod Biomed Online. 2015;31(1):100-7.
152. Marchiani S, Tamburrino L, Maoggi A, Vannelli GB, Forti G, Baldi E, et al. Characterization of M540 bodies in human semen: evidence that they are apoptotic bodies. Mol Hum Reprod. 2007;13(9):621-31.
153. Muratori M, Marchiani S, Tamburrino L, Tocci V, Failli P, Forti G, et al. Nuclear staining identifies two populations of human sperm with different DNA fragmentation extent and relationship with semen parameters. Hum Reprod. 2008;23(5):1035-43.
154. Dominguez-Fandos D, Camejo MI, Ballesca JL, Oliva R. Human sperm DNA fragmentation: correlation of TUNEL results as assessed by flow cytometry and optical microscopy. Cytometry A. 2007;71(12):1011-8.
155. Muratori M, Piomboni P, Baldi E, Filimberti E, Pecchioli P, Moretti E, et al. Functional and ultrastructural features of DNA-fragmented human sperm. J Androl. 2000;21(6):903-12.
156. Cohen-Bacrie P, Belloc S, Menezo YJ, Clement P, Hamidi J, Benkhalifa M. Correlation between DNA damage and sperm parameters: a prospective study of 1,633 patients. Fertil Steril. 2009;91(5):1801-5.
157. Manna C, Barbagallo F, Manzo R, Rahman A, Francomano D, Calogero AE. Sperm Parameters before and after Swim-Up of a Second Ejaculate after a Short Period of Abstinence. J Clin Med. 2020;9(4).
158. Bahadur G, Almossawi O, A II, Al-Habib A, Okolo S. Factors Leading to Pregnancies in Stimulated Intrauterine Insemination Cycles and the Use of Consecutive Ejaculations Within a Small Clinic Environment. J Obstet Gynaecol India. 2016;66(Suppl 1):513-20.
159. Raad G, Mansour J, Ibrahim R, Azoury J, Azoury J, Mourad Y, et al. What are the effects of vitamin C on sperm functional properties during direct swim-up procedure? Zygote. 2019;27(2):69-77.
160. McCallum C, Riordon J, Wang Y, Kong T, You JB, Sanner S, et al. Deep learning-based selection of human sperm with high DNA integrity. Commun Biol. 2019;2:250.
161. Agarwal A, Henkel R, Huang CC, Lee MS. Automation of human semen analysis using a novel artificial intelligence optical microscopic technology. Andrologia. 2019;51(11):e13440.

162. Valiuskaite V, Raudonis V, Maskeliunas R, Damasevicius R, Krilavicius T. Deep Learning Based Evaluation of Spermatozoid Motility for Artificial Insemination. Sensors (Basel). 2020;21(1).

Appendix

A1. Marco Commands, ImageJ

A1.1 Counting number of foci in MCF-7 after incubation with hydrogen peroxide

```
//run("Brightness/Contrast...");

resetMinAndMax();

run("8-bit");

resetMinAndMax();

run("Stack to Hyperstack...", "order=xyzct channels=2 slices=31 frames=1 display=Composite");

run("Duplicate...", "duplicate channels=1");

run("Object Counter3D", "threshold=80 slice=31 min=10 max=1290065 new_results particles dot=3 numbers font=12 summary");
```

A1.2 Counting number of foci in spermatozoa

```
resetMinAndMax();

run("8-bit");

resetMinAndMax();

run("Stack to Hyperstack...", "order=xyzct channels=2 slices=31 frames=1 display=Composite");

Stack.setChannel(2);

run("Blue");

run("Duplicate...", "duplicate channels=1");

run("Object Counter3D", "threshold=135 slice=31 min=10 max=1157728 new_results particles dot=3 numbers font=12 summary");
```

A2. Raw data

A2.1 Number of signals in MCF-7 cells from hydrogen peroxide experiment

Table 8 *Number of signals detected in MCF-7 cells exposed to hydrogen peroxide.*

NT	4 mM 30'	20 mM 30'	20 mM 60'
7	40	200	239
13	36	148	283
10	7	36	299
9	9	106	260
14	2	144	410
6	16	106	314
12	33	45	104
10	22	100	190
6	11	110	198
25	8	76	144
13	117	66	194
12	54	78	148
5	64	30	135
8	21	50	172
5	19	33	141
7	24	35	112
2	44	97	95
3	16	66	227
7	22	126	201
4	29	91	195
3	43	189	200
3	27	222	192
8	14	72	195
7	30	47	243

A2.2 Number of signals in spermatozoa

Table 9 *Number of signals in spermatozoa with open chromatin structure by decondensation (D) and control cells with condensed chromatin.*

C	D
0	0
0	0
0	0
0	0
0	0
0	0
0	0
0	0
0	0
0	0
0	1
0	1
0	1
0	1
0	1
0	1
0	1
0	1
0	1
0	1
0	1
0	1
0	1
0	1
0	1
0	1
0	1
0	1
0	1
0	1
0	1
0	1
0	1
0	1
0	1
0	1
0	1
0	1
0	1
0	1
0	1
0	2
0	2
0	2
0	2
0	2
0	2
0	2
0	2
0	2
0	2
0	2
0	2
0	2
0	2
0	3
0	3
0	3
0	3
0	3
0	3
0	3
0	3
0	3
0	3
0	3
0	4
0	4
0	4
0	4
0	4
0	4
0	5
0	5
0	5
0	5
0	5
0	6
0	6
0	6
0	6
0	6
0	6
0	6
0	6
0	7
0	7
0	8
0	8
0	8
0	9
0	9
0	10
0	10
0	12
0	14
0	14
0	16
0	17
0	19
0	19
0	31
0	36
0	
0	
0	
0	
0	
0	
0	
0	
0	
0	
0	
0	
0	
1	
1	
1	
1	
1	
1	
1	
1	
1	
1	
1	
1	
1	
1	
1	
1	
1	
1	
1	
1	
1	
1	
1	
1	
1	
1	
1	
1	
1	
1	
1	
1	
1	
1	
1	
1	
1	
1	
1	
1	
1	
1	
1	
1	
1	
1	
1	
1	
1	
1	
1	
1	
1	
1	
1	
1	
1	
1	
1	
1	
1	
1	
1	
1	
1	
1	
1	
1	
2	
2	
2	
2	
2	
2	
2	
2	
2	
2	
2	
2	
2	
2	
2	
2	
3	
3	
3	
3	
3	
3	
3	
3	
3	
3	
3	
4	
4	
4	
4	
4	
4	
5	
6	
6	
6	
6	
7	

Table 10 *dSTRIDE signals in spermatozoa treated with different concentrations of hydrogen peroxide.*

0 mM	40 mM	200 mM
0	3	4
0	5	5
0	5	9

0	6	10
0	6	11
0	6	11
0	8	11
0	8	12
0	8	13
0	9	13
0	9	13
1	9	16
1	9	17
1	10	19

1	10	22
2	10	25
2	10	25
2	11	26
3	11	26
4	12	26
4	12	27
4	13	30
4	13	31
4	14	32
4	14	33

5	14	34
6	15	36
6	16	36
7	16	38
7	16	42
8	23	42
8	23	43
8	24	47
8	24	59
10	25	60
13	32	100

15
17
20
21
25
36
40
43
46

Table 11 *Number of signals in spermatozoa after swim-up (SU).*

C	**SU**	0	0	0	0	0	0	0	0	1	0	1	0	1	0	2	1	4	1
0	0	0	0	0	0	0	0	0	0	1	0	1	0	1	0	2	1	4	1
0	0	0	0	0	0	0	0	0	0	1	0	1	0	1	0	2	1	5	1
0	0	0	0	0	0	0	0	0	0	1	0	1	0	1	0	2	1	6	1
0	0	0	0	0	0	0	0	0	0	1	0	1	0	1	0	2	1	6	1
0	0	0	0	0	0	0	0	0	0	1	0	1	0	1	0	2	1	6	1
0	0	0	0	0	0	0	0	0	0	1	0	1	0	1	0	2	1	6	1
0	0	0	0	0	0	0	0	0	0	1	0	1	0	1	0	2	1	7	1
0	0	0	0	0	0	0	0	0	0	1	0	1	0	1	0	2	1		1
0	0	0	0	0	0	0	0	0	0	1	0	1	0	1	0	3	1		1
0	0	0	0	0	0	0	0	0	0	1	0	1	0	1	0	3	1		1
0	0	0	0	0	0	0	0	0	0	1	0	1	0	1	0	3	1		1
0	0	0	0	0	0	0	0	0	0	1	0	1	0	1	0	3	1		1
0	0	0	0	0	0	0	0	0	0	1	0	1	0	1	0	3	1		2
0	0	0	0	0	0	0	0	0	0	1	0	1	0	1	0	3	1		2
0	0	0	0	0	0	0	0	0	0	1	0	1	0	1	0	3	1		2
0	0	0	0	0	0	0	0	0	0	1	0	1	0	1	0	3	1		2
0	0	0	0	0	0	0	0	0	0	1	0	1	0	2	0	3	1		2
0	0	0	0	0	0	0	0	0	0	1	0	1	0	2	0	3	1		2
0	0	0	0	0	0	0	0	0	0	1	0	1	0	2	0	3	1		3
0	0	0	0	0	0	0	0	0	0	1	0	1	0	2	0	4	1		3
0	0	0	0	0	0	0	0	1	0	1	0	1	0	2	1	4	1		3
0	0	0	0	0	0	0	0	1	0	1	0	1	0	2	1	4	1		3
0	0	0	0	0	0	0	0	1	0	1	0	1	0	2	1	4	1		3

Table 12 *Number of signals detected in spermatozoa from samples with known DNA fragmentation.*

301	**503**	**612**	**617**	**1009**	**1010**	**1012**	**1014**	**1015**	**1018**	**1019**
0	0	0	0	0	0	0	0	0	0	0
0	0	0	0	0	0	0	0	0	0	0
1	0	0	0	0	0	0	1	0	0	0
1	0	0	0	0	0	0	1	0	0	0

1	0	0	0	0	0	0	1	0	0	0
1	0	0	0	0	0	0	1	0	0	0
1	0	0	0	0	0	0	1	0	0	0
1	0	0	0	0	0	0	1	0	0	0
1	0	0	0	0	0	0	1	0	0	0
1	0	0	0	0	0	0	1	0	0	0
1	0	0	0	0	0	0	1	0	0	0
1	0	0	0	0	0	0	2	0	0	0
1	0	0	0	0	0	0	2	0	0	0
1	0	0	0	0	0	0	2	0	0	0
1	0	0	0	0	0	0	2	0	0	0
1	0	0	0	0	0	0	2	0	0	0
1	0	0	0	0	0	0	2	0	0	0
1	0	0	0	0	0	0	2	0	0	0
1	0	0	0	0	0	0	2	0	0	0
1	0	0	0	0	0	0	2	0	0	0
1	0	0	0	0	0	0	2	0	0	0
1	0	0	0	0	0	0	3	0	0	0
1	0	0	0	0	0	0	3	0	0	0
1	0	0	0	0	0	0	3	0	0	0
1	1	0	0	0	0	0	3	0	0	0
1	1	0	0	0	0	0	3	0	0	0
1	1	0	0	0	0	0	3	0	0	0
1	1	0	1	0	0	0	3	0	0	1
1	1	0	1	0	0	0	3	0	0	1
2	1	0	1	0	0	1	3	0	0	1
2	1	0	1	0	0	1	3	0	0	1
2	1	0	1	0	0	1	3	0	0	1
2	1	0	1	0	0	1	4	0	0	1
2	1	0	1	0	0	1	4	0	0	1
2	1	0	1	0	0	1	4	0	0	1
2	1	0	1	0	0	1	4	0	0	1
2	1	0	1	0	0	1	4	0	0	1
2	1	0	1	0	0	1	4	0	0	1
2	1	0	1	0	0	1	4	0	0	1
2	1	0	1	0	0	1	4	0	0	1
2	1	0	1	0	0	1	4	0	0	1
2	1	0	1	0	0	1	4	0	0	1
2	1	0	1	0	0	1	4	0	0	1
2	1	0	1	0	0	1	4	0	0	1
2	1	0	1	0	0	1	4	0	0	1
2	1	0	1	0	0	1	4	0	0	1
2	1	0	1	0	0	1	5	0	1	1
2	1	0	1	0	0	1	5	0	1	1
2	1	1	1	1	0	1	5	0	1	1
2	1	1	1	1	0	1	5	0	1	1
2	1	1	1	1	0	1	5	0	1	1
2	1	1	1	1	0	1	5	0	1	1
2	1	1	1	1	0	1	5	0	1	1

2	1	1	1	1	0	1	5	0	1	1
2	1	1	1	1	0	1	5	0	1	1
2	1	1	1	1	0	1	5	0	1	1
2	1	1	1	1	0	1	5	0	1	1
2	1	1	1	1	0	1	5	0	1	1
2	1	1	1	1	0	1	6	1	1	1
3	1	1	1	1	0	1	6	1	1	1
3	1	1	1	1	0	1	6	1	1	1
3	1	1	1	1	0	1	6	1	1	1
3	1	1	1	1	0	1	6	1	1	1
3	2	1	1	1	0	1	6	1	1	1
3	2	1	1	1	0	1	6	1	1	1
3	2	1	1	1	0	1	6	1	1	1
3	2	1	1	1	0	1	6	1	1	1
3	2	1	1	1	0	1	6	1	1	1
3	2	1	1	1	0	1	6	1	1	1
3	2	1	1	1	0	1	6	1	1	1
3	2	1	1	1	0	1	6	1	1	1
3	2	1	1	1	0	1	6	1	1	1
3	2	1	1	1	0	1	6	1	1	2
3	2	1	1	1	0	1	7	1	1	2
3	2	1	1	1	0	1	7	1	1	2
3	2	1	1	1	0	1	7	1	1	2
3	2	1	1	1	0	1	7	1	1	2
3	2	1	1	1	0	1	7	1	1	2
3	2	1	1	1	0	1	7	1	1	2
4	2	1	1	1	0	1	7	1	1	2
4	2	1	1	1	0	1	7	1	1	2
4	2	1	1	1	0	1	7	1	1	2
4	2	1	1	1	0	1	7	1	1	2
4	2	1	1	1	0	1	7	1	1	2
4	2	1	1	1	0	1	7	1	1	2
4	2	1	1	1	0	1	7	1	1	2
4	2	1	1	1	0	1	7	1	1	2
4	2	1	1	1	0	1	8	1	1	2
4	2	1	1	1	0	2	8	1	1	2
4	2	1	1	1	0	2	8	1	1	2
4	2	1	1	1	0	2	8	1	2	2
4	2	1	1	1	0	2	8	1	2	2
4	2	1	1	1	0	2	8	1	2	2
4	2	1	1	1	0	2	8	1	2	2
4	2	1	1	1	0	2	9	1	2	2
4	3	1	1	1	0	2	9	1	2	2
4	3	1	1	1	0	2	9	1	2	2
4	3	1	1	1	0	2	9	1	2	2
4	3	1	2	1	0	2	9	1	2	2
4	3	1	2	1	0	2	9	1	2	2
5	3	1	2	1	0	2	9	1	2	2
5	3	1	2	1	0	2	10	1	2	2

5	3	2	2	1	0	2	10	1	2	2
5	3	2	2	1	0	2	10	1	2	2
5	3	2	2	1	0	2	10	1	2	2
5	3	2	2	1	0	2	10	1	2	2
5	3	2	2	1	0	2	10	1	2	2
5	3	2	2	1	0	2	10	1	2	2
5	3	2	2	1	0	2	10	1	2	2
5	3	2	2	1	0	2	10	1	2	3
5	3	2	2	1	0	2	10	2	2	3
5	3	2	2	1	1	2	11	2	2	3
5	3	2	2	1	1	2	11	2	2	3
5	3	2	2	1	1	3	11	2	2	3
5	3	2	2	2	1	3	11	2	2	3
5	3	2	2	2	1	3	11	2	2	3
6	3	2	2	2	1	3	11	2	2	3
6	3	2	2	2	1	3	11	2	2	3
6	3	2	2	2	1	3	11	2	2	3
6	3	2	2	2	1	3	11	2	2	3
6	3	2	2	2	1	3	11	2	2	3
6	3	2	2	2	1	3	11	2	3	3
6	3	2	2	2	1	3	11	2	3	3
6	3	2	2	2	1	3	11	2	3	3
6	3	2	2	2	1	3	12	2	3	3
6	3	2	2	2	1	3	12	2	3	3
6	4	2	2	2	1	3	12	2	3	4
6	4	2	2	2	1	3	12	2	3	4
6	4	2	2	2	1	3	12	2	3	4
6	4	2	2	2	1	3	12	2	3	4
6	4	2	2	2	1	3	13	2	3	4
6	4	2	2	2	1	3	13	2	3	4
7	4	2	2	2	1	3	13	2	3	4
7	4	2	3	2	1	3	13	2	3	4
7	4	2	3	2	1	3	13	2	3	4
7	4	2	3	2	1	3	13	2	3	4
7	5	3	3	2	1	3	13	2	3	4
7	5	3	3	2	1	3	13	2	3	4
7	5	3	3	2	1	3	13	2	3	4
7	5	3	3	2	1	3	13	2	3	4
7	5	3	3	2	1	3	13	2	3	4
7	5	3	3	2	1	3	14	2	3	4
7	5	3	3	2	1	3	14	2	3	5
7	5	3	3	2	1	4	14	2	3	5
7	5	3	3	2	1	4	15	2	3	5
7	5	3	3	2	1	4	15	2	3	5
8	6	3	3	2	1	4	15	3	4	5
8	6	3	3	2	1	4	15	3	4	5
8	6	3	3	2	1	4	15	3	4	5
8	6	3	3	2	1	4	15	3	4	5
8	6	3	3	3	1	4	15	3	4	5

8	6	3	3	3	1	4	15	3	4	5
8	6	3	3	3	1	4	16	3	4	5
8	6	3	3	3	1	4	16	3	4	5
8	6	3	3	3	1	5	16	3	4	5
8	6	4	3	3	1	5	16	3	4	5
8	6	4	3	3	1	5	16	3	4	5
8	6	4	3	3	1	5	16	3	4	6
9	6	4	3	3	2	5	16	3	4	6
9	6	4	3	3	2	5	17	3	4	6
9	6	4	3	3	2	5	17	3	4	6
9	7	4	4	3	2	5	18	3	4	6
9	7	4	4	3	2	5	18	4	4	6
9	7	4	4	3	2	5	19	4	4	6
9	7	4	4	3	2	5	19	4	4	6
9	7	4	4	3	2	5	19	4	5	7
9	7	5	4	3	2	6	19	4	5	7
9	7	5	4	3	2	6	19	4	5	7
9	7	5	4	3	2	6	20	4	5	7
9	7	5	4	3	2	6	20	4	5	8
9	7	5	4	3	2	7	21	4	5	8
10	8	5	5	3	2	7	21	4	5	8
10	8	5	5	3	2	7	22	4	5	8
10	8	5	5	3	2	7	22	5	5	8
10	8	5	5	3	2	7	22	5	5	9
10	8	6	5	3	2	7	22	5	5	9
11	8	6	5	3	2	7	23	5	5	9
11	8	6	5	3	2	7	23	6	5	9
11	8	6	6	4	2	8	24	6	5	10
11	8	7	6	4	2	8	24	6	6	10
11	8	7	6	4	2	8	24	6	6	10
11	9	7	6	4	2	8	25	6	6	10
12	9	9	6	4	2	8	26	6	6	10
12	9	9	6	4	2	9	26	6	6	11
12	10	10	6	4	2	9	26	7	6	11
12	10	11	7	4	2	9	26	7	6	12
13	10	15	7	4	2	9	26	7	6	12
13	10	16	7	4	3	10	28	7	6	12
13	10	27	7	5	3	10	29	7	7	12
13	10	41	7	5	4	11	30	8	7	13
13	12		8	6	4	11	31	8	7	13
13	12		8	6	4	11	32	9	8	13
13	12		8	6	4	12	32	10	8	16
14	13		8	6	4	12	33	10	8	16
16	14		8	7	5	13	36	10	8	17
16	16		9	7	5	15	37	11	8	17
17	16		9	8	5	17	38	11	8	18
17	19		11	8		19	39	11	9	18
17	25		13	9		20	41	12	9	18
19	27		13	10		20	45	14	10	20

20	28	17	10	20	47	14	19	21
23	30	31	21	24	48	16		23
24	33		21	30	51	16		23
25	33		39	35	67	17		32
36	36							
	45							

A2.3 Different tests for comparing dSTRIDE and SCSA results

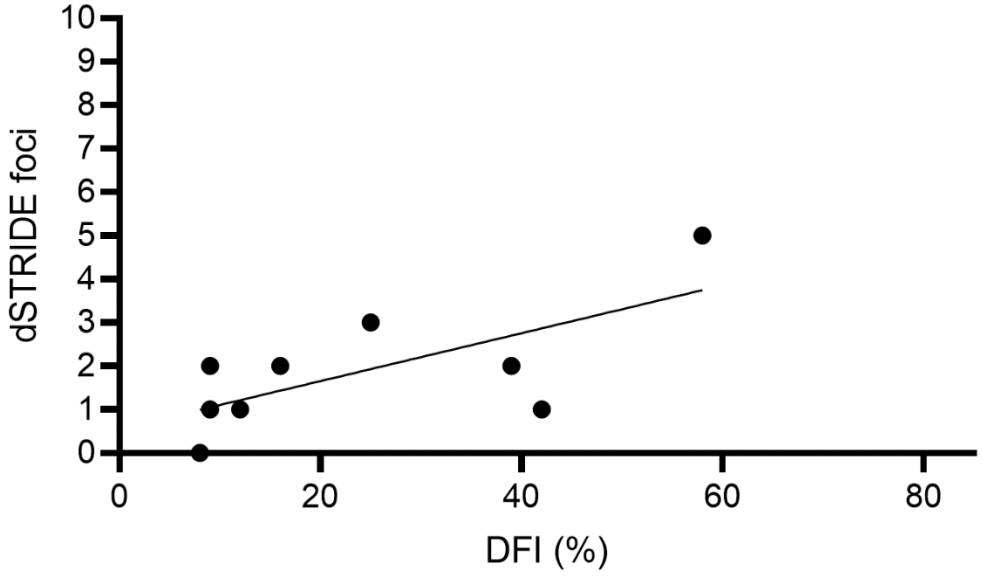

Figure 32 *Simple regression analysis between DFI (%) by SCSA and dSTRIDE foci median by dSTRIDE.*

Table 13 *dSTRIDE foci converted to DFI (%) with variated definitions for a fragmented cell: min. 0, 1, 2, 3, 4 or 5 foci in each cell.*

	0	1	2	3	4	5
301	99 %	86 %	71 %	61 %	51 %	43 %
503	88 %	81 %	54 %	39 %	34 %	29 %
612	75 %	46 %	28 %	18 %	13 %	8 %
617	87 %	51 %	34 %	20 %	15 %	12 %
1009	76 %	44 %	26 %	13 %	8 %	7 %
1010	44 %	20 %	5 %	4 %	2 %	0 %
1012	86 %	57 %	45 %	30 %	25 %	19 %
1014	99 %	95 %	90 %	84 %	28 %	72 %
1015	72 %	75 %	28 %	21 %	15 %	13 %
1018	77 %	55 %	40 %	27 %	17 %	12 %
1019	86 %	65 %	46 %	38 %	30 %	23 %

A3. Materials and solutions

A3.1 Reagents and instruments

Table 14 *Reagents used in this master thesis, listed in alphabetical order.*

Reagents used		
Reagents	**Producer**	**Number**
APO-BrdU™ TUNEL Assay Kit	Invitrogen	Cat. A23210
Biotin-7-dATP	Jena Bioscience	Cat. NU-835-BIO-S
Biotin-16-dCTP	Jena Bioscience	Cat. NU-809-BIO16-S
Biotin-16-dUTP	Jena Bioscience	Cat. NU-803-BIO16-S
Bovin Serum Albumin	Sigma-Aldrich	Prod. A4503-50G
dGTP-solution	Jena Bioscience	Cat. NU-1003L
DMSO	Merc Life Science	Cat. D2650-100ML
DNA polymerase I from *E. coli*	New England Biolabs	Cat. M0209S
DTT	Merck Life Science	Cat. 10197777001
Dulbecco's Modified Eagle Medium	Gibco	Cat. 41965039
Dulbecco's Phosphate buffered saline	Gibco	Cat.14190250
Duolink™ In Situ Detection Reagents Orange	Sigma-Aldrich	Prod. DUO92007-100RXN
Duolink In Situ Wash Buffers	Sigma-Aldrich	Prod. DUO82049-100RXN
Endogenous Biotin-Blocking Kit	Invitrogen	Cat. E21390
Fetal Bovine Serum	Sigma-Aldrich	Prod. A4503-50G
Heparin sodium salt from porcine intestinal mucosa	Merck Life Science	Prod. H3149-10KU
Hydrogenii peroxidum 30 per centum (Hydrogen peroxide)	Apoteksproduksjon AS	Prod. 09N052/4
Immersol™ 518 F	Zeiss	Prod. 10539438
NEBuffer™ 2	New England Biolabs	Cat. B7002S
Paraformaldehyde 4%	Thermo Scientific	Cat. AAJ19943K2
Penicillin-Streptomycin (5000 U/mL)	Gibco	Cat. 15070063
Phosphate buffered saline tablets	Sigma-Aldrich	Prod. 97382
Poly-L-Lysine 0.01%	Sigma-Aldrich	Prod. P8920
Rektifisert sprit ren 1000 ml 96%	Antibac	Cat. 600051
Sperm Preparation Medium 60 mL	Origio	Cat. 10690060A
Sperm Freeze Medium	Origio	Cat. 10670010A
Tween-20	Sigma-Aldrich	Prod. P9416-100ML

Triton® Tx-100	Sigma-Aldrich	Prod. T8787-250ML

Table 15 *Lab equipment and instruments used in this master thesis, listed in alphabetical order.*

Equipment and instruments		
Equipment and instrument	**Producer**	**Number**
Countess™ Automated cell counter	Invitrogen	C10227
Countess™ cell counting chamber slides (includes 0.4% trypan blue)	Invitrogen	C10228
Coverslips (12mm)	VWR	631-1577
Eppendorf Centrifuge 5415 R	Eppendorf	2262140-8
Eppendorf Centrifuge 5810 R	Eppendorf	5810000320
ESCO Class II Biological Safety Cabinet	Nordic Safe	NC2-6L8
Falcon® 15 mL Polypropylene Centrifuge Tube	Falcon	352196
Falcon® 15 mL Polystyrene Centrifuge Tube	Falcon	352095
In-VitroCell Direct Heat CO2 Incubator	Nuaire	NU-5710E
Low Temperature Freezer Vials	VWR	479-1220
Microscope slides (Menzel)	Thermo Scientific	ISO8037/1
Nunc™ Cell-Culture MultiDishes	Thermo Scientific	142475
Nunc™ EasYFlask™ Cell Culture Flasks	Thermo Scientific	156367
Nunc™ EasYFlask™ Cell Culture Flasks	Thermo Scientific	156499
Olympus BX40	Olympus	DP74
Olympus IX71	Olympus	
Olympus CX31	Olympus	
Pipetboy 2	Integra	
Rotofix 32A	Hettich Zentrifugen	1000766
Sarstedt 15 mL	Sarstedt	62.554.502
Sarstedt 1.5 mL	Sarstedt	72.690.301
Vortex Genie 2	Scientific Industries	SI0256

A3.2 Solutions

1x Phosphate Buffered Saline (PBS):

– One tablet dissolved in ddH2O for a total volume of 200 mL

– Sterilized by autoclaving at 121 °C

PBST-BSA (0.01% Tween-20 and 2% BSA):

- 1.0 g BSA

– 5 µl Tween-20

– Dissolved in PBS for a total volume of 50 mL

PBST-BSA with Tx-100 (0.1%):

- 1.0 g BSA

- 50 µl Tx-100

– 5 µl Tween-20

– Dissolved in PBS for a total volume of 50 mL

0.5% PFA

- 1 mL 3% PFA

- 5 mL PBS

0.5% BSA in PBS:

- 0.25 g BSA

- Dissolved in PBS for a total volume of 50 mL

Tx100 (0.1) in PBS:

- 50 µl Tx100

- Dissolved in PBS for a total volume of 50 mL

A3.3 Primary and secondary antibodies

Table 16 *Table of primary antibodies used in relevant methods with detailed information.*

Method	Antigen	Antibody host and clonality	Dilution factor	Producer	Product Number	Lot. Number
IF	Anti-phospho-Histone H2AX	Mouse, monoclonal antibody	1:100	Millipore	05-636	#2310355
dSTRIDE	Anti-BrdU	Mouse, monoclonal antibody	1:500	Abcam	ab8039	#GR301685-32
dSTRIDE	Anti-BrdU	Rabbit, monoclonal antibody	1:200	Abcam	ab152095	#GR3308602-8
sSTRIDE	Anti-Biotin	Mouse, monoclonal antibody	1:200	Abcam	Ab201341	#GR3213949-3
sSTRIDE	Anti-Biotin	Rabbit, polyclonal antibody	1:100	Abcam	Ab53494	#GR3262411-10

Table 17 *Table of secondary antibodies applied in relevant methods, with detailed information.*

Label	Ab	Ab host and clonality	Dilution factor	Producer	Product Number	Lot Number
Cy2	anti-mouse	Donkey polyclonal	1:200	Jackson ImmunoResearch	115-225-166	146498
Cy3	anti-mouse	Donkey polyclonal	1:200	Jackson ImmunoResearch	715-165-150	AB_2340813

Alexa Fluor-594	anti-mouse	Goat polyclonal	1:500	Thermo Fisher	A11005	#1696463
Duolink ™ In Situ PLA® Probe Anti-Mouse MINUS	anti-mouse	Donkey anti-mouse	1:500	Sigma-Aldrich	DUO92004-100RXN	#SLCD9034
Duolink ™ In Situ PLA® Probe Anti-Rabbit PLUS	anti-rabbit	Donkey anti-rabbit	1:200	Sigma-Aldrich	DUO92002—100RXN	#SLCF4321

A4. REC and biobank approval for project 2010/2721 s-08220b

UNIVERSITETET I OSLO
DET MEDISINSKE FAKULTET

Professor Trine Berit Haugen
Høgskolen i Oslo
Avdeling for helsefag
Postboks 4, St. Olavs plass
0310 Oslo

Regional komité for medisinsk og helsefaglig forskningsetikk Sør-Øst B (REK Sør-Øst B)
Postboks 1130 Blindern
NO-0318 Oslo

Telefon: 22 85 06 70
Telefaks: 22 85 05 90
E-post: juliannk@medisin.uio.no
Nettadresse: www.etikkom.no

Dato: 30.04.2008
Deres ref.:
Vår ref.: 08/220b.2008/3957

08/220b.2008/3957 Betydningen av lipidmetabolismen for mannlig reproduksjonsfunksjon

Vi viser til brev datert 29.04.08 med svar på merknader og revidert informasjonsskriv.

Komiteen tar svar på merknader til etterretning.

Komiteen har ingen merknader til revidert informasjonsskriv.

Vedtak
Prosjektet godkjennes.
Komiteen vil videresende skjema for opprettelse av forskningsbiobank, kopi av informasjonsskriv samt komiteens vedtak til Helsedirektoratet for endelig behandling av opprettelse av forskningsbiobank.

Med vennlig hilsen

Tor Norseth
Leder

Julianne Krohn-Hansen
Komitésekretær

Kopi: Helsedirektoratet

Figure 33 *REC approval for the project "Betydningen av lipidmetabolismen for mannlig reproduksjonsfunksjon" 2010/2721 s-08220b.*

Helsedirektoratet

Høgskolen i Oslo
Professor Trine B. Haugen
Avdeling for helsefag
Postboks 4
St. Olavs plass
0310 OSLO

Deres ref.:
Saksbehandler: BEB
Vår ref.: 08/6399-
Dato: 27.05.2008

Høgskolen i Oslo - Melding om opprettelse av forskningsbiobank - Betydningen av lipidmetabolisme for mannlig reproduksjonsfunksjon

Vi viser til brev vedrørende ovennevnte. Helsedirektoratet er delegert å vurdere meldinger om opprettelse av forskningsbiobanker i henhold til biobankloven § 4.

Direktoratet har ingen innsigelser til at forskningsbiobanken opprettes i henhold til biobankloven.

Direktoratet forutsetter at opprettelsen av den planlagte forskningsbiobanken oppfyller nødvendige krav til godkjenning, konsesjon m.v. i henhold til annet relevant regelverk, herunder bioteknologiloven, helseregisterloven og legemiddelloven.

Melding om forskningsbiobank vil registreres ved Biobankregisteret ved Nasjonalt folkehelseinstitutt som har fått ansvaret for å føre et offentlig tilgjengelig register over landets biobanker, jf biobankloven § 6.

Dokumentet er godkjent elektronisk

Vennlig hilsen

Ragnhild Castberg e.f.
avdelingsdirektør

Bente Bryhn
rådgiver

Kopi: Biobankregisteret, ref. 2291
REK Sør-Øst B, ref. 08/220b. 2008/3957

Helsedirektoratet
Avd. bioteknologi og generelle helselover
Bente Bryhn, tlf.: 24 16 32 73
Postadresse: Postboks 7000 St. Olavs plass, 0130 Oslo • Besøksadresse: Universitetsgata 2, Oslo
Tlf.: 810 20 050 • Faks: 24 16 30 01 • Org. nr.: 983 544 622 • postmottak@shdir.no • www.shdir.no

Figure 34 *Approval for creation of biobank at OsloMet related to the project "Betydningen av lipidmetabolisme for mannlig reproduksjonsfunksjon".*